THE THERMOCHEMISTRY OF SOME TRANSITION METAL COMPLEXES

by

Graham Beech, Grad.R.I.C.

A thesis submitted to the University of Keele
in partial fulfilment of the requirements
for the degree of Doctor of Philosophy.

Chemistry Department,
University of Keele.

June, 1967.

ACKNOWLEDGEMENTS

In presenting this thesis I wish to thank Professor H.D. Springall for making available facilities for this work. I also wish to thank Dr. C.T. Mortimer for his guidance and encouragement. Since Dr. Mortimer's secondment to the University of Zambia the supervision of my work has been carried out by Professor Springall, Dr. H.A. Skinner of the University of Manchester, Dr. A.S. Carson of the University of Leeds and Dr. R. Little. I thank them all for their help, and in particular, I thank Dr. Little and Dr. Carson for their patient advice during the preparation of this thesis.

I was fortunate to have useful discussions with Dr. S.M. Nelson of Queen's University, Belfast, and some of his ideas have been incorporated in the discussion in this thesis. In addition, the following have helped in various ways and I thank them:

Dr. L.F. Larkworthy, University of Surrey, for gifts of chromium(II) complexes and helpful advice.

Dr. D.J. Machin, University of Manchester, for help in recording diffuse reflectance spectra and magnetic measurements.

Mrs. R.M. Canadine, I.C.I. (Mond) Ltd., for measuring the magnetic susceptibility of dichloro(2,5-Dimethylpyrazine)cobalt(II).

Dr. A.B.P. Lever, University of Manchester Institute of Science and Technology, for a gift of violet-dichloro(2,5-Dimethylpyrazine)cobalt(II).

Professor J.V. Quagliano, The Florida State University, for a gift of dichlorobis(α-picoline)nickel(II).

Dr. D.R. Douslin, Department of the Interior (U.S.A.), for advice on the heat capacities of heterocyclic bases.

Dr. H.H. Greenwood, for computational assistance.

I also wish to thank the Science Research Council for a Maintenance Grant.

All the experimental work in this thesis was carried out by the author under the supervision of Dr. C.T. Mortimer (and, during his secondment to the University of Zambia, Professor H.D. Springall, Dr. H.A. Skinner, Dr. R. Little and Dr. A.S. Carson) with the exception of some preparations described in Chapter 2.

ABSTRACT

The heats of decomposition of some transition metal complexes have been measured by (a) adiabatic reaction calorimetry and (b) differential scanning calorimetry. Method (a) was applied to dichlorobis(triphenylphosphine)cobalt(II) chloride while method (b) was applied to a considerable number of complexes between divalent metal halides and organic bases. These bases were pyridine, methyl-pyridines, aniline, pyrazine, methylpyrazines and pyrimidine.

The thermal data which were obtained yielded useful information which may be summarised as follows:

(i) Steric interactions

The effect on the strength of the metal-nitrogen bond of methyl substitution was investigated. It was found that, for the methyl pyridines, α-substitution was effective in weakening the bond strength. It is, however, not yet understood why β-substitution appears to weaken the bond still further. Very little weakening, on methyl substitution, could be observed for the pyrazine complexes.

(ii) Crystal field effects

Certain thermal quantities, related to the heats of gas phase reactions, have been calculated from the experimental data. These, when plotted against atomic number for a particular type of complex, vary in the same manner as the crystal field stabilisation energy. One such plot was used to calculate the stabilisation energy of dichlorodipyridinenickel(II) and gave good agreement with a spectroscopic measurement of the same quantity.

(iii) Polarisability

The experimental data appear to support arguments based on the polarisability of the halogen ligand and the effect of this on metal-nitrogen bond strength. π-bonding effects are proposed to account for the apparently constant metal-nitrogen bond strengths in the compounds which contain octahedral molecules. In connection with this, it is shown that there is a convergence of the heats of formation of octahedral and tetrahedral compounds after correction for crystal field effects.

Since many of the decompositions were carried out at high temperatures (up to 500°C) it was necessary to calculate the magnitude of the temperature correction to the heats of decomposition required to refer them all to a common temperature. This required values for the heat capacities of the complexes and these were measured, for representative complexes, in the differential scanning calorimeter. The heat capacity data indicated, also, a rigidity in metal-pyrazine bonds which may be due to back π-donation from the metal to the ring.

CONTENTS

CHAPTER I

INTRODUCTION

All chemical reactions involve changes in energy. These may be detected by the measurement of an intensive or extensive parameter dependent on the energy change of the chemical reaction. The measurement of these parameters and the calculation of the energy changes accompanying chemical processes form the subject matter of thermochemistry. The energy changes must have their origin in the detailed electronic structure of chemical compounds (1) and their determination should yield quantitative information for interpretation by valence theory. Despite the conceptual simplicity of thermochemistry, the terms used in the subject must be rigorously defined. The heat change which accompanies a process is one of the most frequently encountered quantities but the magnitude of this change depends completely upon how the process is carried out. A brief discussion is included here to define some of the terms used in thermochemistry.

The First Law of Thermodynamics (or Law of Conservation of Energy) states that the energy of a system is a state function and is single valued(2).It is necessary to define the properties of a system which describe that system, both in its initial and final states, before interpretation of the accompanying energy change. In addition to heat being exchanged with the surroundings, a system may also perform work. The energy change is given by the sum of the two terms, heat and work,

which are recognized as being interconvertible forms of energy.

The change in (internal) energy of the system

$$\Delta U = q - w \qquad (1)$$

where ΔU = energy change, q = heat absorbed from surroundings and w = work done by the system.

By definition, the derivative of a state function is a complete differential (3,4) so that equation (2) represents such a differential:

$$dU = đq - đw$$

Neither $đq$ nor $đw$ need be complete differentials. For example, if only pressure-volume work is performed by the system,

$$đw = PdV.$$

Integration of PdV can not be carried out unless P as a function of V is known. Therefore, for PV work, $đw$ may possess several values and $w(PV)$ is not a state function. It is immediately obvious that $đq$ is not a state function.

However, $d(PV)$ may be integrated (5) and a new state function formulated, namely, enthalpy (H).

$$dH = dU + d(PV)$$

$$\text{i.e. } H = U + PV$$

In the important case where the initial and final pressures are equal (which does not imply a constant pressure throughout the change) "enthalpy change at constant pressure" is referred to:

$$\Delta H = \Delta U + P\Delta V$$

This is equivalent to the heat of reaction "at constant pressure" and is the quantity most commonly quoted in thermochemical work. If there is

no volume change the heat absorbed is equal to the change in internal energy:

$$q = \Delta U$$

It is the state functional property of enthalpy which is so useful in thermochemistry. This is embodied in the Law of Constant Heat Summation as proposed by Hess (6). The heat of a reaction at constant pressure may be calculated from the heats of other reactions, measured at constant pressure, if these reactions combine to yield the required reaction. Also, by assigning zero enthalpies to elements in their defined standard states, standard enthalpies of formation (ΔH_f°) may be calculated for compounds of those elements. These may then be used to calculate the enthalpy change of a reaction which may be difficult to study experimentally.

It was unfortunate that the early thermochemists, such as Berthelot and Thomsen, used enthalpy changes as the criteria of spontaneity of a chemical reaction (7). Negative enthalpy changes were considered to accompany spontaneous reactions. Several reactions were found, however, to proceed with positive enthalpy changes and a rapid decline of interest in thermochemistry followed. It was soon recognised that the criterion of spontaneity is the existence of a negative free energy change accompanying a chemical reaction. The functions defining free energy are:

$$G = H - TS \quad \text{(Gibbs Free Energy)}$$

$$A = U - TS \quad \text{(Helmholtz Free Energy)}$$

S is the state function, entropy, and the change in entropy $S_B - S_A$.

ΔS is defined as $\int_A^B \frac{dq_{rev}}{T(^\circ A)}$

From what was said at the beginning of this introduction, however, enthalpy changes should reflect the energetics of a chemical reaction directly even though they are not criteria of spontaneity. It is necessary to recognise, therefore, the significance of different measurements in thermodynamics. Firstly, the prediction of the spontaneity of reactions from free energy measurements and, secondly, the interpretation of energy changes in the compounds undergoing reaction. It is the latter aspect which is the concern of thermochemistry and of this thesis.

There is now a considerable collection of thermochemical data and these have been used to test various theories of chemical bonding. As an example, various bond energy schemes have been tested experimentally and found to work reasonably well (8). Discrepancies have been found and have given rise to sophistications in more recent theories. It is also of interest that the parameters of Huckel molecular orbital theory are calculated from experimental measurements while later theories calculate the parameters from first principles and give, generally, worse results (9).

Calorimetric Techniques

Enthalpy changes may be measured either directly or indirectly. Indirect measurements normally involve the determination of equilibrium or kinetic parameters and have been discussed at length elsewhere (10). Spectroscopic methods may be classified as direct but also have been discussed elsewhere (10). Only direct calorimetry is described here.

Calorimeters fall into two classes - isothermal and non-isothermal. In non-isothermal calorimeters, quantities of heat are estimated by the

temperature changes they produce, whereas in isothermal calorimeters the temperature remains constant and the heat effect is measured by the change in some parameter such as the extent of an isothermal phase change at the temperature of measurement. For the purposes of this discussion it is convenient to include temperature controlled calorimeters as was done by O'Neill (11), since in these, the temperature of the sample is the independent reproducible variable just as in an isothermal calorimeter.

Non-Isothermal Calorimeters (3)

Four types of non-isothermal calorimeters are currently in common use. These are: constant temperature environment, Adiabatic, Twin and Heat Leak calorimeters. Since temperature is the measured variable all heat leakage must be minimised so that, ideally, the whole temperature change is due to the heat of reaction. The calorimeters listed above overcome the problem in different ways and are described briefly below:

(i) Constant Temperature Environment

In this mode of operation the calorimeter is surrounded by a constant temperature jacket which may consist of a stirred liquid or, in some cases, a large metal shield. The rate of change of temperature of the calorimeter depends on several factors, the most important being the temperature difference between the jacket and calorimeter and the thermal conductivity between the two. The latter may be decreased by

polishing the adjacent surfaces and also by evacuating the space between the calorimeter and jacket as in Dewar Flasks. The temperature difference may be made as small as practicable but will change during the reaction period. This is overcome by the next method to be described.

(ii) Adiabatic Method

By making the temperature difference between the calorimeter and jacket as small as possible, most of the heat exchange between the calorimeter and jacket is eliminated. This is quite useful since in both methods (i) and (ii) the "corrected temperature rise" needs to be calculated. This requires a "fore" and "after" rating period to establish the rate of change of temperature of the calorimeter due to heat exchange, heat of stirring and evaporation losses. These corrections may be quite large for method (i), especially when slow reactions are involved, so that adiabatic control may be the natural choice in such cases. It has been pointed out, however, (12) that for fast reactions the constant temperature environment calorimeter may be preferable.

(iii) Heat-Leak Calorimeters

Instead of eliminating heat-leakage, this class of calorimeter employs the phenomenon to evaluate heats of reaction. The calorimeters of Calvet (13) and Kitzinger and Benzinger (14) are typical examples which have been extensively used. Essentially, the heat of reaction is measured by plotting the difference in temperature of the calorimeter and jacket against time and integrating graphically:

$$\frac{dq}{dt} = K(T - Tj)$$

where T, Tj are the temperature of the calorimeter and jacket respectively, K is a constant, $\frac{dq}{dt}$ = heat flow with respect to time.

$$\therefore \quad dq = K(T - Tj)dt$$

$$\Delta q = K \int_{t_1}^{t_2} (T - Tj)dt$$

After suitable calibration, Δq is the heat of reaction between t_1 and t_2.

(iv) Twin Calorimeters

If two calorimeter vessels are constructed so that they are as nearly identical as possible and if simultaneous measurements of temperature are made on the vessels in the same environment, a number of advantages are obtained. Almost the whole error due to heat leakage is eliminated and, most important, differential observation is possible by the use of thermocouples, which can be very precise temperature transducers. Differential observation permits the use of a twin system as a scanning calorimeter since the continuous rise in temperature of the scanning system need not be recorded as the ordinate of a graph. The ordinate in this differential process should only depend on the chemical reaction occurring in the calorimeter. This is the basis of differential thermal analysis (DTA)(15), and also of a quantitative scanning calorimeter described by Arndt and Fujita (16). For future reference, the title of "scanning calorimeter" will be applied to a calorimeter designed to undergo a steady temperature rise, or fall, in addition to any such change caused by the heat of reaction.

Isothermal Calorimeters

(i) Labyrinth Flow

In this type, heat is removed from, or added to, the calorimeter by a rapid flow of thermostatted liquid which surrounds the calorimeter. The heat of reaction is estimated by measuring the temperature change of the liquid after passing round the calorimeter. This is properly classified as isothermal since the temperature of the calorimeter is not recorded, in addition to the isothermal operation of the calorimeter. More details are given elsewhere (17, 18).

(ii) Phase Change Calorimeters

This classic type of isothermal calorimeter measures heat effects by the extent of an isothermal phase change produced in the calorimeter. Very precise measurements are possible with this technique and it has several advantages over the non-isothermal type. The heat leak is clearly minimal due to the isothermal nature of the calorimeter and this permits its application to very slow reactions or small heat effects. Among the calorimetric liquids which have been used are ice (fusion), diphenyl ether (fusion), napthalene (fusion) and ammonia (vaporisation). By attaching a fine-bore capillary to the liquid reservoir, the sensitivity of the apparatus is greatly increased. Sensitivity is also increased by using calorimetric liquids with small heats of transformation or which undergo a large volume change during the transformation.

(iii) Temperature Controlled Calorimetry

In this relatively new technique (11), temperature control is maintained by subjecting the calorimeter to various heat flow rates. As in the phase-change calorimeter, temperature is the controlled variable and enthalpy, or its derivative, is the dependent, measured variable. Integration of the heat flow rate with respect to time gives the total heat effect. As in the case of the phase-change calorimeter this method may be used for slow reactions due to the lack of necessity of rating periods, although these are often used. Also, the system may be made extremely small - the only requirement, in addition to a calorimeter vessel, being a temperature controlled surface.

The system lends itself to scanning calorimetry after certain modifications. Clearly, in operating a scanning calorimeter, heat has not only to be supplied for temperature control between the calorimeter vessel and its surroundings but also to raise the temperature of the whole assembly. This is overcome (11) by twin-calorimeter operation. Separate circuits control the temperature of the assembly and the temperature difference between the two calorimeters. In this way the enthalpy change is easily detected, whereas it would not be if superimposed on the heat required for equilibration of the whole assembly. This procedure effectively eliminates spurious effects due to heat losses from the calorimeter which would greatly modify the heat flow rate in the absence of twin operation.

Non-isothermal calorimetry is not suitable for scanning calorimetry for several reasons. Firstly, the technique would become very lengthy because of the large thermal lag of the system. Adiabatic control would only aggravate the situation due to the larger physical size of the enclosure and its consequent higher lag. Rapid temperature increase would give rise to intolerable temperature gradients within the calorimeter enclosure. Adiabatic calorimetry can not cancel the background heat flow since the sample and reference calorimeter temperatures would be neither equal nor reproducible, by virtue of the fact that temperature is the measured variable and is a function of the heat of reaction and heat capacity. It is also extremely difficult to modify an adiabatic calorimeter to scan down in temperature; this precludes the study of reversible phenomena.

Differential isothermal calorimetry is not subject to these limitations. The system is inherently fast and exothermic reactions are studied as easily as endothermic ones simply by decreasing the flow of heat from the temperature controlled surface during such a reaction. The Perkin-Elmer DSC-1 is an example of a differential temperature-controlled twin calorimetric system. Its performance has been examined in detail by O'Neill (11) who has shown that such a calorimeter is ideally suited to the study of sharp transitions. A quantitative instrument which is essentially temperature controlled has been described by Speros and Woodhouse (19). Its operation would not appear to be as convenient as the DSC-1 and, in addition, heats of fusion are the only data which have been obtained with this instrument.

Transition Metal Complexes

The thermochemistry of transition metal complexes has received considerable attention. Many techniques have been used, including direct thermochemical measurements.

Some typical examples are listed in Table 1.

Table 1

Method and application	Author and numerical reference
Direct calorimetry, Cobalt II-ammines	K.B. Yatsimirskii and L.L. Pankova (20).
Direct calorimetry using Calvet calorimeter-pyridine complexes of Cobalt(II)	S.J. Ashcroft, G. Beech and C.T. Mortimer (21).
Argentometric determination of equilibrium constants for thiocyanate complexes. Stepwise heats of reaction	K.G. Poulsen et al. (22).
Determination of equilibrium constants for metal chelates over temperature range by e.m.f. method	A.E. Martell (23).
Spectro-photometric determination of equilibrium constants for copper II complexes	S. Cabani et al. (24).
Bomb calorimetry of metal chelates	J.L. Wood and M.M. Jones (25).

The heats of reaction yield valuable information on the relative donor strengths of co-ordinated groups (normally termed "ligands"). Various authors (26, 27) have correlated such factors as ion size, stereochemistry and ligand type with thermodynamic data. George and McClure (28) have observed the effects of inner-orbital splitting on the

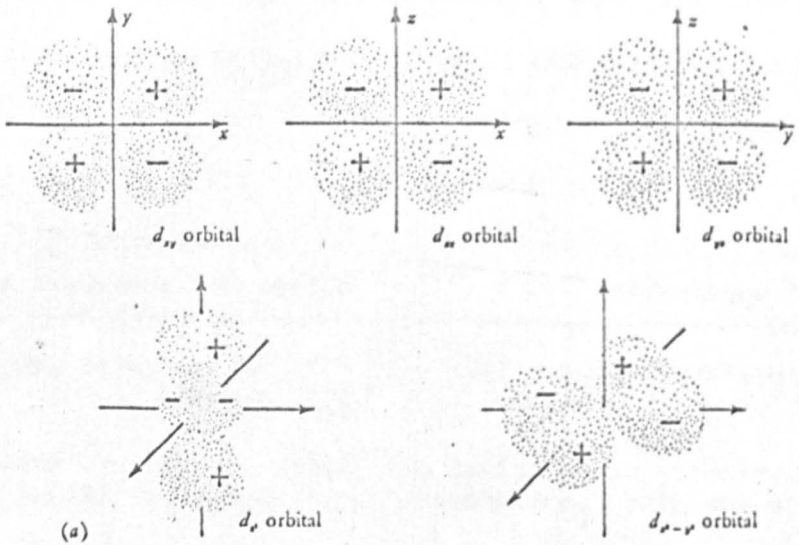

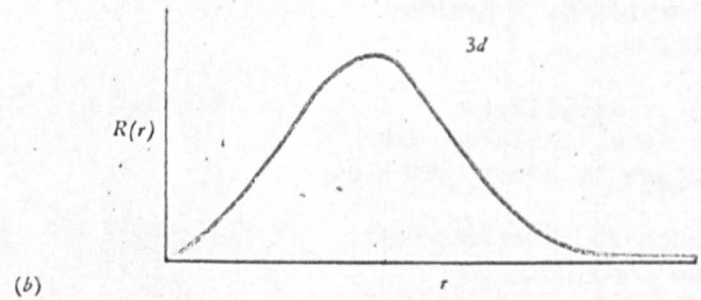

Figure (1) (*a*) Boundary surfaces of the *d* orbitals. (*b*) Plot of $R(r)$ vs. r for a $3d$ orbital.

thermodynamic properties of co-ordination compounds. Inner orbital splitting will be discussed in the following section.

The present work sought to establish, from thermochemical data, the effects of the following on the strengths of metal-ligand bonds:

(i) Steric hindrance between the ligands.

(ii) Ligand basicity

(iii) The relative importance of σ- and π-bonding in metal complexes.

(iv) Inner orbital splitting.

Effect (iv) necessitates some amplification and is dealt with, briefly, below. It is necessary to give a short account of the background theory so that certain symbols and parameters may be defined.

Crystal Field Theory

Crystal field theory is a purely electrostatic theory which describes how the energies of atomic orbitals change when a co-ordination compound is formed. We shall only be concerned with complexes of the first transition series metals - those with partly filled 3d electron shells. The d orbitals have characteristic shapes, as shown in Figure (1). By placing ligands at the corners of an octahedron, the axes along which the $d(x^2-y^2)$ and dz^2 orbitals lie are defined as the metal-ligand axes.

Let us consider the simplest case of a positive ion with one d-electron. The orbitals which this electron may occupy fall into two classes; the dz^2 and $d(x^2-y^2)$ which point towards the ligands and the dxy, dxz and dyz which point between the ligands. The bringing up of the six ligands towards the ion has the following effects:-

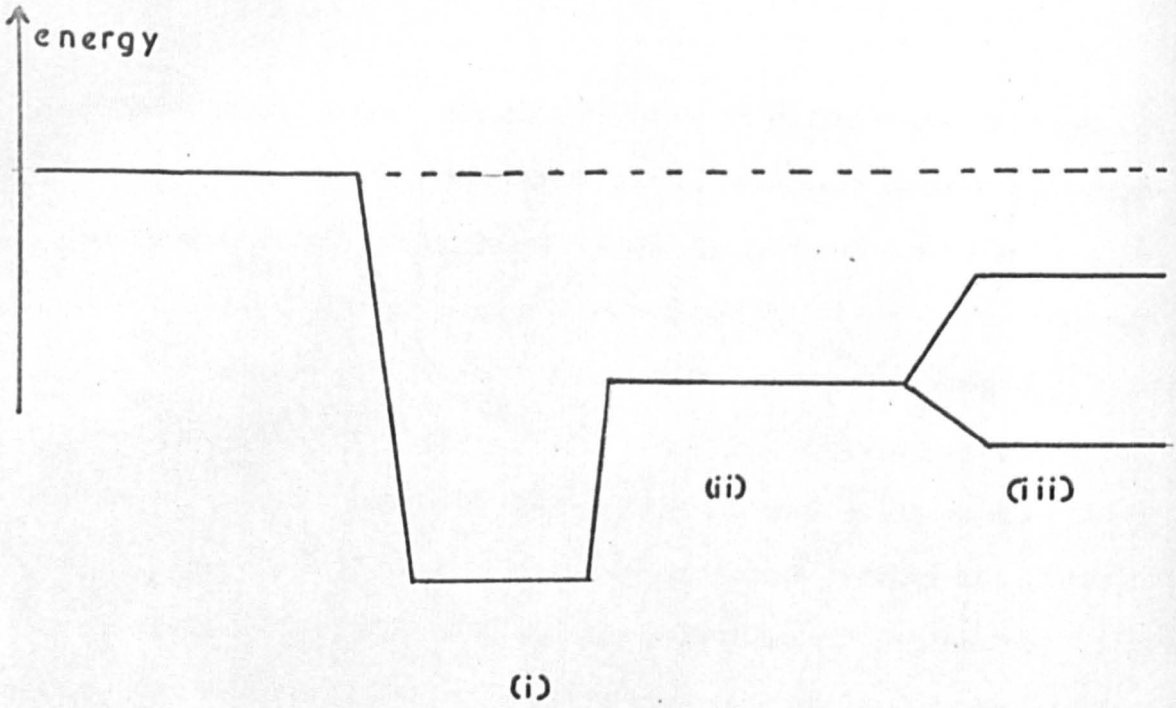

Fig 2 (a)

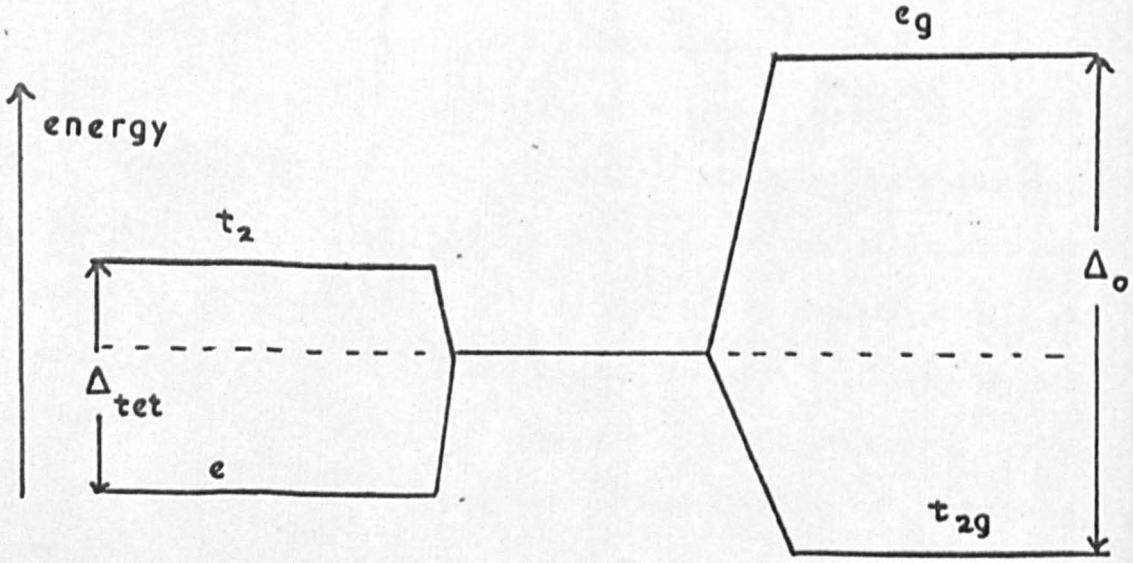

Fig 2(b)

(i) An initial lowering in the metal-ligand energy due to electrostatic attraction.

(ii) A raising of the energy due to electron repulsion between the ligands and between the ligand and central metal ion electron(s).

(iii) A raising in energy of the orbitals pointing towards the ligands (d_{z^2} and $d_{x^2-y^2}$) relative to those which point away from the ligands (dxy, dxz and dyz). The symbols e_g and t_{2g}, respectively, are usually applied to these two degenerate sets of orbitals. Other symbols have also been used (29).

The sequence (i), (ii) and (iii) is shown in Figure 2(a).

For a tetrahedral arrangement of ligands, the splitting pattern is inverted. The upper lying triply degenerate set of orbitals, is given the symbol t_2 and the lower doubly degenerate set the symbol e (see Figure 2(b)).

The magnitude of the splitting for octahedral complexes is typically 10,000 - 20,000cm^{-1} in the first transition series and is referred to as Δ_o or 10Dq. Δ_o is the experimental parameter while 10Dq is a mathematical abbreviation. The symbol Δ_{tet} is the experimental parameter used in tetrahedral symmetry and is about four-ninths of Δ_o for the same metal and ligands. For electron configurations other than d^1, d^5 or d^9, the situation is not so simple since for anything but a strong crystal field the occupation numbers of the t_{2g} and e_g, or t_2 and e, orbitals are not integral. Term wave functions must be considered and an example of the complicated splitting which tends

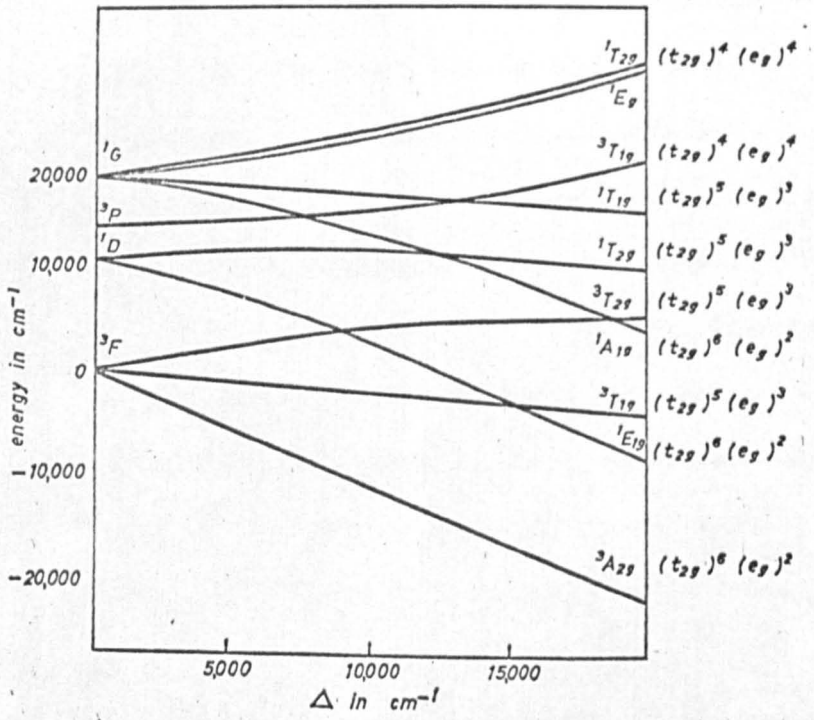

Fig. (3) Energy level diagram for a d^8 ion (Ni^{2+}). The ^1S state is at high energies and is omitted

to occur is shown in Figure 3 for the d^8 configuration (30). For strong cubic crystal fields, the terms are "sorted" into $t_{2(g)}^m \; e_{(g)}^n$ configurations. The first three d-electrons are fed into the t_{2g} set of orbitals (for an octahedral complex). The fourth may go into an e_g orbital or a t_{2g} orbital. The latter will be favoured if the splitting of the two levels is large enough to overcome the "energy of spin pairing" which occurs on double occupation of a t_{2g} orbital.

It may be shown that (31) the energies of the t_{2g} and e_g levels are $^2/_5\Delta_o$ and $^3/_5\Delta_o$ respectively, relative to the originally degenerate energy level (Figure 2(a)). It is a simple matter to calculate the crystal field stabilisation energy for d^n configurations and the results are shown in Table 2. The stabilisation is relative to the originally unsplit d^n energy level resulting from placing the six ligands in their equilibrium positions.

Table 2

Orbital Occupation	Crystal Field Stabilisation Energy
$t_{2g}^o \; e_g^o \; ; \; t_{2g}^3 \; e_g^2$	0
$t_{2g}^1 \; e_g^o \; ; \; t_{2g}^4 \; e_g^2$	$^2/_5\Delta_o$
$t_{2g}^2 \; e_g^o \; ; \; t_{2g}^5 \; e_g^2$	$^4/_5\Delta_o$
$t_{2g}^3 \; e_g^o \; ; \; t_{2g}^6 \; e_g^1$	$^6/_5\Delta_o$
$t_{2g}^3 \; e_g^1 \; ; \; t_{2g}^6 \; e_g^3$	$^3/_5\Delta_o$

If all the other quantities which contribute to the overall heat of formation of a complex compound are constant or vary smoothly in a predictable manner (for example the effective charge of the central ion) then any deviation of the heat of formation of the compound may be attributed to crystal field effects. In fact, it has been found (31) that plots of many thermodynamic properties against atomic number for the compounds of the elements scandium to zinc are neither linear nor smoothly varying but "double-humped".

The deviation from an interpolated baseline is attributed to crystal field stabilisation energy and comparison of crystal field parameters calculated from thermochemical and spectroscopic measurements have been made (31). This present work yields similar non-linear plots and these have been interpreted in terms of crystal field theory.


Gallenkamp
MADE IN ENGLAND

Figure 1 : Adiabatic Reaction Calorimeter

This photograph shows (left to right) the calorimeter can, adiabatic jacket and glass reaction vessel.

CHAPTER 2

2.1 Adiabatic Reaction Calorimeter

The calorimeter, originally designed for combustion calorimetry, was manufactured by A. Gallenkamp and Co. Ltd. (type C.B. 040, Fig. 1). It consists of an inner can, filled with water and containing the glass reaction vessel, and an outer water jacket surrounding the inner can. The temperature of the outer jacket automatically follows that of the inner can by measuring the two temperatures with thermistors which comprise two arms of a Wheatstone bridge. When the temperatures differ, an out of balance signal actuates a relay controlling the jacket heater. The response time of the system is shortened by the use of a cooling coil passing through the jacket.

The reaction vessel, of 400 ml capacity, was provided with a combined stopper and stirrer guide and had raised spikes to facilitate breakage of glass sample ampoules. These ampoules were fitted to the end of the stirring rod, which was driven through a flexible rubber coupling by a constant speed motor.

Temperature measurements were made with a platinum resistance thermometer (Cambridge, No. C.654287) in conjunction with a Smith's Difference Bridge (Cambridge, L303552) and a galvanometer.

Calibrations were performed electrically by using a non-inductively wire wound manganin heater powered by twelve 12V, 40amp.hr, lead accumulators wired in three parallel banks each containing four accumulators in series so that a potential of 48V was available.

Fig (2)

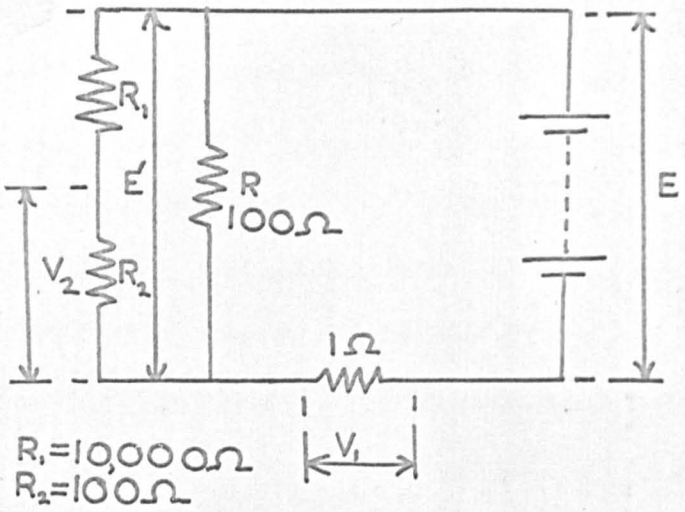

Fig (3)

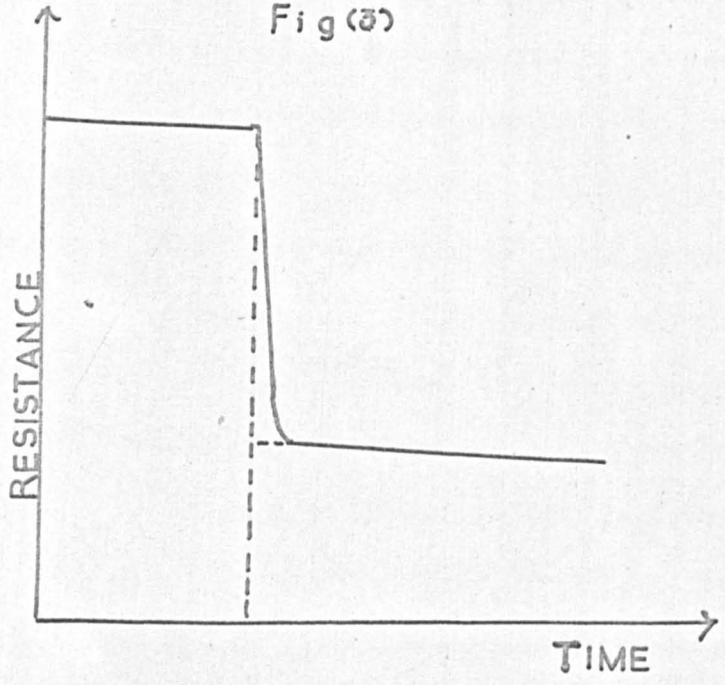

The accumulators were discharged through a dummy heater for 2 to 3 hours before use. The calibration heater (R) was wired in series with the 1Ω and in parallel with the series connected 10,000Ω and 100Ω resistors as in Figure (2).

From Figure (2), $V_2/E' = 100/10,100$

$$\therefore E' = 101V_2 \qquad (1)$$

If the current flow in the 10,100Ω branch is i and that in R is i':

$$i = V_2/100$$

and, $i + i' = V_1$

$$\therefore i' = V_1 - V_2/100 \qquad (2)$$

Equations (1) and (2) give the required current-voltage data. V_1 and V_2 were measured with a Pye precision vernier potentiometer (Pye and Co, Ltd.). The duration of current flow was determined by the use of a transistorized millisecond stopclock (Type T.S.A.4 Venner Electronics Ltd.).

Resistance-time readings were taken every two minutes before the reaction or calibration period and continued after this period until a linear rise or fall in temperature was attained. Ideally, the temperature change in these fore- and after- periods should be zero. The resistance change (ΔR) was evaluated from the resistance-time graph (Figure (3)) by extrapolation of the after period readings

to the commencement of the reaction period and subtraction of the two values.

Knowing the mass of sample, the temperature rise and the energy equivalent of the calorimeter, as determined by electrical calibration, the heat of reaction in Kcals. per mole could be calculated:

$$-\Delta H = E_s \times \Delta R \times \text{M.wt. of sample/wt. of sample(Kcals./mole)}$$

where, ΔR = increase in thermometer resistance (ohms.)

E_s = Energy equivalent in Kcals./ohm.

All measurements were made at approximately 25°C.

2.1.1 Adiabatic Reaction Calorimetry of the Cobalt Chloride, Triphenylphosphine System

The preparation of Dichlorobis (triphenylphosphine) cobalt (II) has been described together with many complexes of related ligands (32, 33). The magnetic moment (4.51 BM) and ultraviolet spectrum of the compound indicate that the local symmetry around the cobalt atom is tetrahedral.

Previous reports of the preparation have given the melting point of the compound as 247-51°C (32) and 231-232°C (33) whereas the compound reported here (see Experimental) has a melting point of 237-239°C. The precise melting point, which is accompanied by decomposition, appears to be a function of the rate of temperature increase and no definite conclusions may be drawn from these figures. Many other phosphine complexes exhibit a similar behaviour.

Procedure

All the reactions were initiated by crushing a thin-walled glass ampoule containing the reactant into the relevant solution. The ampoules were sealed by heating the neck in a gas-oxygen flame after cooling the sample area in liquid nitrogen. The sealed ampoules were attached to the stirrer by a small amount of "Araldite".

The samples were weighed to an accuracy of 2μg and enough sample used to give a measurable temperature change (a change of at least 0.001Ω in the thermometer resistance was achieved).

Since heats of solution are normally concentration dependent, it was desirable to use similar amounts of solutes to those formed in the heat of reaction measurements for the solution measurements. That is, if x gms. of product were formed during reaction then x gms. of that product should be taken to measure the heat of solution. This approach was limited, however, by solubility restrictions.

Calibrations were performed, as previously described, after each reaction in order that the calibration constant should be relevant to the reaction being studied. This was not possible for reaction (1) due to fluctuation of the power supply and the average constant from reaction (2) was used.

After each reaction, it was necessary to ensure that no solid remained from, for example, incomplete ampoule breakage. A visual inspection was adequate for this purpose and in no instance was any solid observed.

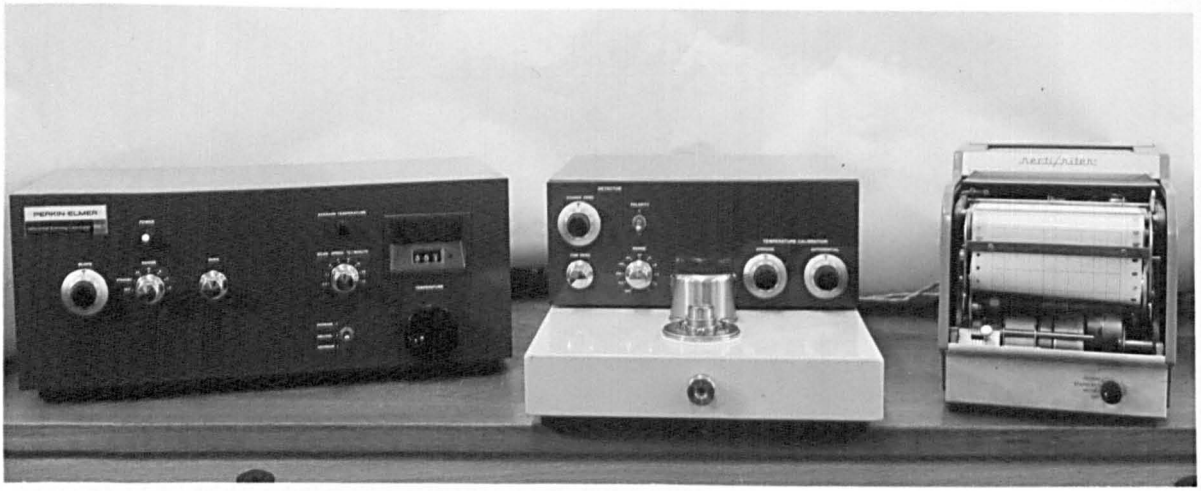
PERKIN ELMER


1
2
3
4
5
6
7

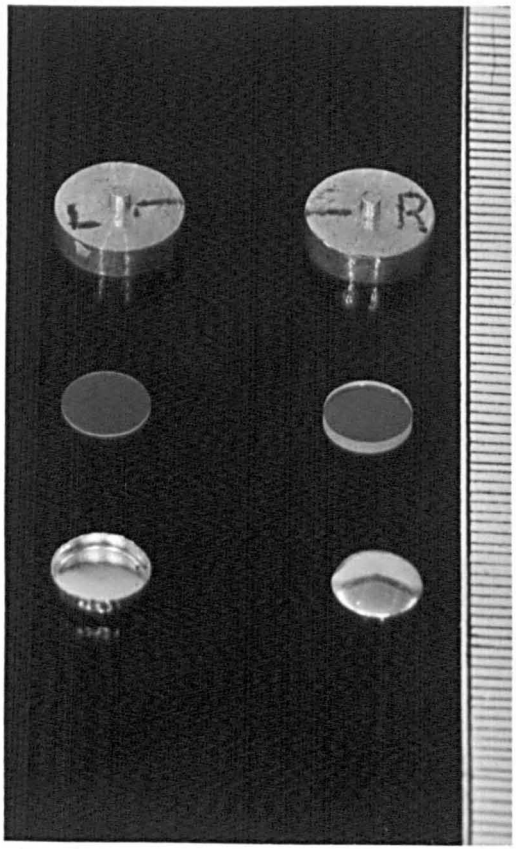
L1
L1R

Figure 4 : Differential Scanning Calorimeter

Top

General view showing (left to right) the control unit, analyser and recorder.

Bottom Left

Close up of sample holder assembly showing sample and reference cups with centimetric scale for comparison.

Bottom Right

This photograph shows some of the specially designed accessories for the DSC-1. At the top is shown a pair of sample holder covers for heat capacity measurements. In the middle are the synthetic sapphires used for heat capacity calibration. At the bottom there is a sample pan with the "domed" cover mentioned in the text. A centimetric scale is shown to the right for comparison.

The heats of the following reactions were determined; the data obtained are summarised in tables (1) to (4) of Chapter 3.

$$CoCl_2.6H_2O_{(cryst.)} + (2.Ph_3P, 563EtOH)_{(liq.)} \rightarrow (Co(Ph_3P)_2Cl_2, 6H_2), 563EtOH)_{(liq.)} \quad (1)$$

$$2\,Ph_3P_{(cryst.)} + 563EtOH_{(liq.)} \rightarrow (2\,Ph_3P, 563EtOH)_{(liq.)} \quad (2)$$

$$6H_2O_{(liq.)} + 563EtOH_{(liq.)} \rightarrow (6H_2O, 563EtOH)_{(liq.)} \quad (3)$$

$$Co(Ph_3P)Cl_{2(cryst.)} + (6H_2O, 563EtOH)_{(liq.)} \rightarrow (Co(Ph_3P)_2Cl_2, 6H_2O, 563EtOH)_{(liq.)} \quad (4)$$

2.2 Differential Scanning Calorimeter

The calorimeter (model DSC-1) is manufactured by the Perkin-Elmer Corporation for the purpose of recording enthalpy changes accompanying physical or chemical changes in a substance while the temperature of the substance is increasing or decreasing at a linear rate. With the DSC-1, the available rates of heating or cooling (scanning speeds) are 0.5, 1, 2, 4, 8, 16, 32 and 64^{o}K per minute. The temperatures of the sample and reference holders are raised by small electrical heaters embedded within them. Temperature control is achieved by two Wheatstone bridge circuits. The first compares the resistance of the sample and reference sensors, also embedded in the sample holders, with a variable resistance, the value of which changes at a rate proportional to the selected scanning speed. When the

temperature of the holders becomes greater or less than the programme temperature, the error voltage from the bridge is amplified and according to its polarity is added to, or subtracted from, the heater supply voltage. The second circuit compares the resistance of the sample sensor with that of the reference sensor. If the ratio of these resistances is equal to the ratio of the resistances in the other arm of the bridge, there will normally be zero output voltage. When the sample temperature changes, due to a reaction occurring, the sensor resistance changes and an error voltage appears at the bridge output. This is amplified and, depending on the polarity of the voltage, is supplied through one of two diodes to one of the two heaters until the bridge output is once more zero and temperature balance reattained.

The first circuit is seen to control the average temperature of the sample holders while the second supplies differential power to the sample holder heater. This differential power is amplified by the readout amplifier and finally presented on a 5ma recorder (Texas Instrument Inc.). Since the ordinate is proportional to the rate at which power is supplied to the sample and the abscissa is proportional to time then integration of the pen deflection gives the total energy change in the time interval studied. This is achieved by measuring the area of the peak obtained during some reaction period. Sensitivities of 2, 4, 8, 16 and 32 milli calories per second per full scale deflection are available.

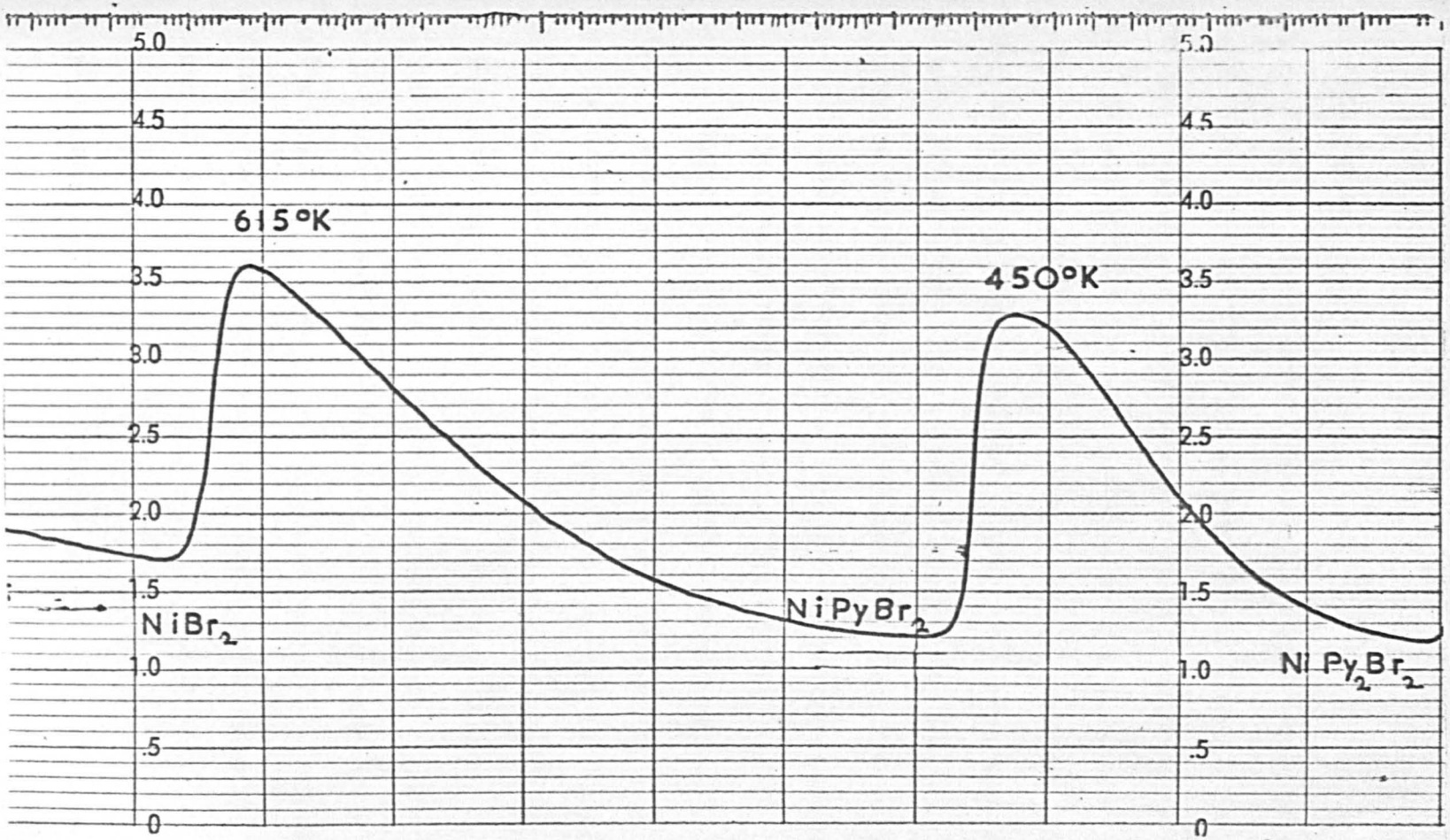

Fig(5)

Thermogram of the thermal decompositition of $NiPy_2Br_2$

The instrument was calibrated by using the heat of fusion of indium as a standard quantity. Indium is available in very high purity (99.999% in this work) and its heat of fusion has been determined to a high degree of accuracy (34). The melting point of indium ($429^{o}K$) was used for temperature calibration. Peak areas were measured with a planimeter (ALLBRIT) to a reproducibility of 1%.

A typical thermogram obtained with the DSC-1 is shown in Figure 5 with all necessary information.

2.2.1 Sample Handling

Samples, normally solids, were enclosed in small pans of 5.5 thousandths of an inch thick aluminium. Lids of the same material were placed over the samples and either "crimped" down tightly with a press or allowed to rest loosely on top. The latter procedure, using slightly domed lids, was favoured since, if gas evolution occurred during or after fusion, the molten sample tended to be forced out from the small available space of the crimped pan. A small number of platinum pans were manufactured for use in highly corrosive systems.

Sample weights were normally 5 to 10 mg and were weighed on an electromicrobalance (EMB-1) manufactured by the Research and Industrial Instruments Company. The weight loss of the sample after thermal decomposition was also noted so that the progress of the reaction could be checked. With compounds having well defined

decomposition paths, this provided a routine purity check. The progress of the decomposition was also noted by using the gas evolution detector of the calorimeter but was found to give only semi-quantitative information.

All decompositions were carried out in an atmosphere of dry nitrogen which passed through the sample enclosure at a rate of 30 ml per minute. It was particularly important to use dry gas at temperatures less than ambient since traces of moisture quickly cause precipitation on the sample holders at low temperatures. These temperatures were attained by the use of a sample holder assembly cover containing liquid nitrogen.

This cover was found to be useful in achieving intermediate temperatures (e.g. $-10^{\circ}C$ to $0^{\circ}C$) by placing it on top of the normal assembly cover. Excessive condensation was avoided in this way but temperatures low enough for collection of easily condensable products of decompositions were obtained. The condensed products, either solid or liquid, were collected from the cover and their infrared spectra recorded. This was most useful in providing proof of the nature of the products of decomposition.

Air sensitive complexes, such as those of iron (II) and chromium (II) were handled in nitrogen.

2.2.2 Measurements of Heat Capacities with a Differential Scanning Calorimeter

The ordinate read-out of the instrument represents the differential heat flow to the sample which, after calibration, may be expressed in calories per second. The heat flow is proportional to the time derivative of the enthalpy of the sample:

$$D(\text{deflection}) = K\frac{dH}{dt} \quad (K \text{ is a constant})$$

$$\text{or} \qquad D = K\frac{dH}{dT}\cdot\frac{dT}{dt} \quad T \text{ is the sample temperature}$$

$$\therefore \qquad D = K\, n_{(i)}Cp_{(i)}\frac{dT}{dt}$$

n_i = number of moles of substance, i

$Cp_{(i)}$ = heat capacity of i.

Knowing the sensitivity of the instrument and, hence, D/K in millicalories per second, $Cp_{(i)}$ could, in principle at least, be calculated.

However, the scanning rate is not quite linear and so the ordinate deflection is temperature dependent to a small extent. This does not in any way affect peak area measurements since the time axis will be lengthened or shortened accordingly.

To eliminate this error, a standard compound having a known heat capacity may be run under the same conditions as the sample. By taking the ratios of the respective deflections, $^{dT}/_{dt}$ and k cancel to leave a simple heat capacity ratio. The deflections are measured relative to a baseline obtained with an empty pan. In order that these measurements refer only to the heat capacities of the sample

pan contents it is essential that heat losses from the holders are reproducible for each run. This was ensured by placing tightly fitting covers over each holder, each cover having a location mark. It was found that removal of the protective disc from the holder assembly gave more reproducible results since the air gap from each holder to the outer cylinder of the assembly was increased. Small errors in positioning of the covers then caused a minimal change in temperature gradient. The practical details of the method are as follows:

(1) An empty pan is placed in a sample holder and the holder covers placed in position.

(2) An isothermal baseline is recorded for a few minutes and the selected temperature and sensitivity.

(3) Scanning is started at 8° or 16°K per minute and continued for 40 - 50°K.

(4) An isothermal baseline at the higher temperature is recorded. This baseline level should not differ from that at the lower temperature by more than ±5%. If it does, the procedure is repeated with varying instrument parameters until the optimum conditions are found.

(5) The procedure is repeated, using the same sample pan with the sapphire and sample respectively. The heat capacity of sapphire has been determined with great accuracy (35).

(6) The higher temperature isothermal baseline is extrapolated back to the temperature attained at the end of the scanning period and a

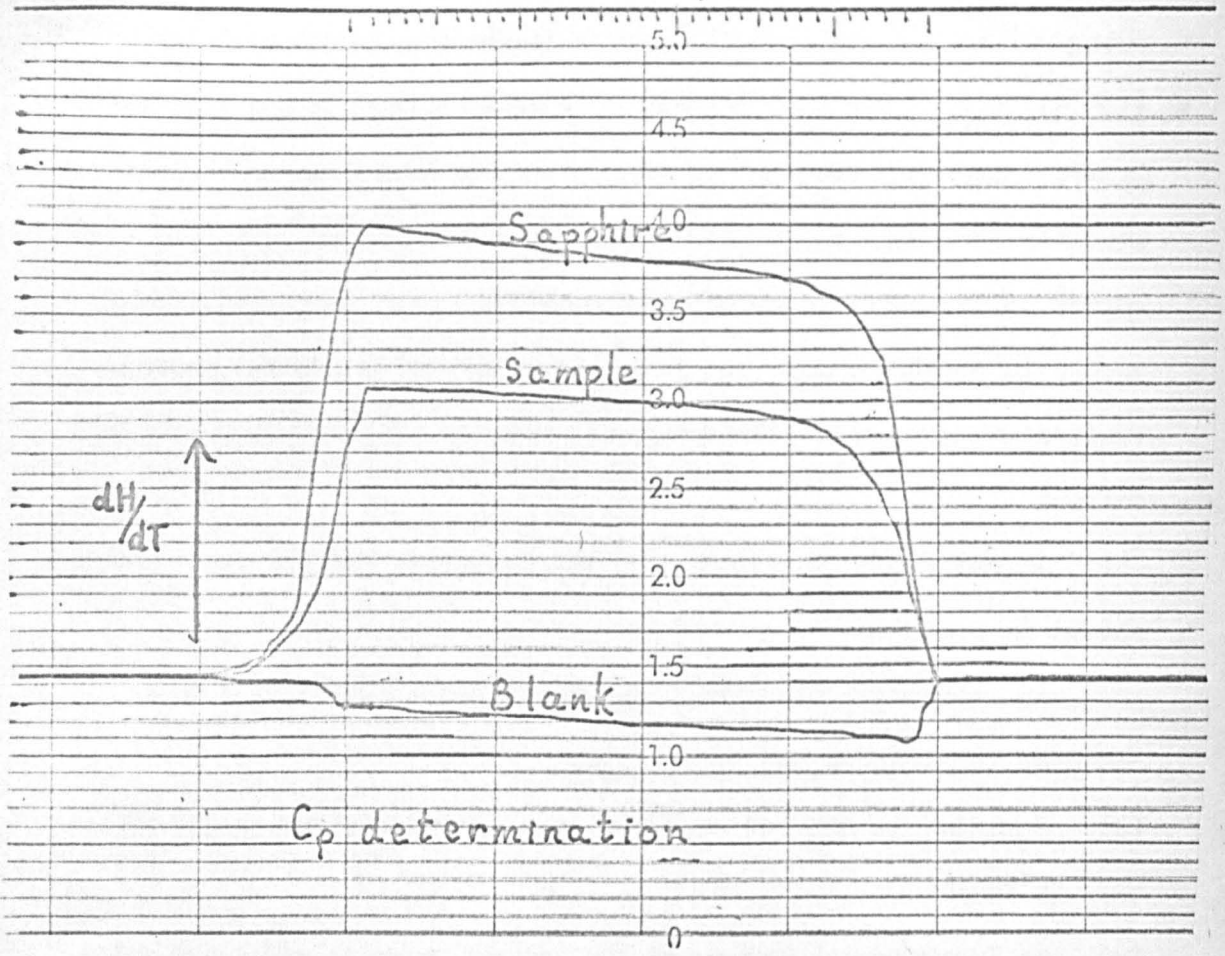
5.5
4.5
4.0
3.5
3.0
2.5
2.0
1.5
1.0
0
Sapphire
Sample
Blank
dH/dT
Cp determination

Fig (6)

baseline drawn between this point and the point on the low temperature isotherm where scanning commenced. The pen deflections for each of the runs are measured at selected temperatures and converted into heat capacities by the equation:

$$D/_{D'} = n\,Cp/_{n'Cp'}$$

where D and D' are the measured pen deflections from the "no-sample" baseline. A typical set of results are shown, superimposed, in Figure (3).

The measurements are repeated over various temperature ranges until sufficient data are obtained.

Heat capacities of polyethylenes have been determined by Wunderlich and Dole in a similar manner and shown to be in good agreement with values calculated from infra-red spectral assignments (36). Heat capacities of gold, nickel and a nylon resin, as determined with a DSC-1, have also been reported (37).

2.2.3

(a) <u>The relation of the total enthalpy change measured over a temperature range to the enthalpy change at a particular temperatur</u>

For the reaction

$$A_{(cryst.)} \rightarrow B_{(cryst.)} + C_{(gas)}$$

let the symbols below characterise the following properties of the system:-

ΔH_{T_i} = Heat of reaction at temperature T_i signifying start of decomposition.

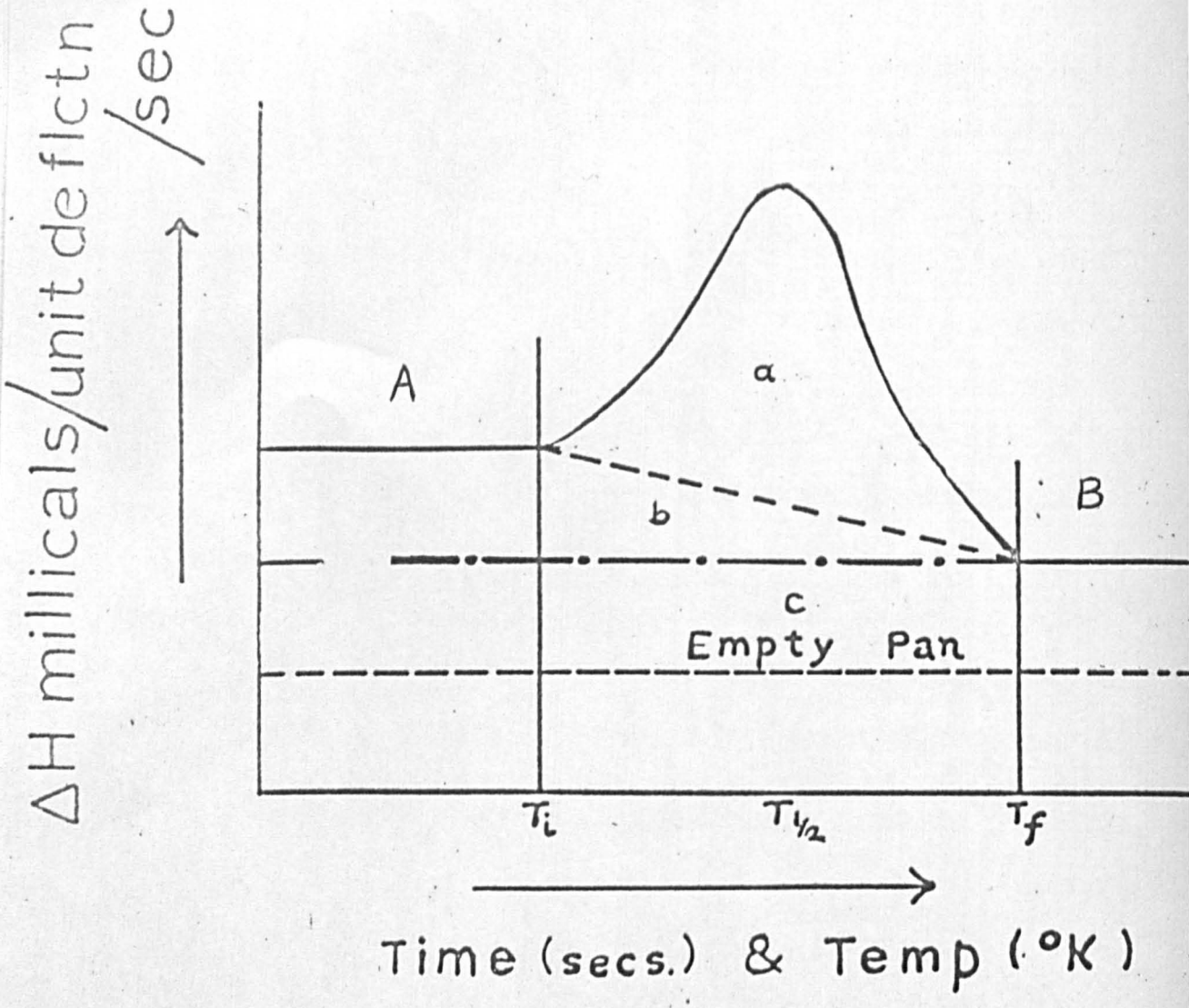
ΔH millicals/unit deflctn /sec
A
a
b
B
c
Empty Pan
T_i
$T_{1/2}$
T_f
Time (secs.) & Temp (°K)

Fig(7)

$\Delta H_{T_{\frac{1}{2}}}$ = Heat of reaction at temperature $T_{\frac{1}{2}}$ midway between T_i and T_f, the latter signifying end of decomposition.

$Cp_{(A)}$, $Cp_{(B)}$, $Cp_{(C)}$ = heat capacities of A, B and C respectively.

$\Delta Cp = (Cp_{(B)} + Cp_{(C)} - Cp_{(A)})$

The general appearance of such a decomposition thermogram is shown in Figure (7). c is the area enclosed by the extrapolated line representing the heat capacity of B and an "empty pan" baseline i.e. it represents the heat required to heat one mole of B from T_i to T_f. The whole area a + b + c represents the heat required to carry out the decomposition in which C is continually evolved. If the evolution is symmetrical about $T_{\frac{1}{2}}$, i.e. as much C is evolved before $T_{\frac{1}{2}}$ as it is after $T_{\frac{1}{2}}$, then the process may be simplified to one having the same energy change but simpler steps:

(1) Decompose A at T_i isothermally (ΔH_{T_i})

(2) Heat B from T_i to T_f ($Cp_{(B)}(T_f - T_i) = C$)

(3) Heat C from T_i to $T_{\frac{1}{2}}$ ($Cp_{(C)}(T_{\frac{1}{2}} - T_i)$)

$$\therefore \quad a + b + c = \Delta H_{T_i} + Cp_{(C)}(T_{\frac{1}{2}} - T_i) + c$$

$$a + b = \Delta H_{T_i} + Cp_{(C)}(T_{\frac{1}{2}} - T_i)$$

but from Figure (6) if the heat capacities are independent of temperature

$$b = \tfrac{1}{2}(Cp_{(A)} - Cp_{(B)})(T_f - T_i) = (Cp_{(A)} - Cp_{(B)})(T_{\frac{1}{2}} - T_i)$$

$$\therefore \quad a = \Delta H_{T_i} + (T_{\frac{1}{2}} - T_i)(Cp_{(C)} + Cp_{(B)} - Cp_{(A)}) \qquad (1)$$

$$\therefore \quad a = \Delta H_{T_i} + (T_{\frac{1}{2}} - T_i)\Delta Cp$$

$$\therefore \quad a = \Delta H_{T_{\frac{1}{2}}} \qquad (2)$$

If the evolution is not symmetrical but is more or less linear, as is more normal, equation (1) should contain an additional term of $Cp_{(C)}(T_x - T_{\frac{1}{2}})$ since half of C will not be evolved until some higher temperature T_x and equation (2) becomes:

$$a = \Delta H_{T_{\frac{1}{2}}} + Cp_{(C)}(T_x - T_{\frac{1}{2}})$$

At some temperature T_y ($T_y > T_x > T_{\frac{1}{2}}$):

$$\Delta H_{T_y} = \Delta H_{T_{\frac{1}{2}}} + \Delta Cp(T_y - T_{\frac{1}{2}})$$

when $a = \Delta H_{T_y}$:

$$Cp_{(C)}(T_x - T_{\frac{1}{2}}) = \Delta Cp(T_y - T_{\frac{1}{2}})$$

$$T_y = \frac{Cp_{(C)}}{\Delta Cp}(T_x - T_{\frac{1}{2}}) + T_{\frac{1}{2}} \qquad (3)$$

For an idealised case in which C is evolved at a linear rate from T_i to T_f it is simple to prove that:

$$T_y - T_i = \sqrt{2}(T_{\frac{1}{2}} - T_i)$$

It is seen, therefore, that the measured area (a) represents the heat of reaction at some temperature slightly above $T_{\frac{1}{2}}$. The exact calculation of this temperature requires not only the form of the equation representing the rate of gas evolution but also $Cp_{(C)}$ and ΔCp. These terms are strictly also temperature dependent so that the equations preceding (1), (2) and (3) should contain integration terms rather than the simple ΔCp term.

The most characteristic temperatures of a thermogram are T_i, T_f and T_p where T_p is the temperature at which the rate of gas evolution and, hence, of reaction is a maximum. These parameters are quoted in

all the data relating to decompositions and no attempt has been made to calculate T_y. Clearly, T_y should lie somewhere between $T_{\frac{1}{2}}$ and T_p but, since the reactions all proceed at relatively high temperatures the uncertainty is quite small and unlikely to be more than 10^o - 20^oK in several hundred degrees.

(b) Relation of ΔH at a high temperature, T, with ΔH at some standard temperature T^o (usually 298^oK)

The relation between these two quantities is normally obtained by the Kirchoff Equation :-

$$\Delta H_T = \Delta H_{T_o} + \int_{TO}^{T} \Delta Cp dT$$

ΔCp is the change in heat capacity for the reaction, i.e.

Σ Cp(products) - Σ Cp(reactants), and is normally temperature dependent to some extent since the heat capacity of a substance is usually given by an equation such as:

$$Cp = a + bT + cT^{-2}$$

Correction of the observed heats of reaction, obtained by use of the Differential Scanning Calorimeter, to 298^oK therefore requires values for the heat capacities of reactants and products. Some heat capacities have been measured with the calorimeter and the corrections calculated in Chapter 4.

2.2.4 An Assessment of the Performance of the Differential Scanning Calorimeter

It was thought to be necessary to check the performance of the DSC-1 by using substances of well defined thermochemistry before proceeding to make measurements of thermal data not previously reported. Speros and Woodhouse (19) used the heats of fusion of several substances to check the performance of their quantitative differential thermal analyser. Since decomposition has been the process studied in this work it was also necessary to measure the heats of some decomposition processes in order to be sure that the instrument was capable of giving good results when used for studying either fusion or decomposition. The selection of suitable starting compounds was subject to the limitations that, firstly, they should be available in high purity and, secondly, that the heats of formation of both the starting compounds and products of decomposition should be well-known. In addition, the decomposition necessarily had to be within the range of temperatures available (-100 to +500^{o}C). The substances chosen were:

(1) Copper sulphate pentahydrate (> 99.9%)

(2) Calcium sulphate dihydrate (> 99%)

(3) Sodium bicarbonate (> 99.5%)

(4) Sodium dihydrogen phosphate (> 99%)

(5) Metallic lead (> 99.9%)

All compounds were of "Analar" quality.

(1) Copper Sulphate Pentahydrate

The compound decomposes in two stages, yielding firstly the monohydrate and then the anhydrous salt. The enthalpy change for each stage was found to be 51.1 ± 0.6Kcals. and 17.3 ± 0.2Kcals. at the respective decomposition temperatures. The values calculated from Circular 500 (38) for the same reactions are 54.3 and 17.2Kcals. respectively at 25°C. Using approximate values of the heat capacities (Cp) of the various substances, it can be calculated, using the Kirchoff expression, $\Delta H_{T_2} - \Delta H_{T_1} = \int_{T_1}^{T_2} \Delta Cp dT$ ($\Delta Cp = \Sigma Cp$ products - ΣCp reactants), that the heats of reaction at room temperature are 0.1Kcals. and 0.2Kcals. greater than the values at the high temperatures at which the decompositions occur. This makes negligible difference to the original answers and agreement is seen to be quite good.

(2) Calcium Sulphate Dihydrate

A great deal of information has been obtained on the calcium sulphate-water system and much of it is very conflicting. An attempt has been made by Posnjak (39) and Kelley (40) to bring some order into the situation. Only one peak appeared in the thermogram so that only the various forms of the anhydrous salt need be considered. These are : Insoluble anhydrite

Soluble α-anhydrite

Soluble β-anhydrite

It is unlikely that the insoluble form is produced since Kelley (40) states that it is only formed in the presence of liquid water above 313°C

and is not formed in the dry state at "ordinary temperatures". It is presumed that these are greater than about 500°C although no definite temperatures are quoted. This leaves only the α and β-forms as possibilities and, using the data in Kelley's paper, the heat of reaction of gypsum being dehydrated to soluble α- or β-anhydrite is calculated to be 26.4 or 27.5Kcals. respectively (no uncertainties were attached to these latter figures). The value of 24.5 ± 0.6Kcals. obtained with the DSC-1 is seen to be similar to the values reported by Kelley and with a probable uncertainty of ±1Kcal. attached to his data agreement is quite good. The most recent value reported by any other worker for this reaction is 22.7 ± 0.5Kcals./mole (41). This worker also used a quantitative differential thermal analyser but employed much slower heating rates than those used in this work.

(3) Sodium Bicarbonate

At the temperature of decomposition, a heat of decomposition of 15.2 ± 0.1Kcals./mole of sodium bicarbonate was found for the reaction:

$$NaHCO_{3(cryst.)} \rightarrow \tfrac{1}{2}Na_2CO_{3(cryst.)} + \tfrac{1}{2}H_2O_{9g)} + \tfrac{1}{2}CO_{2(g)}$$

Circular 500 reports a value of 15.4Kcals. for this reaction at 25°C. The Kirchoff correction only amounts to -0.1Kcal. for correction to room temperature.

(4) Sodium Dihydrogen Phosphate

E. Calvet et al (42) have studied the thermal decomposition of sodium dihydrogen phosphate. In view of the similarity of their

technique to that used in this work, it was thought that the heat of this decomposition would provide a good test for the DSC-1. The data reported here are quite different from that of Calvet and are listed in Tables 53 to 56 of Chapter 3. There are no other independent sources of thermochemical data which may be used as a check on this heat of reaction and a considerable discrepancy still persists. An attempt was made to duplicate Calvet's work by operating at very slow scanning speeds (0.5°C/minute) but this did not bring about any better agreement.

(5) Metallic Lead

The heat of fusion of lead was measured and found to be 1.08 ± 0.02Kcals. The value quoted by Stull and Sinke (43) is 1.14Kcals. Both values refer to the heat of fusion at the melting point of lead.

It would seem that the differential scanning calorimeter provides data which are in adequate agreement with previously published values. These latter values were obtained, for the most part, by solution calorimetry. For the particular substances mentioned above, the Kirchoff integral, $\int_{T_1}^{T_2} \Delta C_p dT$, was very small. In some cases, however, this may be too large to be ignored and should be applied as a correction to the values obtained at elevated temperatures if comparison with room temperature calorimetry is required. Values of Cp for some compounds have been calculated in an attempt to correlate certain data and are discussed later.

2.3 Materials used in Experimental Work

(a) Metals:

Cobalt (Powder)	Koch-Light (99.5%)
Indium (Shot)	Koch-Light (99.999%)
Iron Filings	B.D.H. Laboratory reagent
Lead Foil	B.D.H. (Analar)

(b) Metal Salts:

Calcium chloride (hydrated)	Hopkin and Williams, general purpose reagent
Cadmium chloride (anhydrous)	B.D.H. Laboratory reagent
Calcium sulphate dihydrate	Imperial Chemical Industries Ltd. and Pilkington Bros. Ltd.
Cobalt chloride hexahydrate	B.D.H. (Analar)
Cobalt bromide (hydrated)	B.D.H. Laboratory reagent
Cobalt iodide dihydrate	B.D.H. Laboratory reagent
Copper (II) chloride dihydrate	May and Baker (reagent quality)
Copper (II) sulphate pentahydrate	B.D.H. (Analar)
Iron (III) chloride (anhydrous)	B.D.H. Laboratory reagent
Manganese chloride tetrahydrate	B.D.H. Laboratory reagent
Nickel chloride hexahydrate	B.D.H. (Analar)
Nickel bromide trihydrate	B.D.H. Laboratory reagent

Nickel iodide (hydrated)	B.D.H. Laboratory reagent
Sodium bicarbonate	B.D.H. (Analar)
Sodium dihydrogen phosphate dihydrate	B.D.H. (Analar)

(c) Ligands:

Aniline	B.D.H. Laboratory reagent (Redistilled b.pt. = 185°C)
* Pyrazine	Aldrich Chemical Company
* 2-Methylpyrazine	Ralph N. Emanuel Ltd.
* 2-,5-dimethylpyrazine	Kodak Ltd., Redistilled, b.pt. = 156°C
pyridazine	Koch-Light Ltd.
pyridine	B.D.H. (Analar)
2-Methylpyridine(α-picoline))	Redistilled from b.pt. = 128.1°C
3-Methylpyridine(β-picoline))	B.D.H. Laboratory b.pt. = 143°C
4-Methylpyridine(γ-picoline))	Reagent b.pt. = 143°C
Pyrimidine	Koch-Light Ltd.
s-Triazine	Aldrich Chemical Comaany
Triphenylphosphine	Koch-Light, recrystallised from absolute ethanol

Distillations were carried out on either a Fenske or Dufton column.

* Manufacturers' Analytical report supplied.

Abbreviations used to represent the ligands are:

py = pyridine

α-pic = α-picoline

β-pic = β-picoline

γ-pic = γ-picoline

An = Aniline

Pz = Pyrizine

Mp = 2-Methylpyrazine

Dmp = 2, 5-Dimethylpyrazine

Pmd = pyrimidine

Tz = triazine

The following compounds were prepared by Dr. L.F. Larkworthy (44) of The Battersea College of Technology:

Dichlorodipyridinechromium (II) $Crpy_2Cl_2$

Dibromodiaquodipyridinechromium (II) $Crpy_2(H_2O)_2Br_2$

Diiododiaquodip yridinechromium (II) $Crpy_2(H_2O)_2I_2$

Diiodotetrapyridinechromium (II) $Crpy_4I_2$

Dichlorobis (α-picoline) Nickel (II), $Ni(\alpha\text{-pic})_2Cl_2$ (45) was obtained from Dr. J.V. Quagliano of Florida State University, Tallahassee, Florida, U.S.A. and a sample of violet-Dichloro (2, 5-Dimethylpyrazine) Cobalt (II) (46) from Dr. A.B.P. Lever of the Manchester College of Science and Technology.

The other compounds used in this work were prepared by the methods given below. Where no reference is given after the compound it is believed that the preparation has not been previously reported. Several

2.4 Preparation of Compounds

A general method of preparation of some compounds of the type ML_2X_2 or ML_4X_2 was to mix a hot ethanolic solution of the hydrated metal halide with a similar solution of the appropriate base. In each case, the compound precipitated almost immediately and, after allowing to cool, was filtered. Compounds of the type ML_4X_2 (L = base, X = halogen) were not washed due to the ease with which they lost base to give compounds of the type ML_2X_2:

$$\text{Solvent} + ML_4X_{2(\text{cryst.})} = ML_2X_{2(\text{cryst.})} + 2L_{(\text{soltn.})}$$

The ML_2X_2 compounds were washed with ethanol orether. All the compounds were air dried at room temperature, followed by drying over anhydrous calcium chloride. The compounds prepared by this method were:

(1) Dichlorodipyridinemanganese (II) - $Mnpy_2Cl_2$

(2) Dichlorobis (β-picoline) manganese (II) - $Mn(\beta\text{-pic})_2Cl_2$

(3) Dichlorobis (γ-picoline) manganese (II) - $Mn(\gamma\text{-pic})_2Cl_2$

A previous report (47) of (1), (2) and (3) consisted of refluxing the base with the more appropriate halide.

(4) Dichlorodipyridinecobalt (II) - $Copy_2Cl_2$ (48)

The product was recrystallised from anhydrous acetone.

(5) Dichlorobis (α-picoline) cobalt (II) - $Co(\alpha\text{-pic})_2Cl_2$ (49)

(6) Dibromobis (α-picoline) cobalt (II) - $Co(\alpha\text{-pic})_2Br_2$ (49)

(7) Diiodobis (α-picoline) cobalt (II) - $Co(\alpha\text{-pic})_2I_2$ (49)

(8) Dibromodipyridinecobalt (II) - $Copy_2Br_2$ (49)

(9) Diiodotetrapyridinecobalt (II) - $Copy_4I_2$ (49,50)

(10) Dichlorotetrakis (β-picoline) cobalt (II) - $Co(\beta\text{-pic})_4Cl_2$ (49)

This compound was contaminated with the bis (β-picoline) complex and was converted entirely to the latter by heating at 100°C for one hour.

(11) Dibromotetrakis (β-picoline) cobalt (II) - $Co(\beta\text{-pic})_4Br_2$ (50)

(12) Dichlorotetrakis (γ-picoline) cobalt (II) - $Co(\gamma\text{-pic})_4Cl_2$ (49)

(13) Dibromotetrakis (γ-picoline) cobalt (II) - $Co(\gamma\text{-pic})_4Br_2$ (50)

(14) Diiodotetrakis (γ-picoline) cobalt (II) - $Co(\gamma\text{-pic})_4I_2$ (50)

(15) Diiodotetrapyridinenickel (II) - $Nipy_4I_2$ (51)

(16) Dichlorodipyridinecopper (II) - $Cupy_2Cl_2$ (52)

The following compounds were prepared by heating the appropriate halide with excess base, filtering the solution, and collecting the crystals formed on cooling. The complexes were washed with petroleum ether (60 - 80°C boiling range) and air dried. The calcium compound was very moisture sensitive and was dried in a stream of dry nitrogen.

(17) Dichlorotetrapyridinenickel (II) - $Nipy_4Cl_2$ (51)

(18) Dibromotetrapyridinenickel (II) - $Nipy_4Br_2$ (51)

(19) Dichlorotetrakis (β-picoline) nickel (II) - $Ni(\beta\text{-pic})_4Cl_2$ (51)

(20) Dichlorotetrakis (γ-picoline) nickel (II) - $Ni(\gamma\text{-pic})_4Cl_2$ (51)

(21) Dichlorodipyridinecalcium (II) - $Capy_2Cl_2$ (53)

The cadmium complex also involved a different mode of preparation:

(22) Dichlorodipyridinecadmium (II) - $Cdpy_2Cl_2$ (54)

Aqueous solutions of cadmium chloride and pyridine were mixed and the white solid collected. This was recrystallised from water containing about 2% pyridine.

Complexes of ferrous iron with pyridine and related ligands were prepared as follows:-

Aqueous ferrous chloride was prepared by shaking a solution of ferric chloride with iron filings in a flask fitted with a bunsen valve for several hours until a thiocyanate solution gave no test for ferric iron. A faster reaction resulted if a small amount of dilute hydrochloric acid was added to expose a fresh surface on the iron filings. The mixture was filtered and added to a very large excess of the amine through which nitrogen was passing. Yellow crystals formed in each case which were filtered, washed rapidly with ethanol and dried overnight in a current of nitrogen. The complexes thus obtained were:

(23) Dichlorotetrapyridineiron (II) - $Fepy_4Cl_2$ (55)

(24) Dichlorotetrakis (β-picoline) iron (II) - $Fe(\beta\text{-pic})_4Cl_2$ (56)

(25) Dichlorotetrakis (γ-picoline) iron (II) - $Fe(\gamma\text{-pic})_4Cl_2$ (56)

The pyrazine complexes were prepared by several different methods:

(26) Dichloropyrazinemanganese (II) - $MnpzCl_2$

The compound precipitated as a white solid on adding an ethanolic solution of pyrazine to a similar solution of the halide. The solid was washed with ethanol and air dried.

(27) Dichlorodipyrazineiron (II) - $Fepz_2Cl_2$

Aqueous ferrous chloride (see compounds (23) to (25)) was mixed with an aqueous solution of pyrazine. On warming a red solid precipitated. This was filtered, washed with ethanol and air dried.

(28) Dichlorodipyrazinecobalt (II) - $Copz_2Cl_2$ (57)

Pink crystals of the compound formed on mixing hot aqeuous solutions of the halide and pyrazine. These were washed with cold water, then ethanol and finally with ether.

(29) Dichlorotetrakis(methylpyrazine)cobalt (II))- $CoMp_4Cl_2$ (58)

Pink crystals deposit on recrystallising cobalt chloride hexahydrate from methylpyrazine. They were washed with petroleum ether (60 - 80°C boiling range) and air dried.

(30) Dichloro(2,5-Dimethylpyrazine)cobalt (II) - $CoDmpCl_2$ (58)

This intense blue compound was deposited on mixing ethanolic solutions of cobalt chloride hexahydrate and 2,5-dimethylpyrazine. The powder was washed with ethanol and air dried.

(31) Dibromodipyrimidinecobalt (II) - $Co(Pmd)_2Br_2$

The compound was obtained as pink crystals on mixing ethanolic solutions of the ligand and the halide. The crystals were filtered, washed with ethanol and air dried.

(32) Dichlorodipyrazinenickel (II) - $Nipz_2Cl_2$ (59)

Ethanolic solutions of the halide and the ligand were mixed to give a pale green precipitate. This was dissolved in aqueous ammonia and the resulting solution acidified with dilute hydrochloric acid. Pale green crystals on leaving the solution in a refrigerator overnight.

(33) Dibromodipyrazinenickel (II) - $Nipz_2Br_2$

This was not prepared by the method in reference (59) but by mixing ethanolic solutions of nickel bromide and pyrazine. The pale green precipitate was washed with alcohol and allowed to air dry.

(34) 2-Dichloro(2,5-dimethylpyrazine)nickel (II)-3-water

This was prepared in the same way as compound (32).

In addition to the compounds listed above, it was noted that complexes were also formed on mixing cobalt chloride, nickel chloride or cupric chloride with pyrimidine, pyridazine or s-triazine. The compounds so obtained showed no definite weight loss on heating but gave a black powder or the appropriate metal as the decomposition product. No further investigations were carried out on these compounds.

The aniline complexes were prepared by various methods which are listed below:

(35) Dichlorobisanilinemanganese (II) - $MnAn_2Cl_2$ (60)

White crystals of the ethanolate were deposited on mixing hot ethanolic solutions of the base and the halide. $MnAn_2Cl_2$ was prepared in situ for each run by heating the ethanolate to 350°K. Reference (60) reported the preparation of $MnAn_2Cl_2$ from anhydrous manganese (II) chloride and aniline. It was not found possible to duplicate this preparation and obtain a compound of the correct stoichiometry.

(36) Dichlorohexakisanilineiron (II) - $FeAn_6Cl_2$

Aqueous ferrous chloride was prepared as in preparation (23) and warmed gently while a stream of nitrogen was passed through. Very pale green crystals began to form which were filtered and used immediately. An aqueous solution of the crystals gave no test for ferric iron.

A few grams of the solid ferrous chloride were added to excess aniline through which nitrogen was passing continuously. The mixture was

warmed gently and stirred vigorously until a homogeneous white solid formed. This was filtered under nitrogen and washed quickly with petroleum ether (60 - 80° boiling range). The compound was dried overnight in a stream of nitrogen.

(37) Dichlorobisanilinecobalt (II) - $CoAn_2Cl_2$ (60)

Deep blue crystals of the complex deposited by allowing the solution obtained from refluxing the hydrated halide with aniline to cool slowly.

(38) Dichlorobisanilinenickel (II)-bisethanol - $NiAn_2Cl_2.2EtO$ (60)

The pale green solid, which precipitated on mixing ethanolic solutions of the base and halide, was filtered, washed with ethanol and allowed to air dry.

(39) Dichlorodianilinecadmium (II) - $CdAn_2Cl_2$ (60)

This was prepared in the same way as compound (38).

The preparation of Dichlorobis(triphenylphosphine)cobalt (II) has been reported previously (32, 33, 61)

(40) Dichlorobis(triphenylphosphine)cobalt (II) - $Co(Ph_3P)_2Cl_2$

Cobalt chloride hexahydrate was heated with a solution of triphenylphosphine in glacial acetic acid. On cooling, the solution deposited blue crystals of the compound. These were washed with ethanol and dried in a desiccator over phosphorus pentoxide.

2.5 Analysis of Compounds

In addition to weight loss data, microanalytical data were obtained for most of the complexes. In the case of the cobalt complexes, the percentage metal has been estimated spectrophotometrically by the following method:

Colorimetric estimation of Cobalt (62, 63)

Principle

The absorbing species is the strongly coloured thiocyanate complex. The optical density of the solution, assuming Beer's Law, is given by:

$$\log \frac{I_o}{I} = D = \varepsilon c l$$

where ε is the molecular extinction coefficient, c is the concentration in gram moles per litre and l is the path length in centimetres.

The ratio of two optical densities D and D' should correspond to solution concentrations, c and c', in the same ratio provided l and ε are constant for each solution.

Reagents

(1) Thiocyanate reagent

One hundred millilitres of 50% (weight/volume) aqueous ammonium thiocyanate solution were mixed with 900 mls of Analar acetone.

A standard cobalt solution was prepared by dissolving approximately 1mg cobalt metal (accurately weighed) in 2ml of dilute nitric acid and adding the thiocyanate reagent to give a total solution volume of 50mls. A similar solution was prepared with approximately 1.5mg cobalt.

Sample solutions were prepared in precisely the same manner, sample weights being chosen to give 1 to 1.5mg cobalt metal per 50mls of solution. The reference solution was prepared by taking 2mls dilute nitric acid and making the volume up to 50mls with the thiocyanate reagent.

Duplicate sample solutions were prepared and all optical readings were repeated until reproducible transmittance readings were obtained. Since the instrument (Unicam, SP700) recorded percentage or fractional transmittance, it was necessary to take the negative logarithm of this fraction:

Since $f I_o = I$

$\therefore \log \frac{I_o}{I} = -\log f$

i.e. $D = -\log f$

(f = fractional transmittance, I_o = initial light intensity, I = light intensity after passing through sample).

The results are listed in Chapter 3.

CHAPTER 3

RESULTS

Explanatory notes for Tables

In Tables 6 to 56, the heats of decomposition are the mean of at least five determinations for each compound. All heat effects are endothermic and the uncertainties are standard deviations of the mean. The significance of the temperature parameters is limited and a probable uncertainty of $\pm 10^{o}K$ should be assigned to them since, to a great extent, they are dependent on sample mass. The observed weight losses were found to be reproducible to about 0.5 - 1.0%.

In Tables 57 to 63 the heat capacities are the mean of at least four determinations. No weight loss occurred in any of the determinations.

Microanalytical data are probably correct to ± 0.2% (carbon), 0.1% (nitrogen), 0.05% (hydrogen). The uncertainties in the cobalt analytical data are standard deviations calculated from the expression:

$$\sigma^2 = \sum_{i=o}^{n} \sigma_i^2 \; / \; n-1$$

whereas the standard deviation of the mean is calculated from

$$\sigma^2 = \sum_{i=o}^{n} \sigma_i^2 / n(n-1)$$

Table 1

Reaction (1)

Experiment	1	2	3	4	5
m($CoCl_2.6H_2O$ gm.)	3.079909	2.884858	3.112049	3.028839	3.346420
- ΔR(ohms)	0.00378	0.00379	0.00517	0.00428	0.00454

E_s(Kcal./ohm.) = 24.121 (mean, from reaction (2)).

ΔH(Kcal./mole)	7.043	7.539	-	8.109	7.785

Mean ΔH = + 7.62 ± 0.17Kcal./mole

Table 2

Reaction (2)

Experiment	1	2	3	4
m(Ph_3P,gm.)	4.763801	4.796367	4.903403	5.027112
- ΔR(ohms)	0.00412	0.00415	0.00425	0.00438

Mean of E_s(Kcal./ohm.) = 24.121

ΔH(Kcal./mole)	5.472	5.474	5.484	5.512

Mean ΔH = + 5.486 ± 0.009Kcal./mole

Table 3

Reaction (3)

Experiment	1	2	3	4
m(H_2O, gm.)	1.012194	1.048891	1.045255	1.048761
ΔR(ohms)	0.00103	0.00117	0.00099	0.00085
Mean of E_s(Kcal./ohm.) after reaction (4) = 24.072				
- ΔH(Kcal./mole)	0.441	0.484	0.411	0.352

Mean ΔH = -0.422 ± 0.028Kcal./mole

Table 4

Reaction (4)

Experiment	1	2	3	4
m($Co(Ph_3P)_2Cl_2$)gm.)	1.951974	2.018401	2.019567	2.030478
ΔR(ohms)	0.00096	0.00093	0.00095	0.00104
Mean of E_s(Kcal./ohm) = 24.072				
ΔH(Kcal./mole)	7.747	7.258	7.410	8.069

Mean ΔH = + 7.62 ± 0.18Kcal./mole

Table 5

Reaction Type

$ML_4X_{2(cryst.)} \rightarrow ML_2X_{2(cryst.)} + 2L_{(g)}$ (1)

$ML_2X_{2(cryst.)} \rightarrow ML_2X_{2(liq.)}$ (2)

$ML_2X_{2(cryst.)} \rightarrow MLX_{2(cryst.)} + L_{(g)}$ (3)

$ML_2X_{2(liq.)} \rightarrow MX_{2(cryst.)} + 2l_{(g)}$ (4)

$MLX_{2(cryst.)} \rightarrow ML_{2/3}X_{2(cryst.)} + {}^{1}/_{3}L_{(g)}$ (5)

$ML_{2/3}X_{2(cryst.)} \rightarrow MX_{2(cryst.)} + {}^{2}/_{3}L_{(g)}$ (6)

$ML_4X_{2(cryst.)} \rightarrow MLX_{2(cryst.)} + 3L_{(g)}$ (7)

$ML_6X_{2(cryst.)} \rightarrow ML_4X_{2(cryst.)} + 2L_{(liq.)}$ (8)

$ML_4X_{2(cryst.)} + 2L_{(liq.)} \rightarrow ML_2X_{2(cryst.)} + 4L_{(g)}$ (9)

$ML_2X_{2(cryst.)} \rightarrow MX_{2(cryst.)} + 2L_{(g)}$ (10)

$ML_2X_{2(cryst.,oct.)} \rightarrow ML_2X_{2(cryst.,tet.)}$ (11)

$MLX_{2(cryst.)} \rightarrow MX_{2(cryst.)} + L_{(g)}$ (12)

$ML_2X_2.2H_2O_{(cryst.)} \rightarrow ML_2X_{2(cryst)} + 2H_2O_{(g)}$ (13)

$ML_2X_{2(liq.)} \rightarrow MLX_{2(liq.)} + L_{(g)}$ (14)

$MLX_{2(liq.)} \rightarrow ML_2X_{2(cryst.)} + L_{(g)}$ (15)

$ML_2X_2.2EtOH_{(cryst.)} \rightarrow ML_2X_{2(cryst.)} + 2EtOH_{(g)}$ (16)

$MLX_{2(cryst.)} \rightarrow ML_{\frac{1}{2}}X_{2(cryst.)} + \frac{1}{2}L_{(g)}$ (17)

$ML_{\frac{1}{2}}X_{2(cryst.)} \rightarrow MX_{2(cryst.)} + \frac{1}{2}L_{(g)}$ (18)

$NaH_2PO_{4(cryst.)} \rightarrow \frac{1}{2}Na_2H_2P_2O_{7(cryst.)} + \frac{1}{2}H_2O_{(g)}$ (19)

$\frac{1}{2}Na_2H_2P_2O_{7(cryst.)} \rightarrow NaPO_{3(cryst.)} + \frac{1}{2}H_2O_{(g)}$ (20)

Table 6 : $CuSO_4.5H_2O$

Scan rate : 16°/min. Range : 8mcal./sec.(full scale)

Overall percentage weight loss : 38.1(obs.), 40.5(calc.).

Reaction	T_i(°K)	T_p(°K)	T_f(°K)	ΔH (Kcal./mole)
$CuSO_4.5H_2O_{(cryst.)} \rightarrow$	320	360	400	51.1 ± 0.6
$CuSO_4.H_2O_{(cryst.)} + 4H_2O_{(g)}$		390*		
$CuSO_4.H_2O_{(cryst.)} \rightarrow$	470	520	560	17.3 ± 0.2
$CuSO_{4(cryst.)} + H_2O_{(g)}$				

* two peaks observed

Table 7 : $CaSO_4.2H_2O$

Scan rate : 16°/min. Range : 4mcal./sec.(full scale)

Overall percentage weight loss : 21.1 (obs.), 20.9(calc.)

Reaction	T_i(°K)	T_p(°K)	T_f(°K)	ΔH (Kcal./mole)
$CaSO_4.2H_2O_{(cryst.)} \rightarrow$	370	410	430	24.5 ± 0.6
$CaSO_{4(cryst.)} + 2H_2O_{(g)}$		420*		

* two separate peaks

Table 8 : $NaHCO_3$

Scan rate : 16°/min. Range : 32mcal./sec(full scale)

Overall percentage weight loss : 36.9(obs.), 36.9(calc.)

Reaction	T_i(°K)	T_p(°K)	T_f(°K)	ΔH (Kcal./mole)
$NaHCO_{3(cryst.)} \rightarrow \frac{1}{2}Na_2CO_{3(cryst.)} + \frac{1}{2}H_2O_{(g)} + \frac{1}{2}CO_{2(g)}$	375	435	460	15.2 ± 0.1

Table 9 : Pb

Scan rate : 2°/min. Range : 4mcal./sec.(full scale)

Reaction	Ti(°K)	T_p(°K)	T_f(°K)	ΔH (Kcal./mole)
$Pb_{(cryst.)} \rightarrow Pb_{(liq.)}$	600	603	604	1.08± 0.01

Table 10 : $Capy_2Cl_2$

Scan rate : 16°/min. Range : 8mcal./sec.(full scale)

Overall percentage weight loss : 58.7 (obs.), 58.8(calc.)

No. of reaction type (Table 5)	T_i(°K)	T_p(°K)	T_f(°K)	ΔH (Kcal./mole)
10	480	530,550	560	29.7 ± 0.2

Table 11 : $Crpy_2Cl_2$

Scan rate : 16°/min. Range : 4mcal./sec.(full scale)

Overall percentage weight loss : 56.7(obs.), 56.2 (calc.).

No. of Reaction Type (Table 5)	T_i(°K)	T_p(°K)	T_f(°K)	ΔH (Kcal./mole)
(3)	460	520	530	15.7 ± 0.3
(5)	550	590	605	9.8 ± 0.2
(6)	605	635	660	7.0 ± 0.2

Table 12 : $Mnpy_2Cl_2$

Scan rate : 16°/min. Range : 4mcal./sec.(full scale)

Overall percentage weight loss : 55.1(obs.), 55.6(calc.).

No of Reaction Type (Table 5)	T_i(°K)	T_p(°K)	T_f(°K)	ΔH (Kcal./mole)
(3)	410	460	470	14.7 ± 0.3
(5)	520	540	550	3.1 ± 0.2
(6)	550	600	610	10.7 ± 0.2

Table 13 : $Fepy_4Cl_2$

Scan rate : 16°/min. Range : 4mcal./sec.(full scale)

Overall percentage weight loss : 69.8(obs.), 71.4(calc.)

No. of Reaction Type (Table 5)	T_i(°K)	T_p(°K)	T_f(°K)	ΔH (Kcal./mole)
(1)	310	370	385	27.0 ± 0.4
(3)	400	450	465	15.2 ± 0.2
(5)	500	530	540	5.3 ± 0.1
(6)	545	585	600	10.1 ± 0.2

Table 14 : α-$Copy_2Cl_2$(violet form)

Scan rate : 8°/min. Range : 2mcal./sec.(full scale)

Overall percentage weight loss : 55.5(obs.), 54.9(calc.)

No. of Reaction Type (Table 5)	T_i(°K)	T_p(°K)	T_f(°K)	ΔH (Kcal./mole)
(11)	390	400	410	3.02 ± 0.07
(10)	420	510	600	28.6 ± 0.5

Table 15 : $Nipy_4Cl_2$

Scan rate : 16°/min. Range : 4mcal./sec.(full scale)

Overall percentage weight loss : 70.6(obs.), 70.9(calc.)

No. of Reaction Type (Table 5)	T_i(°K)	T_p(°K)	T_f(°K)	ΔH (Kcal./mole)
(1)	365	415	430	24.5 ± 0.1
(3)	430	470	480	15.6 ± 0.2
(12)	545 570*	610	620	17.0 ± 0.3

* two separate peaks

Table 16 : $Cupy_2Cl_2$

Scan rate : 16°/min. Range : 2mcal./sec.(full scale)

Overall percentage weight loss : 54.2(obs.), 54.1(calc.)

No. of Reaction Type (Table 5)	T_i(°K)	T_p(°K)	T_f(°K)	ΔH (Kcal./mole)
(3)	430	475	480	15.4 ± 1.0
(5)	480	505	515	5.2 ± 0.2
(6)	545	585	590	7.4 ± 0.2

Table 17 : $Cdpy_2Cl_2$

Scan rate : 16°/min. Range : 4mcal./sec.(full scale)

Overall percentage weight loss : 46.3(obs.), 46.3(calc.)

No. of Reaction Type (Table 5)	T_i(°K)	T_p(°K)	T_f(°K)	ΔH (Kcal./mole)
(3)	400	460	470	15.6 ± 0.2
(5)	505	530	545	3.6 ± 0.1
(6)	545	590	600	11.2 ± 0.2

Table 18 : $Crpy_2(H_2O)_2Br_2$

Scan rate*: 16° or 8°/min. Range*: 8 or 2mcal./sec.(full scale)

Overall percentage weight loss : 48.4(obs.), 47.8(Theor.)

No of Reaction Type (Table 5)	T_i(°K)	T_p(°K)	T_f(°K)	ΔH (Kcal./mole)
(13)	340	385	395	28.1 ± 0.4
(3)	490	530	540	14.7 ± 0.4
(12)	545	600	610	16.9 ± 0.4

* Scan rate and range changed to 8°/min. and 2mcal. /sec respectively after reaction (13).

Table 19 : $Copy_2Br_2$

Scan rate : 16°/min. Range : 2mcal./sec.(full scale)

Overall percentage weight loss : 42.1(obs.), 41.9(calc.)

No. of Reaction Type (Table 5)	T_i(°K)	T_p(°K)	T_f(°K)	ΔH (Kcal./mole)
(2) & (4) (not resolved)	450	530	550	27.3 ± 0.9

Table 20 : $Nipy_4Br_2$

Scan rate : 16°/min. Range : 4mcal./sec(full scale)

Overall percentage weight loss : 59.2(obs.), 59.4(calc.)

No. of Reaction Type (Table 5)	T_i(°K)	T_p(°K)	T_f(°K)	ΔH (Kcal./mole)
(1)	370	426	440	23.9 ± 0.2
(3)	440	490	510	16.3 ± 0.2
(12)	546	580	600	17.0 ± 0.3

Table 21 : $Crpy_4I_2$

Scan rate : 8°/min. Range : 2mcal./sec.(full scale)

Overall percentage weight loss : 54.1(obs.), 50.8(calc.)

No. of Reaction Type (Table 5)	T_i(°K)	T_p(°K)	T_f(°K)	ΔH (Kcal./mole
(1)	420	470	480	26.1 ± 0.4
(10)	510	570 600*	610	24.8 ± 0.6

Table 22 : $Copy_4I_2$

Scan rate : 16°/min. Range : 2mcal./sec.(full scale)

Overall percentage weight loss : 52.2(obs.), 50.2(calc.)

No. of Reaction Type (Table 5)	T_i(°K)	T_p(°K)	T_f(°K)	ΔH (Kcal./mole)
(1)	340	370	400	28.4 ± 0.7
(2)	450	475	490	6.3 ± 0.3
(4)	590	610	630	6.0 ± 0.1

Table 23 : $Nipy_4I_2$

Scan rate : 16°/min. Range : 8mcal./sec.(full scale)

Overall percentage weight loss : 51.3(obs.), 50.3(calc.)

No. of Reaction Type (Table 5)	T_i(°K)	T_p(°K)	T_f(°K)	ΔH (Kcal./mole)
(1)	395	445	455	34.2 ± 0.4
(10)	460	490 525*	535	31.6 ± 0.8

* two separate peaks.

Table 24 : $Ni(\alpha\text{-pic})_2Cl_2$

Scan rate : 16°/min. Range : 2mcal./sec.(full scale)

Overall percentage weight loss : 59.5(obs.), 59.0(calc.)

No. of Reaction Type (Table 5)	T_i(°K)	T_p(°K)	T_f(°K)	ΔH (Kcal./mole)
(5)	340	395 420 430*	445	6.7 ± 0.1
(12)	455	485 570*	590	9.1 ± 0.2

* separate peaks.

Table 25 : $Co(\alpha\text{-pic})_2Cl_2$

Scan rate : 16°/min. Range : 4mcal./sec.(full scale)

Overall percentage weight loss : 59.1(obs.), 58.9(calc.)

No. of Reaction Type (Table 5)	T_i(°K)	T_p(°K)	T_f(°K)	ΔH (Kcal./mole)
Not assigned, <3% weight loss	365	375	380	0.73 ± 0.03
(2)	400	425	440	7.6 ± 0.1
(4)	480	520	580	17.9 ± 0.4

Table 26 : $Co(\alpha\text{-pic})_2Br_2$

Scan rate : 8°/min. Range : 2mcal./sec.(full scale)

Overall percentage weight loss : 45.2(obs.), 45.9(calc.)

No. of Reaction Type (Table 5)	$T_i(^{\circ}K)$	$T_p(^{\circ}K)$	$T_f(^{\circ}K)$	ΔH (Kcal./mole)
(2)	420	440	445	6.4 ± 0.4
(4)	500	530	560	14.8 ± 0.8

Table 27 : $Co(\alpha\text{-pic})_2I_2$

Scan rate : 16°/min. Range : 2mcal./sec.(full scale)

Overall percentage weight loss : 38.1(obs.), 37.3(calc.)

No. of Reaction Type (Table 5)	$T_i(^{\circ}K)$	$T_p(^{\circ}K)$	$T_f(^{\circ}K)$	ΔH (Kcal./mole)
(2)	425	440	450	6.0 ± 0.1
(4)	550	570	590	6.3 ± 0.1

Table 28 : $Mn(\beta\text{-pic})_2Cl_2$

Scan rate : 16°/min. Range : 8mcal./sec.(full scale)

Overall percentage weight loss : 58.5(obs.), 59.7(calc.)

No. of Reaction Type (Table 5)	$T_i(^{\circ}K)$	$T_p(^{\circ}K)$	$T_f(^{\circ}K)$	ΔH (Kcal./mole)
(3)	390	450	465	13.6 ± 0.2
(5)	480	510	530	5.1 ± 0.1
(6)	545	615	625	13.4 ± 0.2

Table 29 : $Fe(\beta\text{-pic})_4Cl_2$

Scan rate : 16°/min. Range : 4mcal./sec.(full scale)

Overall percentage weight loss : 75.4(obs.), 74.6(calc.)

No. of Reaction Type (Table 5)	T_i(°K)	T_p(°K)	T_f(°K)	ΔH (Kcal./mole)
(1)	340	390	405	29.2 ± 0.6
(3)	410	450	460	14.4 ± 0.1
(5)	470	500	510	6.1 ± 0.1
(6)	525	590	600	18.3 ± 0.7

Table 30 : $Co(\beta\text{-pic})_2Cl_2$

Scan rate : 16°/min. Range : 2mcal./sec.(full scale)

Overall percentage weight loss : 58.9(obs.), 58.9(calc.)

No. of Reaction Type (Table 5)	T_i(°K)	T_p(°K)	T_f(°K)	ΔH (Kcal./mole)
(2)	410	417	420	5.3 ± 0.2
(14)	470	490	500	5.7 ± 0.2
(15)	550	580	600	12.1 ± 0.4

Table 31 : $Co(\beta\text{-pic})_4Br_2$

Scan rate : 16°/min. Range : 4mcal./sec.(full scale)

Overall percentage weight loss : 63.4(obs.), 63.0(calc.)

No. of Reaction Type (Table 5)	T_i(°K)	T_p(°K)	T_f(°K)	ΔH (Kcal./mole)
(1)	340	385	400	30.0 ± 0.3
(2)	430	435	440	6.4 ± 0.1
(4)	540	570	590	10.5 ± 0.4

Table 32 : $Ni(\beta\text{-pic})_4Cl_2$

Scan rate : 16°/min. Range : 8mcal./sec.(full scale)

Overall percentage weight loss : 73.2(obs.), 74.2(calc.)

No. of Reaction Type (Table 5)	T_i(°K)	T_p(°K)	T_f(°K)	ΔH (Kcal./mole)
(1)	390	430	440	25.7 ± 0.6
(3)	445	490	500	13.9 ± 0.3
(5)	510	550	560	6.9 ± 0.1
(6)	570	600	640	12.8 ± 0.3

Table 33 : $Mn(\gamma\text{-pic})_2Cl_2$

Scan rate : 16°/min. Range : 8mcal./sec.(full scale)

Overall percentage weight loss : 61.3(obs.), 59.7(calc.)

No. of Reaction Type (Table 5)	T_i(°K)	T_p(°K)	T_f(°K)	ΔH (K cal./mole)
(3)	380	440	455	15.1 ± 0.2
(5)	500	540	560	5.4 ± 0.1
(6)	565	615	630	14.0 ± 0.2

Table 34 : $Fe(\gamma\text{-pic})_4Cl_2$

Scan rate : 16°/min. Range : 4mcal./sec.(full scale)

Overall percentage weight loss : 75.1(obs.), 74.6(calc.)

No. of Reaction Type (Table 5)	T_i(°K)	T_p(°K)	T_f(°K)	ΔH (Kcal./mole)
(7)	360	425 440*	460	47.3 ± 0.5
(5)	510	535	545	5.3 ± 0.1
(6)	550	600	610	15.3 ± 0.2

* two separate peaks.

Table 35 : $Co(\gamma\text{-pic})_4Cl_2$

Scan rate : 16°/min. Range : 4, 2mcal/sec.*(full scale)

Overall percentage weight loss : 75.2(obs.), 74.1(calc.)

No. of Reaction Type (Table 5)	T_i(°K)	T_p(°K)	T_f(°K)	ΔH (Kcal/mole)
(1)	360	390	430	32.9 ± 0.7
(2)	4.5	420	425	5.2 ± 0.3
(4)	440	530	600	25.8 ± 0.6

* 2mcal/sec after reaction (1)

Table 36 : $Co(\gamma\text{-pic})_4Br_2$

Scan rate : 8°/min. Range : 2mcal./sec.(full scale)

Overall percentage weight loss : 64.0(obs.), 63.0(calc.)

No. of Reaction Type (Table 5)	T_i(°K)	T_p(°K)	T_f(°K)	ΔH (Kcal./mole)
(1)	350	390	420	38.9 ± 0.8
(10)	500	560	590	17.6 ± 0.9

Table 37 : $Co(\gamma\text{-pic})_4I_2$

Scan rate : 16°/min. Range : 2mcal./sec.(full scale)

Overall percentage weight loss : 55.9(obs.), 54.3(calc.)

No. of Reaction Type (Table 5)	T_i(°K)	T_p(°K)	T_f(°K)	ΔH (Kcal./mole)
(1)	350	400	415	30.5 ± 0.6
(2)	420	425	430	5.1 ± 0.2
(4)	600	630	650	5.8 ± 0.5

Table 38 : $Ni(\gamma\text{-pic})_4Cl_2$

Scan rate : 16°/min. Range : 2mcal./sec.(full scale)

Overall percentage weight loss : 75.4(obs.), 74.1(calc.)

No. of Reaction Type (Table 5)	T_i(°K)	T_p(°K)	T_f(°K)	ΔH (Kcal./mole)
(7)	405	470	485	45.8 ± 0.6
(12)	535	575, 605*	620	20.8 ± 0.4

* two separate peaks.

Table 39 : $FeAn_6Cl_2$

Scan rate : 16°/min. Range : 8mcal./sec.(full scale)

Overall percentage weight loss : 82.0(obs.), 81.5(calc.)

No. of Reaction Type (Table 5)	T_i(°K)	T_p(°K)	T_f(°K)	ΔH (Kcal./mole)
(8)	330	340	350	13.3 ± 0.2
(9)	360	440	455	36.1 ± 0.6
(3)	460	490	500	16.3 ± 0.3
(12)	505	530	550	11.6 ± 0.2

Table 40 : $MnAn_2Cl_2$

Scan rate : 16°/min. Range : 8mcal./sec.(full scale)

Overall percentage weight loss : 58.9(obs.), 59.7(calc.)

No. of Reaction Type (Table 5)	T_i(°K)	T_p(°K)	T_f(°K)	ΔH (Kcal./mole)
(10)	420	480 510 540*	565	30.1 ± 0.7

* three separate peaks.

Table 41 : $CoAn_2Cl_2$

Scan rate : 16°/min. Range : 4mcal./sec.(full scale)

Overall percentage weight loss : 59.0(obs.), 58.9(calc.)

No. of Reaction Type (Table 5)	T_i(°K)	T_p(°K)	T_f(°K)	ΔH (Kcal./mole)
(10)	460	525 555*	570	35.5 ± 0.5

* two separate peaks.

Table 42 : $NiAn_2Cl_2.2EtOH$

Scan rate : 16°/min. Range : 4mcal./sec.(full scale)

Overall percentage weight loss : 68.6(obs.), 68.2(calc.)

No. of Reaction Type (Table 5)	T_i(°K)	T_p(°K)	T_f(°K)	ΔH (Kcal./mole)
(16)	310	350	375	28.1 ± 0.4
(10)	450	510 555*	570	32.2 ± 0.7

* two separate peaks.

Table 43 : $CdAn_2Cl_2$

Scan rate : 16°/min. Range : 8mcal./sec.(full scale)

Overall percentage weight loss : 49.6(obs.), 50.4(calc.)

No. of Reaction Type (Table 5)	T_i(°K)	T_p(°K)	T_f(°K)	ΔH (Kcal./mole)
(10)	400	460 480 520*	535	32.9 ± 0.4

* three separate peaks

Table 44 : $NiDmpCl_2$

Scan rate : 16°/min. Range : 4mcal./sec.(full scale)

Overall percentage weight loss : 51.5(obs.), 51.0(calc.)

No. of Reaction Type (Table 5)	T_i(°K)	T_p(°K)	T_f(°K)	ΔH (Kcal./mole)
(10)	490	550* 580	600	21.2 ± 0.5

* two separate peaks

Table 45 : $MnpzCl_2$

Scan rate : 16°/min. Range : 4mcal./sec.(full scale)

Overall percentage weight loss : 40.5(obs.), 38.9(calc.)

No. of Reaction Type (Table 5)	T_i(°K)	T_p(°K)	T_f(°K)	ΔH (Kcal./mole)
(12)	600	690	700	22.1 ± 0.5

Table 46 : $Fepz_2Cl_2$

Scan rate : 16°/min. Range : 4mcal./sec.(full scale)

Overall percentage weight loss : 56.1(obs.), 55.8(calc.)

No. of Reaction Type (Table 5)	T_i(°K)	T_p(°K)	T_f(°K)	ΔH (Kcal./mole)
(3)	450	500	510	15.5 ± 0.2
(12)	640	710 730*	740	22.5 ± 0.6

* two separate peaks

Table 47 : $Copz_2Cl_2$

Scan rate : 16°/min. Range : 8mcal./sec.(full scale)

Overall percentage weight loss : 56.3(obs.), 55.2(calc.)

No. of Reaction Type (Table 5)	T_i(°K)	T_p(°K)	T_f(°K)	ΔH (Kcal./mole)
(3)	450	495	510	15.0 ± 0.2
(12)	660	730	745	20.8 ± 1.0

Table 48 : $CoDmpCl_2$ (blue form)

Scan rate : 16°/min. Range : 8mcal./sec.(full scale)

Overall percentage weight loss : 45.3(obs.), 45.4(calc.)

No. of Reaction Type (Table 5)	T_i(°K)	T_p(°K)	T_f(°K)	ΔH (Kcal./mole)
(17)	490	525	535	7.9 ± 0.2
(18)	535	580	590	11.4 ± 0.3

Table 49 : $Co(Mp)_4Cl_2$

Scan rate : 16°/min. Range : 8mcal./sec.(full scale)

Overall percentage weight loss : 73.4(obs.), 74.4(calc.)

No. of Reaction Type (Table 5)	T_i(°K)	T_p(°K)	T_f(°K)	ΔH (Kcal./mole)
(1)	310	335	380	33.8 ± 0.3
(3)	385	420	430	11.9 ± 0.2
(5)	490	540	550	5.8 ± 0.2
(6)	560	610	630	15.9 ± 0.3

Table 50 : $Nipz_2Cl_2$

Scan rate : 16°/min. Range : 8mcal./sec.(full scale)

Overall percentage weight loss : 57.9(obs.), 55.3(calc.)

No. of Reaction Type (Table 5)	T_i(°K)	T_p(°K)	T_f(°K)	ΔH (Kcal./mole)
(3)	490	550	565	15.7 ± 0.2
(12)	700	755	765	22.6 ± 0.7

Table 51 : $Nipz_2Br_2$

Scan rate : 16°/min. Range : 8mcal./sec.(full scale)

Overall percentage weight loss : 44.5(obs.), 42.3(calc.)

No. of Reaction Type (Table 5)	T_i(°K)	T_p(°K)	T_f(°K)	ΔH (Kcal./mole)
(3)	520	570	580	15.8 ± 0.6
(12)	670	740	750	19.8 ± 0.6

Table 52 : $Co(Pmd)_2Br_2$

Scan rate : 16°/min. Range : 4mcal./sec.(full scale)

Overall percentage weight loss : 43.4(obs.), 42.3(calc.)

No. of Reaction Type (Table 5)	T_i(°K)	T_p(°K)	T_f(°K)	ΔH (Kcal./mole)
(3)	410	460	480	14.7 ± 0.5
(12)	660	730	750	26.9 ± 1.0

Table 53 : NaH_2PO_4

Scan rate : 32°/min. Range : 8 or 4mcal./sec*(full scale)

Overall percentage weight loss : 15.2(obs.), 15.0(calc.)

No. of Reaction Type (Table 5)	T_i(°K)	T_p(°K)	T_f(°K)	ΔH (Kcal./mole)
(19)	480	500	510	6.7 ± 0.1
(20)	550	580 620**	630	9.3 ± 0.1

* 4mcal. after Reaction (19); ** two separate peaks.

Table 54 : NaH_2PO_4

Scan rate : 16°/min. Range : 8 or 4mcal./sec.*(full scale)

Overall percentage weight loss : 15.4(obs.), 15.0(calc)

No. of Reaction Type (Table 5)	T_i(°K)	T_p(°K)	T_f(°K)	ΔH (Kcal./mole)
(19)	475	500	505	6.6 ± 0.1
(20)	550	570 590 610**	625	9.4 ± 0.1

* 4mcal. after Reaction (19); ** three separate peaks.

Table 55 : NaH_2PO_4

Scan rate : 8°/min. Range : 4mcal./sec.(full scale)

Overall percentage weight loss : 15.2(obs.), 15.0(calc.)

No. of Reaction Type (Table 5)	T_i(°K)	T_p(°K),	T_f(°K)	ΔH (Kcal./mole)
(19)	480	490 500*	505	6.7 ± 0.1
(20)	540	555 575*	600	8.8 ± 0.1

* two separate peaks

Table 56 : NaH_2PO_4

Scan rate : 0.5°/min. Range : 4mcal./sec.(full scale)

Overall percentage weight loss : 15.2(obs.), 15.0(calc.)

No. of Reaction Type (Table 5)	T_i(°K)	T_p(°K)	T_f(°K)	ΔH (Kcal./mole)
(19)	480	490	500	6.6 ± 0.4
(20)	Unsatisfactory thermogram.			

Heat Capacity Results

The heat capacities of some compounds were measured by the method described previously and the results obtained are shown in tables 57 to 63.

Originally it was intended to fit the data to an equation of the type:

$$Cp = A + BT + CT^2$$

A least squares procedure indicated that C was very small and could be neglected. The data were, therefore, fitted to a linear equation:

$$Cp = A + BT$$

The equation is given for each substance in the appropriate table. Details of the least squares procedure are given in Appendix 1.

Table 57 : C_p of $Copy_2Cl_2$(violet)

Range : 2mcal./sec. (full scale)

Scan : 16°K/min.

T(°K)	320	330	340	350	360	370	380
C_p(cal./°/mole)	69.9	72.4	73.5	75.0	75.9	77.1	79.5

$$Cp = 24.0 + 0.145T \text{ cal./°/mole}$$

Table 58 : C_p of $Co(\gamma\text{-pic})_2Cl_2$

Range : 2mcal./sec. (full scale)

Scan : 16°K/min.

T(°K)	330	340	350	360	370
Cp (cal./°/mole)	85.7	86.9	88.5	92.4	94.6

$$Cp = 12.6 + 0.22T \text{ cal./°/mole}$$

Table 59 : Cp of $Co(\alpha\text{-pic})_2Cl_2$

Range : 2mcal/sec. (full scale)

Scan : 16°K/min.

T(°K)	290	300	310	320	330	340	350	360
Cp(cal./°/mole)	80.2	84.4	86.0	87.4	89.7	92.1	94.8	97.4

$C_p = 14.3 + 0.23T$ cal./°/mole

Table 60 : Cp of $CoAn_2Cl_2$

Range : 2mcal./sec (full scale)

Scan : 16°K/min.

T(°K)	330	340	350	360	370	380	390	400	410	420	430
Cp(cal/°/mole)	79.1	80.9	82.2	84.9	86.1	87.1	88.8	93.6	94.2	95.2	96.8

$C_p = 16.6 + 0.19T$ cal./°/mole

Table 61 : Cp of $FePz_2Cl_2$

Range : 2mcal./sec.(full scale)

Scan :: 16°K/min.

T(°K)	320	330	340	350	360	370	380	390	400	410	420	430
Cp(cal./°/mole)	60.7	63.0	63.6	65.7	71.3	72.2	72.6	74.3	75.4	76.5	77.5	78.4

$C_p = 7.1 + 0.17T$ cal/°/mole

Table 62 : Heat capacity of sodium chloride

Range : 2mcal./sec.(full scale)

Scan : 16°K/min.

T(°K)	200	220	250	270	320	340	360	380	410
Cp(cal./°/mole)	10.9	11.5	11.5	11.8	11.9	11.8	12.1	12.2	12.5

T(°K)	430	450	470	490	510
Cp(cal./°/mole)	12.8	12.7	12.8	12.6	12.8

$$C_p = 10.1 + 0.0056T \text{ cal./°/mole}$$

Table 63 : Heat capacity of Indium

Range : 2mcal./sec.(full scale)

Scan : 16°K/min.

T(°K)	330	350	370	390	410	425
Cp(cal./°/mole)	6.43	6.56	6.67	6.88	6.91	7.09

$$C_p = 4.18 + 0.0068T \text{ cal./°/mole}$$

Analytical Results

The analytical data for the analysis of the compounds prepared in this work are listed in Tables (64) and (65).

Table 64 : Cobalt analyses

Sample	Sample weight (mg)	Optical Density	%Co found	%Co theory
1) Cobalt	1.050	0.694		
Metal	1.635	1.103		
2) $Copy_2Cl_2$	5.090	0.654	19.5 ± 0.5	20.4
	4.620	0.570		
3) $Co(\alpha\text{-pic})_2Cl_2$	2.815	0.540	19.0 ± 0.2	18.6
	2.785	0.536		
4) $Co(\gamma\text{-pic})_4Cl_2$	4.205	0.308	11.2 ± 0.2	11.7
	3.395	0.241		
5) $Copy_2Br_2$	5.970	0.627	16.1 ± 0.3	15.6
	7.005	0.718		
6) $Co(\alpha\text{-pic})_2Br_2$	7.090	0.705	15.4 ± 0.3	14.6
	9.155	0.910		
7) $Co(\gamma\text{-pic})_4Br_2$	4.050	0.274	10.3 ± 0.2	10.0
	8.495	0.558		
8) $Copy_4I_2$	7.070	0.412	9.0 ± 0.1	9.2
	8.700	0.507		
9) $Co(\alpha\text{-pic})_2I_2$	6.805	0.510	11.2 ± 0.2	11.8
	6.100	0.457		
10) $Co(\gamma\text{-pic})_4I_2$	7.030	0.379	8.4 ± 0.1	8.6
	7.655	0.379		

Table 65 : Microanalytical (Carbon, Hydrogen, Nitrogen) Data

Sample	% : C	H	N(found)	% : C	H	N(theory)
$Mnpy_2Cl_2$	41.9	3.56	10.0	42.2	3.52	9.9
$Mn(\beta\text{-pic})_2Cl_2$	45.4	4.54	8.7	46.2	4.52	9.0
$Mn(\gamma\text{-pic})_2Cl_2$	46.3	4.42	8.7	46.2	4.52	9.0
$Copy_2Cl_2$	41.5	3.48	9.3	41.7	3.50	9.7
$Co(\beta\text{-pic})_2Cl_2$	44.9	4.39	8.4	45.6	4.47	8.9
$Co(\beta\text{-pic})_4Br_2$	48.8	4.62	9.1	48.7	4.78	9.5
$Nipy_4Cl_2$	53.0	4.44	12.1	53.8	4.49	12.6
$Ni(\beta\text{-pic})_4Cl_2$	56.9	5.56	11.0	57.4	5.62	11.2
$Ni(\gamma\text{-pic})_4Cl_2$	57.9	5.63	11.2	57.4	5.62	11.2
$Nipy_4Br_2$	44.6	3.59	10.1	44.9	3.74	10.5
$Nipy_4I_2$	38.7	3.20	8.8	38.2	3.20	8.9
$Cupy_2Cl_2$	40.9	3.36	9.3	41.0	3.42	9.6
$Cdpy_2Cl_2$	34.8	2.82	7.9	35.2	2.9	8.2
$CoAn_2Cl_2$	45.6	4.42	8.9	45.6	4.46	8.9
$NiAn_2Cl_2.2EtOH$	47.4	6.28	7.2	47.1	6.4	6.9
$CdAn_2Cl_2$	38.4	3.72	7.3	39.0	3.82	7.6
$MnpzCl_2$	23.1	2.17	13.1	23.3	1.96	13.6

(Table 65 continued)

Sample	% : C	H	N(found)	% : C	H	N(theory)
$Fepz_2Cl_2$	33.5	2.79	19.4	33.5	2.81	19.5
$Copz_2Cl_2$	32.7	2.75	18.6	33.1	2.8	19.3
$CoDmpCl_2$	30.0	3.28	11.6	30.2	3.39	11.8
$Nipz_2Cl_2$	33.3	3.08	18.9	33.1	2.78	19.3
$2NiDmpCl_2.3H_2O$	26.9	3.84	10.4	27.2	4.1	10.5
$Nipz_2Br_2$	24.7	2.16	13.9	25.4	2.13	14.8
$Co(Ph_3P)_2Cl_2$	65.7	4.58	-	66.0	4.59	-

Due to the instability of iron(II) complexes in air, no analytical data were obtained for these compounds.

Dichlorodianiline manganese(II) was obtained with an indefinite number of attached ethanol molecules. These were removed prior to each thermal decomposition as described in preparation number (22), chapter 3.

There was only sufficient dibromodipyrimidinecobalt(II) for thermal decomposition studies but with this compound, as with the others for which no analytical data are available, the weight losses found in the decompositions indicate that the compounds were sufficiently pure.

CHAPTER 4

DISCUSSION

4.1 A Thermochemical Study of Dichlorobis(triphenylphosphine)cobalt(II)

The heats of reaction (1) to (4) were measured at 298°K in an adiabatic reaction calorimeter.

$$CoCl_2.6H_2O_{(cryst)} + \{2PPh_3, 563EtOH\}_{(liq)} \rightarrow \{Co(PPh_3)_2Cl_2, 6H_2O, 563EtOH\}_{(liq)} \quad (1)$$

$$2P(Ph)_{3(cryst)} + 563EtOH_{(liq)} \rightarrow \{2PPh_3, 563EtOH\}_{(liq)} \quad (2)$$

$$6H_2O_{(liq)} + 563EtOH_{(liq)} \rightarrow \{6H_2O, 563EtOH\}_{(liq)} \quad (3)$$

$$Co(PPh_3)_2Cl_{2(cryst)} + \{6H_2O, 563EtOH\}_{(liq)} \rightarrow \{Co(PPh)_3Cl_2, 6H_2O, 563EtOH\}_{(liq)} \quad (4)$$

The data obtained are summarised in Tables (1) and (4) of Chapter 3.

The heat of hydration of cobalt(II) chloride to the hexahydrate was reported (64) to be -21.9 ± 0.4KCal./mole (ΔH_5). The heat of sublimation of triphenylphosphine was estimated (65) to be +21.0 ± 0.5Kcal./mole ($\Delta H(6)$). Using the data from Tables (1) to (4) and multiplying the heats of reaction (in Kcal./mole) by the number of moles of reactant, the heat of the reaction

$$CoCl_2.6H_2O_{(cryst)} + 2PPh_{3(cryst)} \rightarrow Co(PPh_3)_2\,Cl_{2(cryst)} + 6H_2O_{(liq)}$$

was found to be +13.5 ± 0.3Kcal./mole. Using $\Delta H(5)$ and $\Delta H(6)$, the heat of the reaction

$$CoCl_{2(cryst)} + 2PPh_{3(g)} \rightarrow Co(PPh_3)_2Cl_{2(cryst)}$$

was found to be -50.4 ± 0.7KCal./mole.

It was thought that this reaction could also be carried out in the differential scanning calorimeter. Thermal decomposition did not yield reproducible weight losses, however, and difficulty was experienced with corrosion of the sample holders by the molten complex.

4.2 The Structures of Compounds of the type ML_2X_2 and ML_4X_2

(L is a heterocyclic base)

4.2.1 Complexes of pyridine and related ligands

N.S. Gill et al. (66) have discussed the structures of pyridine complexes of the type MPy_2X_2, where X is a halogen. In this paper, the two forms of dichlorodipyridinecobalt(II)have received the most attention since their structures are typical of most of the compounds of this type. The α and β forms are violet and blue respectively, the violet form being stable at room temperature and the blue form stable at temperatures greater than 100°C. The transformation is reversible, the violet form being obtained when the blue form is allowed to stand for a few hours.

The above authors report the magnetic moments of the α- and β-forms as 5.15 and 4.42 Bohr Magnetons respectively. It can be predicted that divalent cobalt in a tetrahedral field should give a smaller orbital contribution to the susceptibility than should divalent cobalt in an octahedral field. This has been confirmed for many cobalt complexes of known stereochemistry and suggest that the α- and β-forms are, respectively, octahedral and tetrahedral compounds. Furthermore, diffuse reflectance measurements (49) on the two forms indicate that they have quite different spectra, the β form giving rise to very intense ligand field bands. When dissolved in organic solvents, however, both forms give rise to an intense set of ligand field bands. The more intense spectrum is characteristic of a transition metal in an environment lacking a centre of symmetry, for example, tetrahedral symmetry. Finally, the crystal

structures of the two forms have been determined (67, 68). These show that the α-form is an octahedral polymeric compound, having equatorial chlorine bridges and axial pyridines, while the β-form is a tetrahedral monomer.

Gill et al. then suggested that since the X-ray powder patterns of MPy_2X_2 type compounds were similar to those of either the α- or β-forms of the cobalt complex, described above, they could be divided into Class A (octahedral) and Class C (tetrahedral) compounds. Class A includes $FePy_2Cl_2$, $MnPy_2Cl_2$, $MnPy_2Br_2$ and $Nipy_2Cl_2$. Class C comprises $Copy_2Br_2$, $Copy_2I_2$, $Znpy_2Cl_2$ and $Znpy_2I_2$. There is also a Class B, closely related to Class A except that the M-X bond lengths are not equal. The compounds in this class are derived from Class A by a tetragonal distortion and include $Crpy_2Cl_2$, $Cupy_2Cl_2$ and $Cupy_2Br_2$.

Making use of the intensities of certain spectral bands in the visible to ultra-violet regions, J.R. Allan et al. (47, 49, 51) have assigned the following compounds to Classes A or C:

Class A $Mn(\beta\text{-pic})_2Cl_2$, $Mn(\gamma\text{-pic})_2Cl_2$

$Ni(\beta\text{-pic})_2Cl_2$, $Nipy_2Br_2$

Class C $Co(\alpha\text{-pic})_2Cl_2$, $Co(\beta\text{-pic})_2Cl_2$, $Co(\gamma\text{-pic})_2Cl_2$, $Copy_2Br_2$, $Co(\alpha\text{-pic})_2Br_2$, $Co(\beta\text{-pic})_2Br_2$, $Co(\gamma\text{-pic})_2Br_2$, $Copy_2I_2$, $Co(\alpha\text{-pic})_2I_2$, $Co(\beta\text{-pic})_2I_2$, $Co(\gamma\text{-pic})_2I_2$, $Ni(\alpha\text{-pic})_2Cl_2$, $Nipy_2I_2$

Holah and Fackler (69) have assigned the compound $Crpy_2Br_2$ to Class C.

Compounds of the general formula ML_4X_2 are thought to have trans-octahedral structures by analogy with the compounds Mpy_4X_2 (M = Co, Ni, X = Cl, Br, NCS). X-ray investigations of these compounds (70, 71, 72) show that the pyridine molecules are twisted out of plane and halogens or thiocyanate groups placed axially. Spectral data suggest that cobalt and nickel complexes with L = pyridine, β or γ-picoline have similar structures while the similarity of X-ray powder photographs has confirmed that the structures of FeL_4X_2 are very similar to those of the nickel analogues (56).

4.2.2 Aniline Complexes

It has been inferred (60) that since the ultra-violet spectra of the MAn_2Cl_2 compounds are all, with the exception of the cobalt compound, compatible with octahedral symmetry then the structures should be similar to the Class A type pyridine complexes referred to previously. This is quite reasonable since the Class A structure is the only octahedral structure which may be proposed for a compound of the proposed stoichiometry. Similarly, the assignment of $CoAn_2Cl_2$ to Class C is reasonable, even though distortions may be present in all the "tetrahedral" complexes which tend to put them into a C_{2v} symmetry class. Spectral data were used by Ahuja et al. (60) for this assignment.

4.2.3. Complexes of Pyrazine and Related Ligands

These complexes are unique in that there exists the opportunity of co-ordination by each nitrogen of the ligand. Pyrazine complexes of cobalt, nickel and copper have been studied by Lever et al. (74, 57, 59).

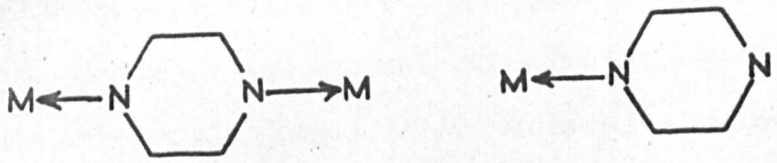

Fig (1)

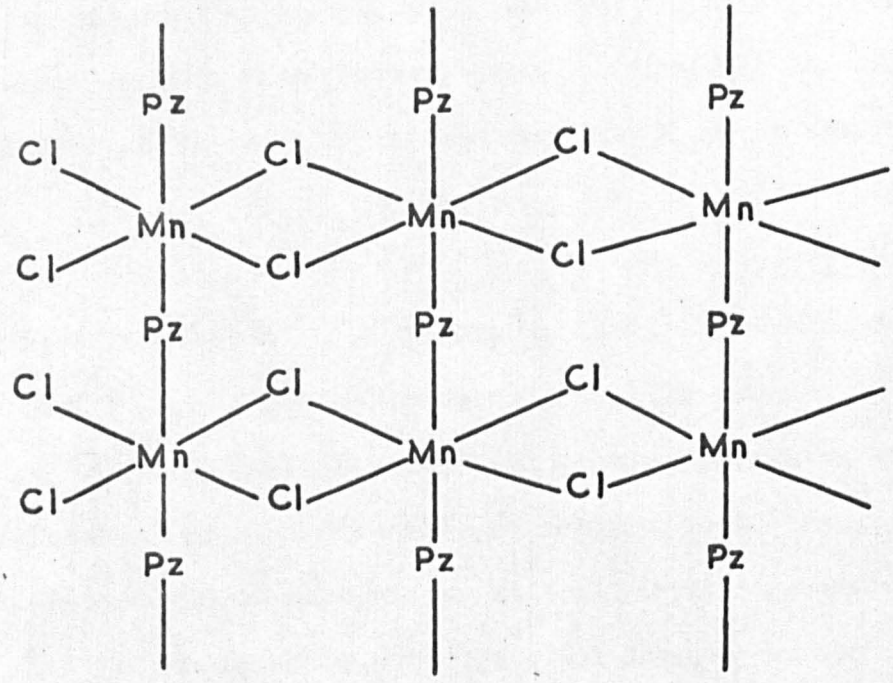

Fig (2)

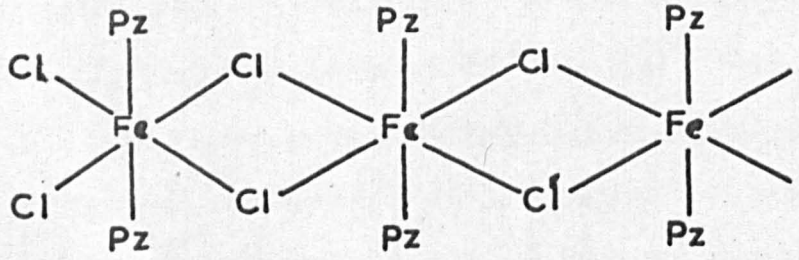

Fig (3)

Briefly, their method was to determine the local symmetry around the metal by magnetic susceptibility and ultra-violet spectroscopic measurements. Infra-red measurements were used to establish whether the pyrazine was acting as a mono- or bi-dentate group by the following method: In Figure (1) it is clearly seen that for a ring stretching vibration, the dipole moment of the system will change in (b) but not in (a). It would be expected, therefore, that one more absorption band would be present in the infra-red spectrum of type (b) compounds. Since at least one more vibration would be infra-red active.

Using this criterion, the above workers argued that the ligand acted as a monodentate group in the complexes:

$Copz_2Cl_2$, $CoDmpCl_2$(violet), $Nipz_2Cl_2$, $Nipz_2Br_2$.

$CoDmpCl_2$(blue) is thought to be a tetrahedral polymeric complex (58) using bridging 2, 5-Dimethylpyrazine groups while the compounds, $CopzCl_2$ and $NiDmpCl_2$, have the ligand bound at both ends, with an overall octahedral symmetry about the metal.

Two compounds, $MnpzCl_2$ and $Fepz_2Cl_2$ have not been previously described. $MnpzCl_2$ has the characteristically weak diffuse reflectance spectrum associated with manganese (II) in an octahedral environment. The infra-red spectrum shows no absorption band at around $1000cm^{-1}$, the frequency at which terminal pyrazine molecules normally absorb. With this limited information it is suggested that the compound has a three dimensional pyrazine bridged structure with normal chlorine bridges such as those found in the class A Mpy_2Cl_2 compounds, described previously.

The suggested structure is shown in Figure (2) and is similar to that suggested by Lever for some $MpzCl_2$ compounds (57, 59, 74).

$Fepz_2Cl_2$ is an intense orange-red compound. Its magnetic moment was found to be 5.28BM, after correction for diamagnetism. This is acceptable for octahedrally co-ordinated iron (II). A d <-> d band was found in the diffuse reflectance spectrum at 11,600cm^{-1} which gives a value of 10Dq (= 11,600cm^{-1}) also compatible with octahedral iron (II). The infra-red spectrum has a band ot 987cm^{-1} which is indicative of a terminal pyrazine group. This band is not present in the spectrum of the decomposition product, $FepzCl_2$. $Fepz_2Cl_2$ would seem to be a polymeric octahedral compound with chlorine bridges and terminal pyrazine groups while the structure of $FepzCl_2$ probably resembles that of $MnpzCl_2$. The structure of $Fepz_2Cl_2$ is probably as shown in Figure (3) and is seen to be similar to that of the dipyridine complexes of Class A described previously.

The magnetic moment of the complex $CoDmpCl_2$ was also measured and found to be 4.45BM, indicative of tetrahedral cobalt (II). The compound exists in two forms but these are not readily inter-convertible, unlike the two forms of $Copy_2Cl_2$. The other form of $CoDmpCl_2$ is violet and may have an octahedral structure (57).

4.3 The Heats of Solid State Reactions

4.3.1 ML_2X_2 Compounds

Consider the decomposition of a compound of the type ML_2X_2,

$$ML_2X_{2(cryst)} \xrightarrow{\Delta H_r^2} MX_{2(cryst)} + 2L_{(g)}$$

This heat of reaction, ΔH_r^2, is the experimentally measured quantity. It may be related to the heats of the analogous gas phase reaction by a thermodynamic cycle (Figure 4).

$$\begin{array}{ccc} ML_2X_{2(g)} & \xrightarrow{\Delta H_g} & MX_{2(g)} + 2L_{(g)} \\ \uparrow S_1 & & \downarrow -S_2 \\ ML_2X_{2(cryst)} & \xrightarrow{\Delta H_r^2} & MX_{2(cryst)} + 2L_{(g)} \end{array}$$

Figure 4

From this cycle, $\Delta H_g = \Delta H_r^2 - S_1 + S_2$

Thus, a more fundamental enthalpy change is obtained which is independent of the states of aggregation of the solids involved. The states of aggregation of the gaseous halides and their stereochemistries must still, however, be uncertain.

Ablov and Konunova (75) have estimated S_1, the heat of sublimation of the complex, for certain aniline complexes from the known boiling points of organometallic compounds of similar molecular weights. An approximate value was obtained by the use of Trouton's rule.

They also considered the process in Figure 5 as a means of interpreting ΔH_r^2:

$$MX_{2(cryst)} + 2L_{(g)} \xrightarrow{U_{exp}} MX_{2(cryst,exp)} + 2L_{(g)}$$

$$-\Delta H_r^2 \qquad\qquad \downarrow Q_g$$

$$ML_2X_{2(cryst)}$$

Figure 5

U_{exp} is the work done in expanding the crystalline MX_2 lattice until it can accept the molecules of L in the positions they are to occupy in the complex. By comparison with the first cycle, shown above, it is clear that: $U_{exp} + Q_{(g)} = S_2 - S_1 - \Delta H_g$. If Q_g and $(-\Delta H_g)$ were equal, which is most unlikely but which was assumed by Ablov, then U_{exp} would equal $S_2 - S_1$. Their arguments, therefore, in considering a possible connection between U_{exp} and $S_1 - S_2$ can not be considered valid, which conclusion detracts from the possible value of their work.

J.L. Wood and M.M. Jones (76) have devised a thermochemical cycle similar to the one used in this work which differs only in the ligands used and the type of calorimetric measurements employed. Whereas heats of decomposition are used in this work, Wood and Jones made use of heats of combustion which lead to a rather more complicated cycle. The cycle used here is shown in Figure 6.

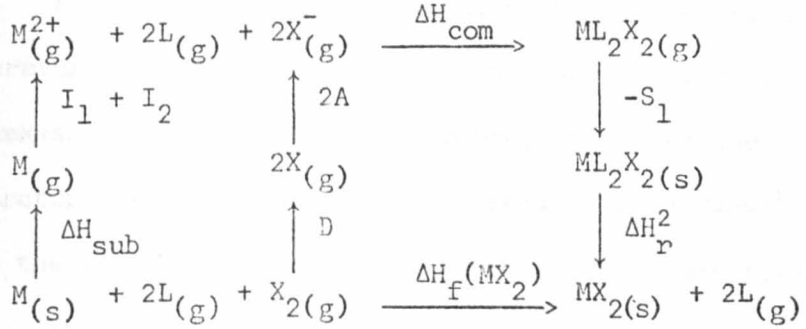

Figure 6

From this, one arrives at the following equation:-

$$\Delta H_{com} = \Delta H_f(MX_2) - \Delta H^2_r - (D + 2A) - (\Delta H_{sub} + I_1 + I_2) + S_1$$

where: ΔH_{com} = heat of the gas phase complexation reaction

$\Delta H_f(MX_2)$ = the heat of formation of the metal halide

ΔH^2_r = the measured heat of decomposition

D = the heat of dissociation of the halogen molecule

A = the electron affinity of the halogen atom

ΔH_{sub} = the heat of sublimation of the metal

I_1, I_2 = the first and second ionisation potentials of M

S_1 = the heat of sublimation of $ML_2X_{2(s)}$.

S_1 is not known with accuracy but for many pyridine and picoline complexes it is expected to be fairly constant since it is known that the heats of solution, in chloroform, of many such complexes do not differ by more than ±0.75Kcal./mole (77). If this is taken to indicate that the interactions within the crystal are similar, then S_1 should be invariant for the same reason.

All the values in the cycle should be referred to the temperature of measurement. The heat capacities of only a few of the complexes have been measured, however, which precludes such a temperature correction. It would necessarily be superfluous, however, since the uncertainties in many of the other quantities are large.

In order to detect a variation in the heats of the gas phase complexation reactions, S_1 may be neglected since it has been assumed constant. The remaining data are summarised in tables (1), (2) and (3).

Table 1 : Electron Affinities and Dissociation Energies

Halogen	Electron Affinity (Kcal./g.atom)	Dissociation Energy (Kcal./mole)
Cl	87.2	57.2
Br	81.7	45.4
I	74.7	35.5

Table 2 : Heats of sublimation and first and second ionisation potentials

Metal	Heat of sublimation (Kcal./g. atom)	First and second ionisation potentials (Kcal./g. atom)
Ca	42	415
Cr	95	536
Mn	67	532
Fe	100	555
Co	102	574
Ni	101	594
Cu	81	646
Cd	27	597

4.3.2 ML_4X_2 Compounds

The ML_4X_2 compounds normally decompose firstly to ML_2X_2 compounds. Since the latter are thought to have similar intermolecular forces it may be assumed that the same is true for the ML_4X_2 type of compound, especially since these are all discreet octahedra. The solid state heats of decomposition may be compared, therefore, for these compounds directly.

4.4 The Pyridine and Picoline Complexes

These complexes fall into three categories:

(1) Octahedral - ML_4X_2 (monomer)

(2) Octahedral - ML_2X_2 (polymer)

(3) Tetrahedral - ML_2X_2 (monomer)

In addition, there are intermediate decomposition products of the types MLX_2 and $ML_{2/3}X_2$ which appear to be distorted octahedral polymeric compounds (49).

In connection with the stereochemistry of the complexes, dichlorodipyridinecobalt (II) is of particular interest. This compound exists in both octahedral and tetrahedral forms, as previously mentioned. The heat of transformation, ΔH, from the octahedral to tetrahedral forms, was found to be $+3.02 \pm 0.07$Kcal./mole, which is very close to the value reported by Wendlandt (78) of $+ 3.2 \pm 0.1$Kcal./mole.

(1) ML_4X_2 Compounds

These compounds usually decompose firstly to the bis ligand complex, ML_2X_2. Less frequently, MLX_2 compounds are the first stage decomposition products and these mono ligand complexes are always formed by the decomposition of the bis ligand complexes. It is convenient to group the compounds according to the stereochemistry of the decomposition product:

(a) Giving octahedral ML_2X_2(cryst.)

Compound	Reference	Heat of the decomposition $ML_4X_{2(cryst.)} \rightarrow ML_2X_{2(cryst.,oct.)} + 2L_{(g)}$
$CrPy_4I_2$		26.1 ± 0.4
$FePy_4Cl_2$	56	27.0 ± 0.4
$Fe(\beta\text{-pic})_4Cl_2$	56	29.2 ± 0.6
$Nipy_4Cl_2$	51	24.5 ± 0.1
$Ni(\beta\text{-pic})_4Cl_2$	51	25.7 ± 0.6
$Nipy_4Br_2$	51	23.9 ± 0.2

(b) Giving tetrahedral ML_2X_2(cryst.)

Compound	Reference	Heat of the decomposition $ML_4X_{2(cryst.)} \rightarrow ML_2X_{2(cryst.,tet.)} + 2L_{(g)}$
$Co(\gamma\text{-pic})_4Cl_2$	49	32.9 ± 0.8
$Co(\gamma\text{-pic})_4Br_2$	49	32.8 ± 0.8
$Co(\beta\text{-pic})_4Br_2$	49	30.0 ± 0.3
$Copy_4I_2$	49	28.4 ± 0.7
$Co(\gamma\text{-pic})_4I_2$	49	30.4 ± 0.6
$Nipy_4I_2$	51	34.2 ± 0.4

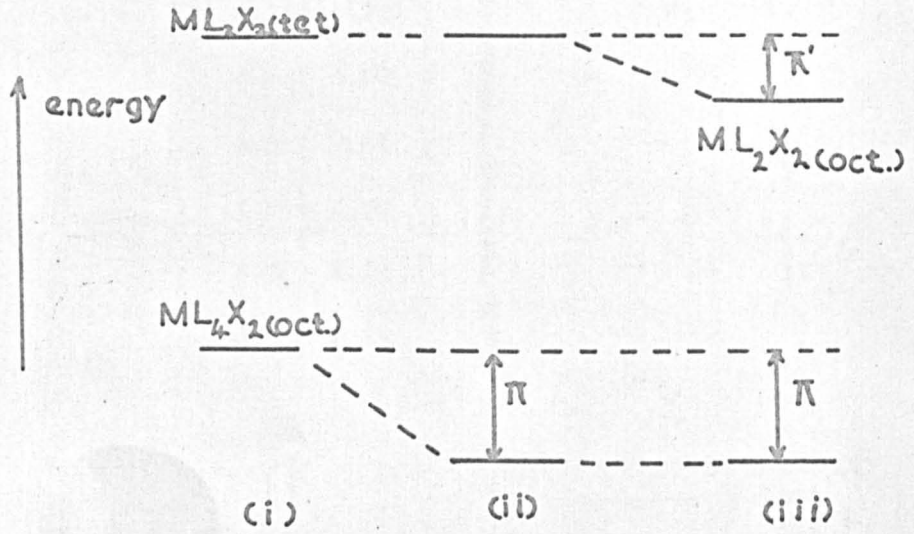

Fig (7)

(c) Giving octahedral MLX_2(cryst.) as a first, or second, stage decomposition product

Compound	Reference	Heat of the decomposition $ML_4X_{2(cryst.)} \rightarrow MLX_{2(cryst.,oct.)} + 3L_{(g)}$
$Fepy_4Cl_2$	56	42.2 ± 0.5
$Fe(\beta\text{-pic})_4Cl_2$	56	43.6 ± 0.6
$Fe(\gamma\text{-pic})_4Cl_2$	56	41.3 ± 0.5
$Nipy_4Cl_2$	51	40.1 ± 0.2
$Ni(\beta\text{-pic})_4Cl_2$	51	39.0 ± 0.6
$Ni(\gamma\text{-pic})_4Cl_2$	51	45.8 ± 0.6
$Nipy_4Br_2$	51	40.2 ± 0.3

Figure (7) shows an idealised energy scheme wherein the compounds initially (i) have only σ metal-ligand bonds. In (ii), π-bonding is also present in the starting material and in (iii), π-bonding is also present in the decomposition product. It would be expected that π-bonding between the metal and the ligands should be more important in octahedral than in tetrahedral complexes since, in the former, the t_{2g} set of orbitals are conveniently oriented towards the ligands. In the tetrahedral molecules, the t_2 set point between the ligand and dπ-bonding is not expected to be so efficient.

From Figure (7) we see that heats of decomposition of the ML_4X_2 compounds which give tetrahedral decomposition products should be greater than those obtained from the compounds which give octahedral products. Not only is the π-bonding ability lost in the tetrahedral

compounds but also there must be a sizeable heat effect on formation of the polymeric lattice. In fact, the heats of decomposition are in the predicted order which would seem to give some support to the proposals outlined above.

Also, it would be expected that the electron densities at the 2 and 6 positions of the pyridine nucleus would affect the extent of back π-bonding. If these positions have large negative charges, the t_{2g} set will be repelled and, conversely, they will be less repelled if the 2 and 6 positions are not highly charged. Electron releasing substituents at the 2, 4 or 6 positions should increase the electron densities at positions 1, 3 and 5 whereas substituents at the 3 or 5 positions will tend to increase the electron densities at positions 2, 4 and 6. 3 or 5 substitution (the β-positions) should, therefore, hinder back π-donation whereas 4 substitution (γ) should have little effect. Since all positions are slightly increased in electron density by either β or γ substitution of an electron releasing group for a proton, then back π-donation should be inhibited with all the substituted ligands; at the same time, the σ contribution should increase with the increased basicity of the substituted bases. Also, the ability of the metal ion to back-donate should increase with the number of t_{2g} electrons, if only because back donation should decrease the repulsive forces between these electrons. It also will increase when more polarisable ligands are used. The tendency of atoms to dispose of an acquired high charge is familiar as "Pauling's Electro-neutrality Principle", which suggests that atoms decrease their charge, by some mechanism, to between ±1 electronic charges if possible.

In group (b) it is seen that the heats of reaction for the dihalogenotetrakis (γ-picoline) cobalt(II) complexes are very nearly the same, regardless of which halogen is present in the complex. A possible explanation of these facts is that on replacing chlorine with a more polarisable halogen, the σ bond strength will decrease; at the same time, the high acquired charge on the metal which should weaken the σ bonds is disposed of by back π-bonding onto the ligands. This synergic process should ensure a constancy of bond strength in the tetrakis complexes. Dibromotetrakis(β-picoline)cobalt(II) has a slightly lower heat of decomposition than its γ-picoline analogue, possibly reflecting the lesser ability of β-picoline to accept back donated charge. Diiodotetrapyridinecobalt (II) has a heat of decomposition lower than that of the corresponding γ-picoline complex which may be due to the greater basicity of γ-picoline in the latter case.

The group (a) compounds do not show such interesting variations in heats of reaction as do the group (b) compounds since the products are octahedral and, presumably, retain a considerable amount of π-bonding. The heats of decomposition of $Ni(\beta\text{-pic})_4Cl_2$, $Nipy_4Cl_2$ and $Nipy_4Br_2$ are all closely similar and much lower than the heat of decomposition of $Nipy_4I_2$. This may reflect the absence of π-bonding in the tetrahedral compound, $Nipy_2I_2$, but the latter is monomeric and changes in intermolecular forces may be considerable.

Although we do not have corresponding data for the γ-picoline complexes of nickel, it is of interest to compare the heats of decomposition of the compounds in group (c) wherein it is seen that the compound $Ni(\gamma\text{-pic})_4Cl_2$ has a markedly higher heat of decomposition than its β-picoline or pyridine analogues. It is suggested that this is a π- rather than σ-bonding effect since there is little difference between the heats of decomposition of the pyridine and β-picoline complexes and the latter ligand is only slightly less basic than γ-picoline. Precisely similar effects are seen for the group (c) heats of decomposition of complexes of iron (II); the γ-picoline complex gives the highest value while the β-picoline and pyridine complexes have quite similar, lower, heats. This would seem to indicate that β-picoline offers quite a high resistance to back π-donation.

It is convenient, at this point, to review the data obtained by other workers concerning other physical properties of these complexes to show that there is some correlation between them. In particular, spectroscopic and thermodynamic measurements should lead to similar conclusions regarding the bonding in these compounds.

Infra-red Spectroscopic Measurements

Some of the compounds discussed here have been studied by infra-red methods by Clark and Williams (79) and Frank and Rogers (80). The value of their results is lessened by the incompleteness of many series of compounds and by the fact that it is difficult to attach too much significance to such data which are not precise to better than $\pm 3cm^{-1}$

since this uncertainty is frequently greater than the differences in the metal-ligand vibrational frequencies. These frequencies should be most sensitive to metal-nitrogen bond strength. It should be emphasised that the uncertainties quoted above are quite normal in this work and that this should be borne in mind when comparing very small frequency differences.

However, taking the results from the Clark and Williams paper as the more complete set, the metal ligand stretching frequencies can be arranged in the order:-

$$Copy_4Cl_2 \sim Copy_4Br_2 < Ni(\beta\text{-pic})_4Cl_2 < Nipy_4Br_2 \sim Nipy_4Cl_2 \sim Nipy_4I_2$$

Incomplete as the series is, the similarity of the stretching frequencies in compounds with the same ligand and various halogens parallels the thermochemical data reported above. The ß-picoline nickel (II) complex has a lower stretching frequency than the corresponding pyridine complex but this is misleading since the masses of the ligands differ. This will alter the stretching frequency since this frequency is inversely proportional to the square root of the reduced mass of the oscillator. Assuming a nickel atom and ligand to be the oscillator and by calculating the reduced mass of the system in each case, an approximate estimate may be made of the force constant in each oscillator. This is found to be 1.1×10^5 dynes/cm for each complex so that, despite the simplicity of the argument, it would seem that the bond strengths are very similar in the two compounds, as predicted from the thermochemical data.

Ultra-Violet Spectroscopic Measurements

Detailed electronic spectra have been recorded for some of the compounds reported here by Sharp et al.(49, 51) and Goodgame et al.(73). Lever et al.(81) have also calculated the crystal field parameters 10Dq and B for complexes of the type NiL_2X_2. 10Dq was found to be greater in bromides than in chlorides and this was explained in terms of greater metal to ring π-bonding being induced by the greater polarisability of the bromine atom. It was further demonstrated that β-substitution is more effective than γ-substitution in repelling back-co-ordinated charge.

Nelson and Shepherd have published details of further work on the subject of Nickel(II)halide and pseudo-halide complexes with heterocyclic ligands in which the same general conclusions are reached (85) namely that there is significant π-bonding in such complexes and that the positions of the ring substituents govern the degree of such bonding.

Thermodynamic Measurements

Nelson and his co-workers (82, 83, 84, 86) and Libus and Uruska (87) have made thermodynamic measurements on compounds similar or identical to these reported here. Using a pyridine-chlorobenzene solvent, Libus and Uruska have calculated equilibrium constants for the equilibrium

$$Mpy_2Cl_{2(soltn)} + 2Py_{(soltn)} = MPy_4Cl_{2(soltn)}$$

by measuring the concentrations of the various species involved.

They found that the equilibrium constants had a minimum value at manganese, rising to nickel and falling again to zinc. These authors suggested that all the MPy_2Cl_2 complexes are tetrahedral and that their results reflect the differences in crystal field stabilisation energies of the octahedral and tetrahedral compounds. In fact, only the cobalt and zinc compounds are thought to be tetrahedral and, therefore, this part of their argument should be disregarded.

Nelson's work was found to be more interesting, since, in addition to measurements of equilibrium constant, he has reported heats of reaction for reactions similar to those reported in this thesis. Nelson's measurements were made for both solid state decompositions and for solution equilibria and all of these are referred to room temperature. It is of interest to note that he found parallel trends in the various heats of reaction in spite of the differences in the absolute values obtained by the two calorimetric techniques. Table 3 summarises some of Nelson's results and compares them, where possible, with those reported here.

Table 3

Heats of decomposition for $ML_4X_{2(s)} \rightarrow ML_2X_{2(s)} + 2L_{(g)}$

Compound	Nelson et al (86) (Kcal./mole)	This work (K.cal/mole)
$Copy_4Br_2$	33.7	
$Copy_4I_2$	36.2	28.4
$Co(\beta\text{-pic})_4Cl_2$	34.5	
$Co(\beta\text{-pic})_4Br_2$	33.3	30.0
$Co(\beta\text{-pic})_4I_2$	31.9	

Table 3 (continued)

Compound	Nelson et al (Kcal./mole)	This work (Kcal./mole)
$Co(\gamma\text{-pic})_4Cl_2$	38.5	32.9
$Co(\gamma\text{-pic})_4Br_2$	38.1	32.8
$Co(\gamma\text{-pic})_4I_2$	34.7	30.4

Nelson has concluded that the results he obtained are best explained by invoking π-bonding. As was stated previously, β-picoline should have poor π-bonding capability, whereas pyridine should be rather better and γ-picoline should be intermediate. Consequently, the heat of decomposition for the pyridine complexes increases on going from bromide to iodide but decreases for the complexes of β- and γ-picoline from chloride to iodide. In this work, we were only able to obtain data for the γ-picoline complexes but it is seen that these parallel those reported by Nelson. There is a difference in the absolute magnitudes of the heats of reaction and this may be due to the fact that the data reported here were obtained at higher temperatures than those of Nelson and a Kirchoff correction would be required before such a comparison could be made.

Nelson has also calculated the entropy changes for the various reactions from the equation $\Delta G = \Delta H - T\Delta S$. We found these changes to be in excess of those required for loss of translational degrees of freedon and dependent on the ligand used. This was attributed to a degree of rigidity in the metal-nitrogen band which could be caused by π-bonding. Measurements of heat capacities are reported later in this thesis which would seem to support this argument.

The Convergence of the Heats of Formation of Octahedral and Tetrahedral Complexes after Correction for Crystal Field Stabilisation

Nelson (82) in studying the reaction

$$P\ Mpy_2I_{2(s)} + 2Py_{(g)} \rightarrow Mpy_4I_{2(s)}$$

has compared the experimental difference in the heats of reaction for M = Co and Ni with that expected from crystal field theory. Assuming that the heats of formation of octahedral Mpy_4I_2 and of tetrahedral Mpy_2I_2 parallel each other, the difference in the heats of reaction should be given by the following expression, in which the crystal field stabilisation energy of the various species is represented by CFSE:

$$\{CFSE(Ni_{oct}) - CFSE(Ni_{tet})\} - \{CFSE(Co_{oct}) - CFSE(Co_{tet})\}$$

For the medium field case, this reduces to:

$$\{12Dq(Ni_{oct}) - 8Dq(Ni_{tet})\} - \{8Dq(Co_{oct}) - 12Dq(Co_{tet})\}$$

Nelson assumed a value for 10Dq of $9200cm^{-1}$ for the octahedral cobalt and nickel complexes and of $5000cm^{-1}$ and $3800cm^{-1}$ for the tetrahedral nickel and cobalt complexes respectively. The calculated difference in the heats of reaction, using these data, is then calculated to be -12.1Kcal./mole. Allowing for the uncertainties involved in this calculation, Nelson allowed this figure to be in error by not more than ±2Kcal. The experimental difference was found by Nelson to be -7.2Kcal and in this work to be -5.8Kcal., using the differential scanning calorimeter. Our results support, therefore, the suggestion made by Nelson that there is a convergence of the heats of formation of the

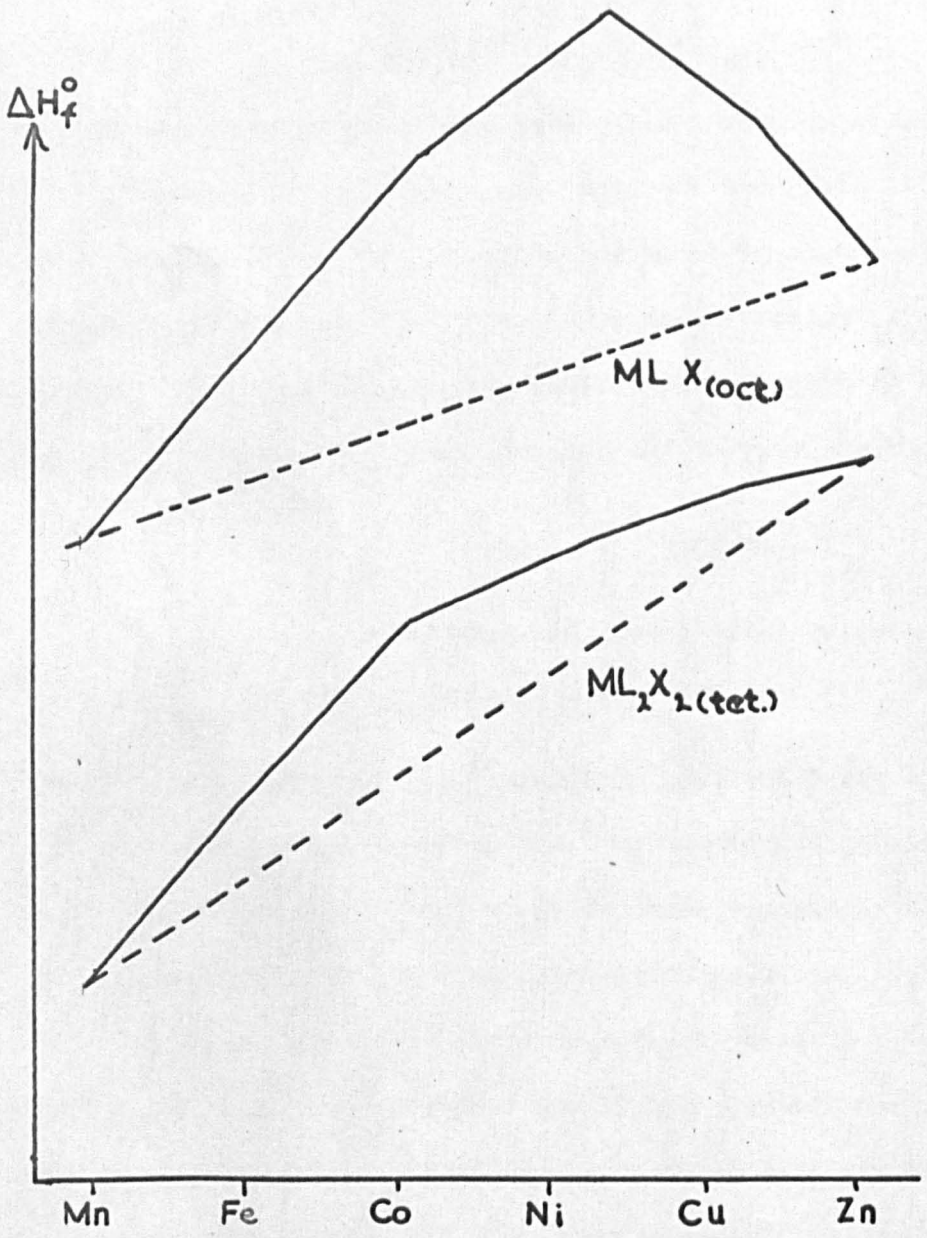

Fig (8)

octahedral and tetrahedral complexes studied on passing from cobalt to nickel after correction for crystal field effects. This is illustrated in Figure 8.

Gill and Nyholm came to similar conclusions on the basis of qualitative arguments (88) and Blake and Cotton (89) observed a similar convergence during their thermochemical investigations of the reactions:

$$MCl_4^{2-}{}_{(aq)} + aq \rightarrow M(H_2O)_6^{2+}{}_{(aq)} + 4Cl^-_{(aq)}$$

These authors found the closing of the gap on passing from cobalt to nickel to be 5.5 to 7.0Kcal./mole, but the overall convergence from manganese to zinc was found to be rather smaller, on the average, between each pair of elements. This could not be confirmed in this work since most of the ML_2X_2 reaction products were octahedral rather than tetrahedral.

(2) ML_2X_2 Compounds

It has been discussed in an earlier section that by using thermochemical cycles, quantities may be derived from the measured heats of decomposition which should be of greater interest than the latter. The first of these quantities is $\Delta H_{(g)}$ (see Figure 4) which is the heat required to remove two moles of ligand from the metal complex leaving the metal halide, all substances being in the gaseous state. ΔH_{com} is the second quantity of interest; this is the heat of the gas phase complexation reaction (Figure 6) but is usually replaced by $\Delta H'_{com}$ which differs from ΔH_{com} only by the heat of sublimation of the metal complex. S_1, the heat of sublimation of the complexes has been assumed to be approximately 15Kcal./mole. This could be considerably in error

Table 4

Compound	ΔH_r [2]	$-\Delta H_f(MX_2)$(49)	$I_1+I_2+\Delta H_{sub}$	$-(D+2A)$	S_2	S_1	$-\Delta H'_{com}$	ΔH_g
$Copy_2Cl_2$	28.6						674	75
$Co\alpha pic_2Cl_2$	26.2						672	73
$Co\beta pic_2Cl_2$	23.1	77.8		108	61.9(a)		669	69
$Co\gamma pic_2Cl_2$	31.0						676	78
$Copy_2Br_2$	27.3		676				636	72
$Co\alpha pic_2Br_2$	21.2	51.0		118	Not Known **	Estimated to be -15 Kcal./mole	630	66
$Co\beta pic_2Br_2$	16.9						626	61
$Co\gamma pic_2Br_2$	23.7						633	69
$Copy_2I_2$	12.3						586	57
$Co\alpha pic_2I_2$	12.2	21.0		123	Not Known **		586	57
$Co\gamma pic_2I_2$	11.0						585	56
$Mnpy_2Cl_2$	28.5				55.0(a)		632	73
$Mn\beta pic_2Cl_2$	32.1	112.0	599	108	Heat of fusion from (b)		635	77
$Mn\gamma pic_2Cl_2$	34.5						638	80
$Fepy_2Cl_2$	30.6				50.6(a)		659	67
$Fe\beta pic_2Cl_2$	38.8	81.5	655	108	Heat of fusion from (17)		667	75
$Crpy_2Cl_2$	32.5	97.0		108	63.0(b)		653	80
$Crpy_2Br_2$	31.6	76.0*	631	118	67*		621	79
$Crpy_2I_2$	24.8	37.8		123	71.4(c)		571	81
$Nipy_2Cl_2$	32.6						693	77
$Ni\alpha pic_2Cl_2$	15.8	73		108	59.1(a)		676	60
$Ni\beta pic_2Cl_2$	33.6		695				694	78
$Nipy_2Br_2$	33.3	33.3		118	** Not		662	77
$Nipy_2I_2$	31.6	31.6		123	Known **		627	78
$Cupy_2Cl_2$	28.0	28.0	727	108	Not Known		696	
$Cdpy_2Cl_2$	30.4	30.4	624	108	41.2(b)		639	56

* estimated ** estimated to be about 60Kcal./mole

(a) H. Schafer, L. Bayer, G. Breil, K. Etzel and K. Krehl, Z. Anorg. Chem. 278, 300 (1955).

(b) "Metallurgical Thermochemistry" O. Kubaschewski & E.LL. Evans Pergamon Press (1958)

(c) "Selected Values of Chemical Thermodynamic Properties" National Bureau of Standards, Circular 500.

but no measurements have been reported and this estimate is based on a calculation by Ablov (75) concerned with complexes of aniline which are of similar stoichiometry to the pyridine complexes studied here. Certain heats of sublimation of the metal halides were not obtainable and these, also, have been estimated where applicable.

The calculation of ΔHg permits comparison between compounds of various metal halides and also gives an estimate of the metal-nitrogen bond energy - that is, the energy evolved when the gaseous nitrogen-containing ligand combines with an isolated gaseous molecule of the metal halide. For cobalt chloride, this was found to be 75Kcal./mole of $Copy_2Cl_2$ for the removal of two moles of pyridine. Ablov (75) found that the corresponding heat for the aniline complex was 95Kcal./mole at room temperature. All our data use heats of reaction obtained at the temperatures of decomposition and do not include Kirchoff corrections.

From Table 4, it is seen that the complexes fall into two groups. The heats of decomposition, ΔHg, of the cobalt decrease in the order:

iodides < bromides < chlorides

The chromium and nickel complexes yield ΔHg values which do not depend strongly on the halogen used with the exception of $Ni(\alpha\text{-pic})_2Cl_2$ which has a very low value of ΔHg. This may be explained by the fact that the cobalt complexes are all tetrahedral whereas most of the remaining ones are octahedral. In the latter, on passing from chloride to iodide, increasing charge will be acquired by the metal atom which should weaken the nitrogen to metal sigma bonds. At the same time, back π-donation from the metal to the ligand should be enhanced with the result that the bonds remain

essentially constant in strength regardless of the halogen ligand. This in turn suggests that the heats of decomposition should stay fairly constant. In tetrahedral compounds, in which π-bonding is not expected to be as effective as in octahedral compounds, this π-bond enhancement should not occur to such a marked extent and substitution of bromide or iodide for chloride would be expected to progressively weaken the metal-nitrogen bond and hence lower the heat of decomposition. It would be expected that ΔHg for $Nipy_2I_2$ would be lower than ΔHg of the analogous chloride and bromide complexes. This was not found to be so but it should be emphasised that this may have its origin in the estimated value of the heat of sublimation of nickel iodide. For a particular metal halide, either ΔH_r[2]or ΔHg values may be compared since they differ only by a constant term involving heats of sublimation. As ΔHg values have been used so far this will be continued for the sake of consistency. ΔHg values of the cobalt chloride complexes are at a maximum for the γ-picoline complex. The pyridine complex (β-$Copy_2Cl_2$), which contains a less basic ligand has a lower ΔHg while the α-picoline complex falls still lower, presumably for steric reasons. The position of the β-picoline complex is, as yet, inexplicable since there seem to be no factors, steric or otherwise, to significantly weaken the metal-nitrogen band. The analogous complexes of cobalt bromide were prepared and a similar result obtained: the β-picoline complex having the lowest ΔHg while the other complexes of cobalt bromide gave ΔHg values which fell into a similar order to that obtained for the cobalt chloride complexes. This behaviour was not found for any of the other complexes examined in

this work. ΔHg for the manganese complexes, for example, is in the order which might be expected:

$$Mn(\gamma\text{-pic})_2Cl_2 > Mn(\beta\text{-pic})_2Cl_2 > Mnpy_2Cl_2$$

It was found that the complex $Ni(\alpha\text{-pic})_2Cl_2$ has a very low ΔHg when compared with the other complexes of nickel chloride and also when compared with $Co(\alpha\text{-pic})_2Cl_2$. Both of these complexes are tetrahedral and it might at first seem surprising that the bonding is much weaker in one than in the other when they differ only in the central atom. It would not be expected that this difference would give rise to any steric interactions due to the similar sizes of the two atoms (or ions) concerned. It is of interest to compare the loss in crystal field stabilisation energy (CFSE) for the cobalt and nickel complexes which occurs when each of the complexes decompose into their parent halides, which possess octahedral structures. It was thought that this might explain the data since cobalt(II) possesses the greatest CFSE for tetrahedral divalent ions whereas nickel(II) has the greatest CFSE for octahedral divalent ions. Nelson and Shepherd (81) calculated 10Dq for octahedral-$NiCl_{2(s)}$ to be 7,200cm^{-1} and this value has also been used for $CoCl_{2(s)}$. As an approximation 10Dq for the tetrahedral $M(\alpha\text{-pic})_2Cl_2$ was presumed to be half this value. The calculated difference in the change of CFSE for the nickel and cobalt complexes decomposing to the parent metal halides is given by the following:

$$(\text{CFSE Ni}_{oct} - \text{CFSE Ni}_{tet}) - (\text{CFSE Co}_{oct} - \text{CFSE Co}_{tet})$$

$$= 12\ Dq\ Ni_{oct} - 8\ Dq\ Ni_{tet} - 8\ Dq\ Co_{oct} + 12\ Dq\ Co_{tet}$$

$$\simeq 6\ Dq\ M_{oct}$$

Therefore, the calculated stability difference is -4,300cm^{-1} or -12.2Kcal.

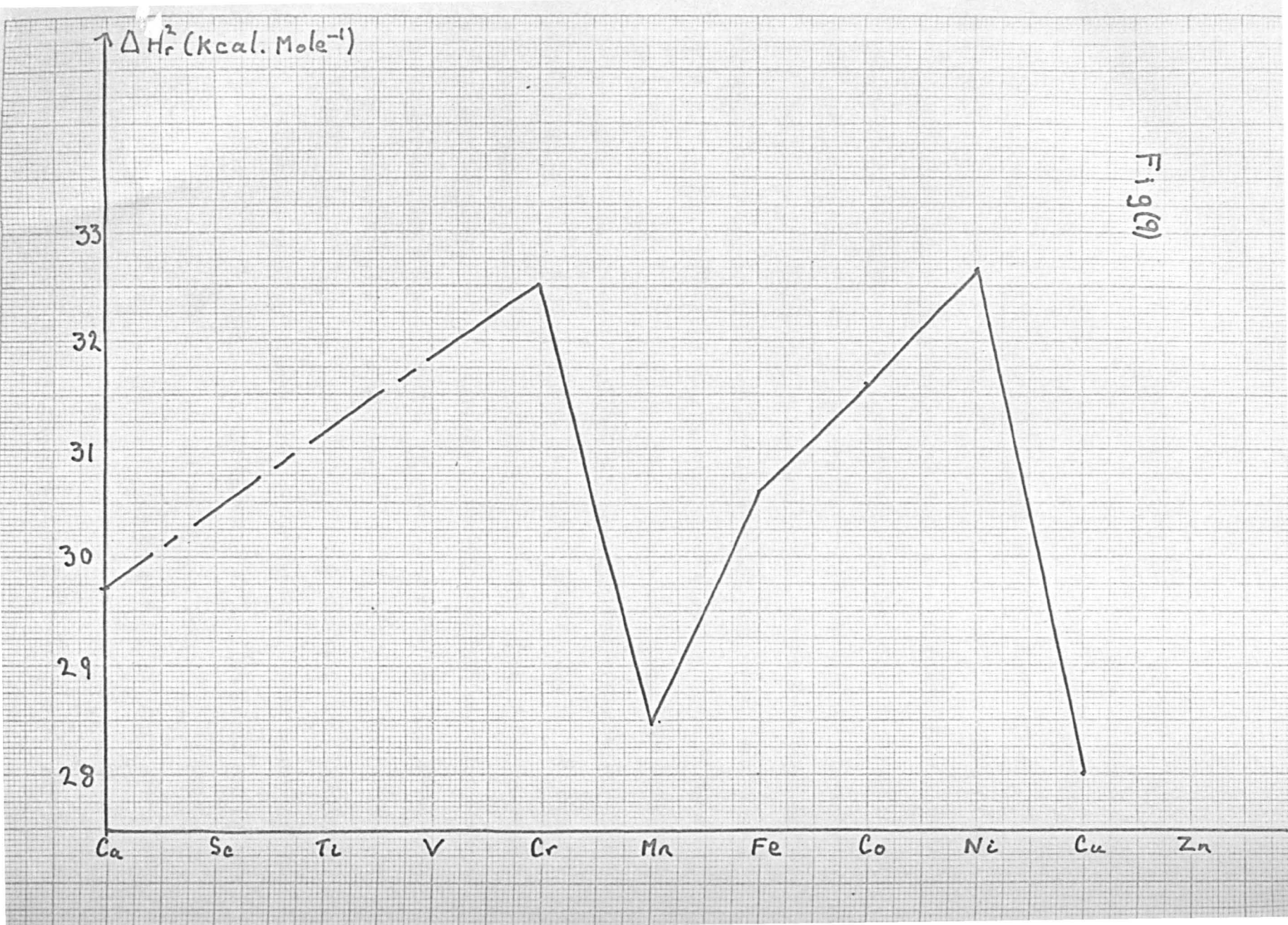
ΔH_r^2 (Kcal. Mole^{-1})
33
32
31
30
29
28
Ca
Sc
Ti
V
Cr
Mn
Fe
Co
Ni
Cu
Zn

Fig (9)

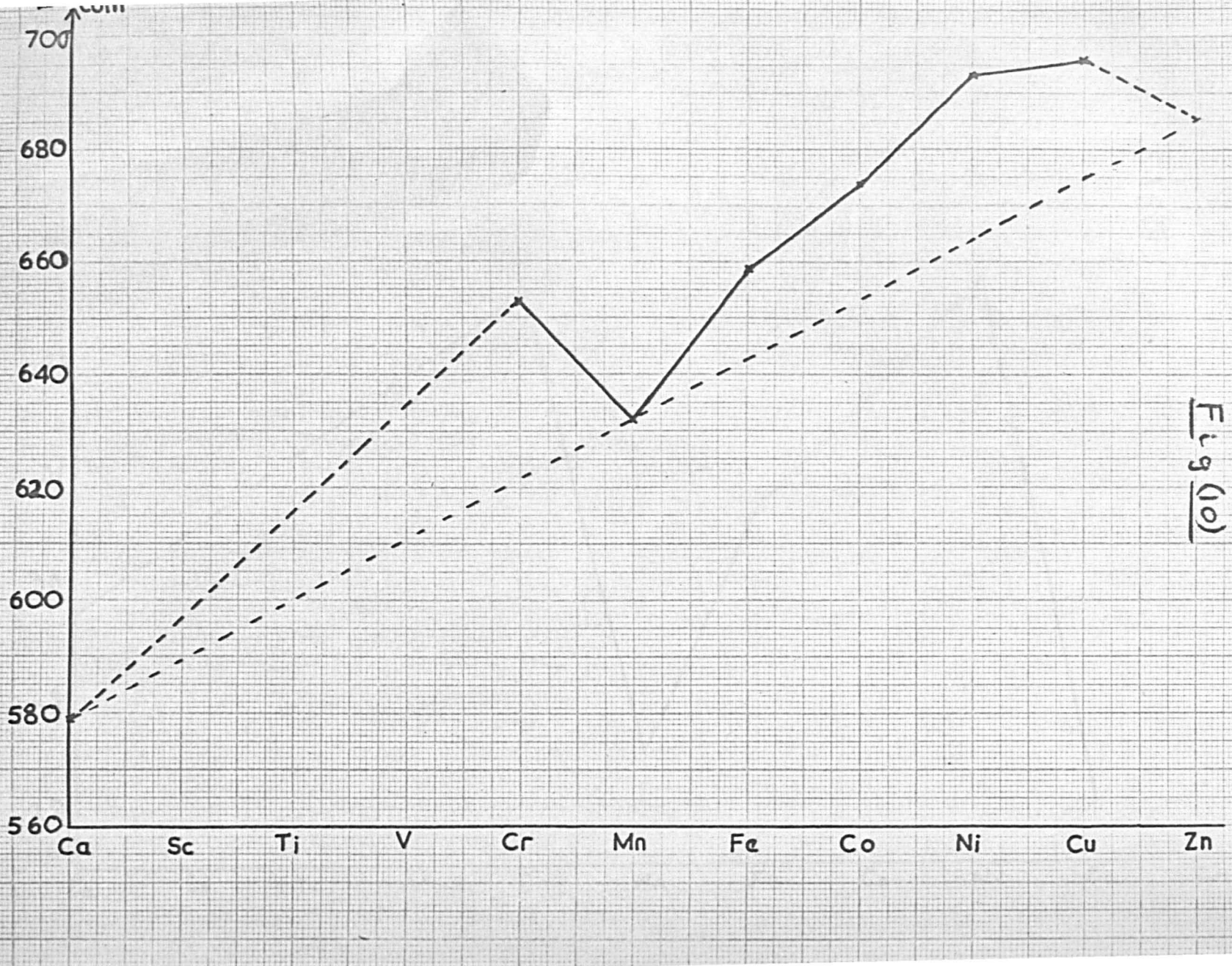

Fig (10)

The experimental difference is approximately -11 Kcal. so that it would seem that the data are in fact explained by purely crystal field arguments.

Crystal field theory predicts that CFSE should be a function of the atomic number of the transition metal ion present in a complex compound. This stabilisation energy is expected to manifest itself in the thermodynamic properties of these complexes. It might be expected that the heat of decomposition, ΔH_r^2, or the heat of the gas phase reaction, ΔHg, would be suitable quantities to illustrate this variation. There are objections to using these, however, since ΔH_r^2 includes solid state interaction energies and ΔHg refers to gaseous metal halides for which the structures are largely unknown. A more useful quantity is ΔH^1_{com} (Figure 6) since, firstly, the only stereochemistry involved is that of the complex and, secondly, the gas phase complexation reaction (Figure 6) introduces the crystal field stabilisation energy as a first order effect rather than as a change on going from the metal halide to the complex. Therefore, a plot of ΔH^1_{com} against atomic number show a greater variation than either ΔHg or ΔH_r^2.

ΔH_r^2 and ΔH^1_{com} have been plotted in Figures (9) and (10) for the dichlorodipyridine complexes. Similar plots for other complexes may be drawn but it is not then justifiable to include the cobalt complexes which are all, with the exception of α-$Copy_2Cl_2$, tetrahedral monomers whereas the other metal complexes are octahedral polymers. From Figure (10) it is seen that ΔH^1_{com} is minimal at manganese, rises to chromium on the one side and through iron, cobalt, nickel and copper on the other. ΔH_r^2 is rather low for copper and this may be caused by the different crystal structure

of copper chloride compared to the other metal halides. The variation of ΔH^l_{com} is just that expected from crystal field theory (31) and similar to the variation of other thermochemical quantities (28). If a line is drawn, on the graph of ΔH^l_{com} vs. atomic number, from calcium through manganese, the deviation from this line of the experimental points is found to be between 5 and 10% of ΔH^l_{com}. This indicates the percentage of the total binding energy due to crystal field effects and serves to emphasise the smallness of these effects.

ΔH^l_{com} decreases rapidly with increasing atomic number of the halogen in all cases due to the lower electronegativity of the heavier halogens.

Estimation of 10Dq, the crystal field splitting parameter

In the absence of crystal field effects, the heat of complexation of a metal ion would be expected to rise smoothly, if not linearly, with increasing atomicnumber of the metal ion due to theincreasing nuclear charge of that ion. Any deviation from this smoothly varying quantity is attributed to crystal field effects.

Since calcium, manganese and zinc are not stabilised by a cubic crystal field, the heats of complexation of the ions of these metals should lie on the line which represents the heat of complexation in the absence of crystal field effects. The heats of complexation of the remaining metals should then lie above this line and the extra stabilisation is the crystal field stabilisation energy of the metal ion. Data were not available for $Znpy_2Cl_2$ but by extrapolating a line from calcium through manganese (Figure 10), the heat of complexation for Ni^{2+} was found to be about 28Kcal. above the extrapolated line. In terms of wave numbers, this becomes

9825cm^{-1} and, since the CFSE of octahedral divalent nickel is 12Dq 10Dq is calculated to be about 8,200cm^{-1}. An uncertainty of about ± 10% is expected but the value is in good qualitative agreement with the spectroscopic value of ~8,500cm^{-1} (81). As pointed out by Figgis (31), it is unreasonable to expect exact agreement due to the arbitrary nature of the interpolation procedure since the change in, for example, lattice energy (which he quoted) with the number of d electrons is by no means linear in the absence of CFSE.

4.5 The Aniline Complexes

Many aniline complexes have been prepared since the early work of Leeds (90) and more recent work has been mentioned by Ahuja et al (60). These workers studied the thermal decomposition of many aniline complexes and isolated new complexes as decomposition products. In this work we were not able to resolve separate peaks in the thermograms except in the case of the iron complex. Calorimetric measurements have been reported by Ablov (75, 91) for the reaction

$$CoA_2X_{2(s)} \rightarrow CoX_{2(s)} + 2A_{(l)} \qquad (A = \text{aniline or substituted aniline})$$

at room temperature.

The data we obtained are summarised in table 5 using the usual abbreviations.

Table 5 : MAn_2Cl_2 Complexes

Compound	ΔH_r^2(Kcal./mole)	$-\Delta H_{com}^1$(Kcal./mole)
$CdAn_2Cl_2$	32.9	642
$MnAn_2Cl_2$	30.1	633
$FeAn_2Cl_2$	27.9	655
$CoAn_2Cl_2$	35.5	681
$NiAn_2Cl_2$	32.2	697

$FeAn_6Cl_2$ was the only aniline complex studied in this work which had more than two molecules of aniline per metal atom. Hexakis-aniline complexes are rare, but a report of such complexes with metal perchlorates has been published (92). The infra-red spectrum of the compound indicated the presence of aniline and the gas evolved during decomposition gave a spectrum identical to that of aniline. Initially, the complex lost four molecules of aniline to form $FeAn_2Cl_2$. This decomposition recurred in two stages - the first of which was not accompanied by a weight loss since it occurred below the boiling point of aniline. The weight loss in the second stage corresponded to the loss of four molecules of aniline and almost 50Kcal./mole of complex were required for these two stages. This is rather less, per mole of ligand, than in the case of the ML_4Cl_2 compounds (L = picoline) and may be attributed to the weaker basicity of aniline and its inability to participate in metal-ring π-bonding.

As for the pyridine and picoline complexes, the decomposition into metal halide occurs at relatively high temperatures. This may preclude an absolute comparison of the ΔH_r^2 values for the aniline and pyridine complexes because of the uncertainty in the magnitude of the Kirchoff correction, $\int \Delta C_p dT$.

It was found that, as for the pyridine complexes, ΔH^1_{com} rose from manganese through to nickel, Less data are available for the aniline complexes since it has not been possible to obtain useful data from the copper complex and the chromium(II) complex has not yet been prepared.

For the reaction

$$CoCl_{2(g)} + 2An_{(g)} \rightarrow CoAn_2Cl_{2(g)}$$

Ablov has calculated that the heat of addition is 95Kcal/mole. Using Ablov's estimate of the heat of sublimation of $CoAn_2Cl_2$ (~14Kcal./mole) we calculated the heat of the same reaction to be about 83Kcal./mole. Our estimate, using data obtained at high temperatures, is much less than that of Ablov, obtained at room temperature. This suggests that there is a considerable heat capacity correction to be made before a direct comparison may be made between the two sets of data. It has already been mentioned (see "Heats of solid state reactions") that Ablov confused certain thermochemical data concerning the reaction:

$$CoAn_2Cl_{2(s)} \rightarrow CoCl_{2(s)} + 2An_{(g)}$$

Ablov's value of 43.2Kcal./mole for this reaction is considerably higher than the value reported here of 35.5Kcal./mole. This discrepancy may also have its origin in the Kirchoff correction.

There does not appear to have been any other thermochemical work reported for these compounds. Some ultra-violet spectral data have been reported (60) but no quantitative conclusions have been drawn from them.

Using infra-red spectroscopic measurements, Clark and Williams (93) have established that all the complexes used in this work, with the exception of the cobalt complex, are distorted octahedral polymers. Unlike the analogous pyridine complex, $CoAn_2Cl_2$ is tetrahedral at room temperature and this form persists down to liquid nitrogen temperatures. Evidently, for the octahedral and tetrahedral forms of $CoAn_2Cl_2$, there is a large energy difference which may originate from the lack of π-acceptor orbitals in aniline which, for pyridine, may stabilise the octahedral structure as described previously.

4.6 Complexes of Pyrazine and Related Ligands

The preparations and structures of many metal-diazine complexes have been discussed by Lever, Lewis and Nyholm (57, 59, 74, 94). Reimann and Gordon (95) have discussed the preparations and properties of some diazine and triazine complexes and Koros and his co-workers have reported the thermal decomposition of some cobalt-diazine complexes (58). This latter work served as a useful comparison with our own work and good agreement was found between the two sets of data.

The diazines used in this work were mostly those derived from pyrazine (1,4-diazine) by substitution of ring protons with methyl groups. The weight losses which accompanied thermal decomposition could be assigned to definite stoichiometric reactions in which only integral, or simple

fractional losses of diazine occurred for the complexes of 1, 4-diazines. Complexes of 1, 2- and 1, 3-diazine were also prepared but thermal decomposition of these complexes resulted in the formation of a black residue of ill-defined stoichiometry except in the case of dibromobis (pyrimidine) cobalt(II) bromide which decomposed cleanly to cobalt(II) bromide. Poor results were also obtained with complexes of sym-triazine (1, 3, 5-triazine). It may be that ring fragmentation occurs when these black residues are formed and, although no black residues were formed from 1, 4-diazine complexes it was thought to be necessary to ensure that the gas evolved during decomposition of these complexes was not a product of ring fragmentation. A sample of the gas was condensed and its infra-red spectrum recorded which proved to be identical to that of a pure sample of the diazine. This was considered adequate proof that the decomposition did not involve the formation of any other gaseous product than the diazine and it was possible to proceed with the thermochemical measurements. The presence of two nitrogen atoms in the ring will induce quite a high positive charge at the centre of the ring. Back donation to the ring would be favoured due to stabilisation of the π-electron cloud and the results we obtained would appear to support this suggestion. As an example, it is of interest to note that the ferrous complex, $Fepz_2Cl_2$, is unusually stable towards air oxidation. The high charge acquired by the ferrous atom from the ligands which normally results in the oxidation to ferric iron in other compounds, will be delocalised by back π-donation to the pyrazine rings and no further electron loss is required for stability.

It was expected that chromium(II) should be similarly stabilised but, on mixing aqueous or ethanolic solutions of chromous chloride and pyrazine, a black tarry solid was formed to leave a green solution characteristic of chromium(III). Methylpyrazine formed a green solution, without formation of a black solid, and in both cases it would seem that extreme charge transfer occurred onto the pyrazine rings resulting in oxidation of the chromium(II) ion.

The most common stoichiometry of the diazine complexes is ML_2X_2, although methylpyrazine reacts with cobalt or nickel chloride to give complexes of the type $M\ Mp_4Cl_2$ and 2, 5-dimethylpyrazine forms complexes of the type MLX_2. The occurrence of these complexes needs explanation in view of the steric factors involved. In view of the non-existence of a tetrakis α-picoline complex, it is probable that methylpyrazine is bonded through the non sterically hindered nitrogen. Bis-ligand complexes are readily formed with α-picoline and complexes of similar stoichiometry would be expected for 2, 5-dimethylpyrazine. That this is not so may be due to a particular steric interaction which causes the rings to be oriented in a particularly favourable way for metal-ring π-bonding. This was proposed by Coates (96) to explain the stability of some organo-metallic compounds which had substituents ortho to the metal-carbon bond and may also be applicable here. A one to one complex of manganese is also formed, $MnpzCl_2$, in which similar arguments may not be invoked but other methods of preparation may yield the bis-ligand complex. Further coordination of 2, 5-dimethylpyrazine could not be induced even by using the ligand as solvent for the reaction.

The complex, $CoDmpCl_2$, exists in two forms: one is a polymeric octahedral complex (a sample of which was supplied by Dr. A.B.P. Lever) and the other is a polymeric tetrahedral complex, the preparation of which has been described earlier. Unlike the two forms of $Copy_2Cl_2$, it was not possible to interconvert the two forms. The sample of the octahedral form decomposed, on heating, to a charred compound of indefinite composition whereas the tetrahedral form decomposed cleanly to the metal halide.

The heats of decomposition of the dipyrazine complexes into the monopyrazine complex and the metal halide respectively are quite different, the second stage being several kilocalories per mole greater than the first. This would seem to indicate a possibly greater stability of the monodiazine complexes. In view of the very low basicity of 1, 4-diazines, it was surprising to find that the heats of decomposition of the diazine complexes were slightly higher than those of the analogous pyridine complexes. The pK_B values of various bases are summarised in Table 6, wherein it is seen that pyrazine is $10^{4.6}$ times less basic than pyridine.

Table 6 : pK_B of Various Bases (97)

Base	Pyridine	Aniline	β,γ-picoline	Pyrazine	Pyrimidine
pK_B	8.77	9.42	8.00	13.4	12.7

If σ-bonding were the only bonding between metal and nitrogen, the lower basicity of pyrazine would be expected to result in a weak bond compared with the metal-pyridine complexes. This would, presumably,

manifest itself in relatively low heats of decomposition for pyrazine complexes. If the σ-bonding were reinforced with back π-bonding it would be expected that the bond strengths could be similar to those found in the pyridine complexes. Since the heats of decomposition of the pyrazine complexes are slightly higher than those of analogous pyridine complexes it would seem that π-bonding may well be important in these complexes as was expected from the observations, mentioned previously, made on the iron complex.

The complex $CoMp_4Cl_2$, readily lost two molecules of ligand at relatively low temperatures with an accompanying heat of reaction of 33.8Kcal/mole. The heat of reaction for the loss of two further molecules of ligand is 33.6Kcal./mole and is almost equal to that of the complex $Copz_2Cl_2$ from which it may be inferred that the non-sterically hindered nitrogen of the ring bonds to the metal. 21.7Kcal./mole are required to remove the final molecule of ligand from this complex whereas only 19.3Kcal are required to remove one mole of 2, 5-dimethylpyrazine from $CoDmpCl_2$. This may suggest greater steric hindrance in the latter compound but a comparison is not really possible since the structures of the starting compounds differ.

The most complete set of heats of reaction refer to the decomposition

$$MLX_{2(cryst.)} \rightarrow MX_{2(cryst.)} + 2L_{(g)}$$

which may be referred to, following the convention adopted in the experimental section, as ΔH(12). For the octahedral polymeric compounds,

$NipzCl_2$ and $NiDmpCl_2$, $\Delta H(12)$ has almost the same value. As has been said before, it may be that the dimethylpyrazine molecule may adopt a favourable configuration so that steric interactions which would otherwise decrease the bond strengths of its complexes are overcome. Lever et al.(94) were unable to detect any dependence of 10Dq, the crystal field splitting parameter on methyl substitution of the pyrazine ring. On a molecular orbital approach, 10Dq is the separation of the non-bonding and anti-bonding orbitals in the complex and, as such, reflects the interaction of the metal and ligand orbitals. It would seem, therefore, that Lever's observations support our own, namely that the bond strength is little affected by ortho-substitution. Lever's explanation of the observation was that the increased σ-bonding ability would be offset by decreased π-bonding due to the higher negative charge induced on the ring by the methyl groups. If this were true, α-picoline, which participates to a lesser degree in π-bonding than pyrazine, should form stronger bonds than pyridine. Our results do not appear to support this and, therefore, Lever's suggestion does not seem to be acceptable. As a general observation, the $\Delta H(12)$ values do not exhibit any such regular dependence on the nature of metal, ligand or halogen, as was found for the complexes of pyridines and picolines. The pyrimidine complex, $Co(pmd)Br_2$ has a $\Delta H(12)$ of 26.9Kcal./mole which is considerably greater than that of any of the pyrazine complexes. The structures of pyrimidine complexes are not known with certainty (95) but are thought to be very similar to the structures of 1-4 diazine complexes. If this is so, it is difficult to see why pyrimidine should form a more stable structure than pyrazine unless a simple

4.7 Heat Capacity Results

As outlined previously, the differential scanning calorimeter may be used to determine the heat capacities of chemical substances relatively quickly and with good accuracy. It was considered necessary to measure the heat capacities of representative complexes and to calculate the Kirchoff correction, $\int \Delta C_p dT$, which has been mentioned previously, in order to see if there was any correlation between the heats of decomposition obtained from room temperature solution calorimetry and from higher temperature scanning calorimetry. It was desirable to use complexes which did not decompose at low temperatures and this excluded the tetrakis-ligand complexes. Also, the heat capacities of the gaseous products had to be known; fortunately, the heat capacities of most of the ligands used in this work have been measured or calculated to high accuracy. The first compound chosen for this work was dichlorodipyridinecobalt(II). It is thermally stable over a reasonable temperature range, which permitted extrapolation of our data to higher temperatures, and two independent determinations have been made of its heat of decomposition at room temperature (64, 98). The heat of the similar reaction for dichlorobis-(α-picoline)cobalt(II) has also been reported (99) and the heat capacity of this compound has been measured. It was also of interest to measure the heat capacities of complexes for which the ligand skeleton had been changed slightly, from pyridine to pyrazine for example; it was thought that this would permit a comparison of the temperature corrections for each ligand skeleton so that it could be seen if a sensible comparison could be

made between scanning calorimetry data without temperature corrections being applied in each case.

It was necessary to ensure that the differential scanning calorimeter gave meaningful results when used for the measurement of heat capacities. Certain standard substances were chosen for this purpose. These were high purity (99.999%) metallic indium and dried "Analar" sodium chloride. The heat capacity of indium was found to fit the equation:

$$C_p = 4.18 + 0.0068T \text{ cals } {}^{o}K^{-1} \text{ g.atom}^{-1} \qquad (a)$$

over the range 330°K to 425°K. Other data have been reported which fit the equations:

$$C_p = 5.81 + 0.0025T \text{ cals } {}^{o}K^{-1} \text{ g.atom}^{-1} \text{ (101)} \qquad (b)$$

$$C_p = 4.90 + 0.0050T \text{ cals } {}^{o}K^{-1} \text{ g.atom}^{-1} \text{ (100)} \qquad (c)$$

These latter equations relate to data obtained over a similar temperature to that used in this work. Agreement between any two of the equations would not appear to be good. If, however, heat capacities are calculated from each of the equations, a point by point comparison is found to be good. For example, the maximum difference of heat capacities calculated from equation (a) and equation (b) was found to be 3% which is only slightly greater than the experimental uncertainty of ±1 to 2%. The heat capacity of sodium chloride was found to fit the equation:

$$C_p = 10.1 + 0.0056T \text{ cals } {}^{o}K^{-1} \text{ g.atom}^{-1}$$

Kubaschewski and Evans (101) report the equation

$$C_p = 10.98 + 0.0039T \text{ cals } {}^{o}K^{-1} \text{ g.atom}^{-1}$$

for this compound. The discrepancies between the two equations are well within experimental error when a point by point comparison is made.

The calorimeter was then used to measure the heat capacities of some of the complexes which have been studied. The Kirchoff correction is given by:

$$\Delta H_{Tf} = \Delta H_{Ti} + \int_{Ti}^{Tf} \sum_{p} Cp_{(p)} - Cp_{(r)} \; dT$$

ΔH refers to the heat of reaction at the lower temperature (Ti) or the higher temperature (Tf). Ti, in this case, was room temperature. Tf was estimated as a weighted mean for a multi-stage decomposition by summing the products of the individual heats of reaction and their average temperatures and equating this sum to the product of the total heat of reaction and Tf. $\Sigma Cp_{(p)}$ is the sum of the heat capacities of the products and $Cp_{(r)}$ is the heat capacity of the reactant. These had the form:

Heat capacity of $CoCl_{2(s)}$ = $a + bT$ cals $^{o}K^{-1}$ $mole^{-1}$

Heat capacity of base = $c + dT + cT^2$ cals $^{o}K^{-1}$ $mole^{-1}$

Heat capacity of complex = $f + gT$ cals $^{o}K^{-1}$ $mole^{-1}$

It is implied that the heat capacity of the complex can be extrapolated to within the temperature range of decomposition since the integration must be carried out to within this range. This is a dubious assumption but necessary for the calculation. Data for the equations are available and are summarised in Table 7.

Table 7

Compound	Heat capacity cals^{o}K^{-1}mole^{-1}	Reference and Temperature range
$CoCl_{2(solid)}$	$14.41 + 14.60 \times 10^{-3}T$	(101) 298^{o}K - m.pt.
$Aniline_{(gas)}$	$-10.2216 + 1.56200 \times 10^{-1}T - 1.31860 \times 10^{-4}T^2$	(102) 298.15^{o}K - 1.000^{o}K
$Pyrazine_{(gas)}$	$2.1977 + 3.99752 \times 10^{-2}T + 9.63829 \times 10^{-5}T^2$	(103) 200 - 1000^{o}K
α-$picoline_{(gas)}$	$-4.097 + 1.00658 \times 10^{-1}T - 6.0026\ z\ 10^{-6}T^2$	(104) 273 - 600^{o}K
$Pyridine_{(gas)}$	$-8.262 + 10.608 \times 10^{-2}T - 5.4662 \times 10^{-5}T^2$	(105) 374 - 500^{o}K

The Kirchoff correction was integrated and the results are listed below:

Table 8

Compound	$(\Delta H_{Tf} - \Delta H_{Ti})$Kcal./mole
$Copy_2Cl_{2(cryst.)}$	- 2.2
$Co(\alpha\text{-pic})_2Cl_{2(cryst.)}$	- 3.1
$CoAn_2Cl_{2(cryst.)}$	- 1.9
$FePz_2Cl_{2(cryst.)}$	+ 5.4

It was not possible to calculate the correction for $Co(\gamma\text{-pic})_2Cl_2$ since the heat capacity of γ-picoline has not yet been reported. Thermodynamic data should soon be available for this base but the writer

has been informed that some slight decomposition occurs at high temperatures which has delayed publication of results (105).

The corrections, $\Delta H_{(T_f)} - \Delta H_{(T_i)}$ are all small and, with the exception of $Fepz_2Cl_2$, negative. The heats of the reaction

$$CoL_2Cl_{2(cryst.)} \quad CoCl_{2(cryst.)} + 2L_{(g)}$$

have been measured at room temperature (64, 99) for L = pyridine or α-picoline (ref. 64 only). The results obtained were

L = pyridine, ΔH = 45.3Kcal./mole (64)

= 45.1Kcal./mole (99)

L = α-picoline, ΔH = 41.1Kcal./mole (64)

The heats of reaction obtained with the scanning calorimeter were found to be 31.6 and 26.2Kcal./mole for L = pyridine and α-picoline respectively. Using these data and the $\Delta H_{(T_f)} - \Delta H_{(T_i)}$ corrections it is calculated that $\Delta H_{(T_i)}$ should be 33.8Kcal./mole for α-$Copy_2Cl_2$ amd 29.3Kcal./mole for $Co(\alpha\text{-pic})_2Cl_2$. Each of these values is smaller than the experimental values quoted above by about 12Kcal. The reason for this discrepancy may lie in the assumption that the heat capacity of the complex may be extrapolated to within the temperature range of decomposition. This is almost certainly true and a non-linear rise in the heat capacity in this range would result in a larger negative value of $\Delta H_{(T_f)} - \Delta H_{(T_i)}$. However, it is not possible to test this assumption experimentally. In the absence of these data, it is noteworthy that the difference between the heats of decomposition of $Copy_2Cl_2$(violet) and $Co(\alpha\text{-pic})_2Cl_2$ is 5.4 ± 1.1Kcal./mole at the higher temperature and 4.2 ± 1.7Kcal./mole at the lower temperature.

It would seem, therefore, that since the differences in the heats of decomposition so appear to be similar at either high or low temperatures then it may be reasonable to compare the scanning calorimeter data as an internally consistent set. It does not seem likely that a useful comparison can be made with room temperature measurements. It may also be true that a comparison is only possible between complexes which differ only slightly, for example by minor changes in the ligand skeleton as in this work; major changes may bring about quite different Kirchoff corrections which thereby preclude comparison of data.

The heat capacities of the various complexes were obtained at a number of temperatures and some of the experimental data are summarised in Table 9.

Table 9

Compound	Temperature	Cp cals/^{o}/mole
$Copy_2Cl_2$	330	72.4
	350	75.0
	370	77.1
$Co(\gamma\text{-pic})_2Cl_2$	330	85.7
	350	88.5
	370	94.6
$Co(\alpha\text{-pic})_2Cl_2$	330	89.7
	350	74.8
	370	97.4

Table 9 (continued)

Compound	Temperature	Cp cals/^{o}/mole
$CoAn_2Cl_2$	330	79.1
	350	82.2
	370	86.1
	400	93.6
	430	96.8
$Fepz_2Cl_2$	330	63.0
	350	65.7
	370	72.2
	400	75.4
	430	78.4

Theoretically, one may calculate the energy associated with the translation, rotation or vibration of a substance. These three modes are generally separable and, at ordinary temperatures, electronic excitation is normally excluded. Differentiation of the energy of a substance yields its heat capacity at constant volume since work of expansion has not been allowed for. This work contains data obtained at constant pressure and the heat capacity at constant pressure is related to that at constant volume by:

$$Cp = Cv + T\left(\frac{\partial V}{\partial T}\right)_P \left(\frac{\partial P}{\partial T}\right)_V$$

For similar compounds, Cp should parallel Cv and, in any case, Cp - Cv is often quite small for liquids and solids. For a solid, the major contribution to its heat capacity is given by the vibrations of the crystalline lattice. At high temperatures, the maximum heat capacity of 3R gm.mole^{-1} for a particular element is obtained.

A useful rule (Kopp's Rule) states that the heat capacity of a solid compound is frequently equal to the sum of the heat capacities of the constituent solid elements in proportion to the numbers of gram atoms per gram molecule of the compound. This rule will be used later.

The heat capacities of solid pyridine, picoline and aniline have been measured and are listed in Table 10.

Table 10

Temp.(^{o}K)	Cs(pyridine)(54)	Cs(α-picoline)(55)	Cs(aniline)(58)
140		18.4	16.1
160		19.9	18.2
180	17.2	21.4	20.4
200	19.0	23.0	22.7
220	21.3		25.2

There is little difference in the heat capacities of solid aniline and α-picoline, particularly as the temperature is raised, since they each have identical numbers of carbon, hydrogen and nitrogen atoms. Pyridine has fewer atoms, and a lower heat capacity. On the basis of the differences in heat capacities, it would be expected that the ML_2X_2 complexes for which L = aniline or picoline should have similar heat capacities which should be greater than that of the pyridine complex. This is seen to be true (Table 9) for the aniline complex but the picoline complexes have rather higher heat capacities. This may suggest

that rotation is more restricted in the aniline complex than in the picoline complexes. The α-picoline complex has a heat capacity which is slightly greater than that of the γ-picoline complex but the difference is only just outside experimental error. The heat capacity of the pyrazine complex is much lower than that of the pyridine complex. From Table 10 it is seen that the heat capacities of α-picoline and aniline are greater than that of pyridine in the solid state by about 4 cals.mole^{-1} $^{o}K^{-1}$. Since α-picoline or aniline contain one carbon and two hydrogen atoms more than pyrazine, one gram atom of hydrogen must contribute less than 4 cals. to the heat capacity in the solid state. It would be expected therefore that the heat capacity of the pyrazine complex should be smaller than that of the pyridine complex by much less than 8 cals.mole^{-1} $^{o}K^{-1}$. Both complexes have similar polymeric structures but the heat capacity of the pyrazine complex is 5 to 9 cals. less than that of the pyridine complex. This is rather greater than expected and may be due to loss of rotational freedom about the metal-nitrogen bond. π-bonding from metal to pyrazine has previously been proposed and this may support such a suggestion since π-bonds should induce greater rigidity of a bond.

It would seem that there may be some correlation between the data obtained from the heats of decomposition and heat capacity measurements reported here insofar as the same general conclusions are reached, albeit in a semi-quantitative manner.

APPENDIX I

Least Squares Curve Fitting (3)

If y depends on x by

$$y_i = A + Bx_i + Cx_i^2$$

and if the experimental value at x_i be y_i^1

$$y_i^1 + \delta y = y_i = A + Bx_i + Cx_i^2 + ...$$

$$\therefore \delta y = -y_i^1 + A + Bx_i + Cx_i^2 + ...$$

$$\therefore \delta y^2 = (-y_i^1 + A + Bx_i + Cx_i^2 \quad .....)^2$$

Differentiating with respect to A and minimising, summing over i yields:-

$$\sum_i (A + Bx_i + Cx_i^2 + ...) = \sum_i y_i^1$$

Similarly, differentiation with respect to B, C etc yields equations of the form:

$$AS_m + BS_{m+1} + CS_{m+2} + ... = V_m$$

m = 0, 1, 2... until as many equations as unknowns are attained.

$$S_m = \sum_i x_i^m \ , \quad V_m = \sum_i y_i \, x_i^m$$

The equations are then solved for A, B, C and so on.

REFERENCES

1. L. Pauling and D.M. Yost, Proc. Nat. Acad. Sci., Wash., 18, 414 (1932).
2. See, for example, "Chemical Thermodynamics", Kirkwood and Oppenheim, McGraw-Hill Ltd., New York, 1961, Chapter 3.
3. H. Margenau and G.M. Murphy, "The Mathematics of Physics and Chemistry", D. van Nostrand Inc., New York, 1943.
4. See also reference (2), appendix.
5. See, for example, D.F.Eggers, N.W. Gregory, G.D. Halsey and B.S. Rabinovitch, "Physical Chemistry" John Wiley & Sons, New York, 1964.
6. G.H. Hess, Ann. Physik., 50, 385 (1840).
7. See, for example, M. Berthelot, Ann. Chim. (Phys.) 1884-1904
8. G. Pilcher and H.A. Skinner, Quart. Rev., 17, 264 (1963).
9. J.N. Murrell, S.F.A. Kettle and J.M. Tedder, "Valence Theory" John Wiley & Sons Ltd., London, 1965.
10. T.L. Cottrell, "The Strengths of Chemical Bonds", 2nd Ed., Butterworths, London, 1958.
11. M.J. O'Neill, Anal. Chem., 36, 1238 (1964).
12. W.P. White, "The Modern Calorimeter", The Chemical Catalog. Co., New York, 1928.
13. See, for example, p. 546 of "Physical Methods of Organic Chemistry", Part One, Vol. One of "Technique of Organic Chemistry, edited by A. Weissberger, Interscience Inc., New York, 1959.
14. C. Kitzinger and T. Benzinger, Z. Naturforsch., 10b, 365 (1955).
15. See, for example, W.J. Smothers and Y. Chiang, "Differential Thermal Analysis", Chemical Publishing Co., New York, 1958.
16. R.A. Arndt and R.E. Fujita, Rev. Sci. Inst., 34, 868 (1963).

17. H. Junkers, J. Gasbeleucht 50, 520 (1907).

18. W. Swietoslawski, "Microcalorimetry", Reinhold, New York, 1946, Chapter X.

19. D.M. Speros and R.L. Woodhouse, J. Phys. Chem. 67, 2164 (1963).

20. K.B. Yatsimirskii and L.L. Pankova, Zhur. Obshshei. Khim., 18, 2051 (1948).

21. S.J. Ashcroft, G. Beech and C.T. Mortimer, J. Chem. Soc. (In Press).

22. K.G. Poulsen, J. Bjerrum and I. Poulsen, Acta. Chem. Scand., 8, 921 (1954).

23. A.E. Martell, Rec. Trav. Chim., 75, 781 (1956).

24. S. Cabani, G. Moretti and E. Scrocco, J. Chem. Soc., 88 (1962).

25. J.L. Wood and M.M. Jones, J. Phys. Chem., 67, 1049 (1963).

26. See, for example, J. Lewis and R.G. Wilkins, "Modern Coordination Chemistry", Interscience, New York - London (1960).

27. See, for example, M.C. Day and J. Selbin, "Theoretical Inorganic Chemistry", p.315, Reinhold Pub. Co., New York, 1962.

28. P. George and D.S. McClure in Progress in Inorganic Chemistry (Vol. I) Interscience Inc., New York (1959).

29. See, for example, C.K. Jørgensen, "Absorption Spectra and Chemical Bonding", Pergamon Press, London, 1962.

30. L.E. Orgel, "An Introduction to Transition Metal Chemistry", Methuen Ltd., London 1966 (2nd Ed.).

31. B.N. Figgis, "Introduction to Ligand Fields", Interscience Publishers, New York, 1966.

32. M.C. Browning, R.F.B. Davies, D.J. Morgan, L.E. Sutton and L.M. Venanzi, J. Chem. Soc. 4816 (1961).

33. J. Chatt and B.L. Shaw, J. Chem. Soc., 285 (1961).

34. W. Oelsen, Arch. Eisenhuttenw 26, 519 (1955).

35. D.C. Ginnings and G.T. Furukawa, J. Am. Chem. Soc., 75, 522 (1953).

36. B. Wunderlich and M. Dole, J. Poly. Sci., 24, 201 (1957).
and B. Wunderlich, J. Phys. Chem., 69, 2078 (1965).

37. N. Brenner and M.J. O'Neill, Perkin-Elmer Instrument News 16 (2), 12 (1965).

38. National Bureau of Standards, Circular 500, Washington, D.C.

39. E. Posnjak, Am. Jour. Sci., 35A, 247 (1938).

40. K.K. Kelley, J.C. Southard and C.T. Anderson, U.S. Bureau of Mines, Paper 625 (1941).

41. G. Williams, Pilkington Bros. Ltd., personal communication.

42. E. Calvet, M. Gambino and M.L. Michel, Bull. Soc. Chim.France 2208 (1964).

43. D.R. Stull and G.C. Sinke, "Thermodynamic Properties of the Element", American Chemical Society (1958).

44. A. Earnshaw, L.F. Larkworthy and K.S. Patel, Chem. and Ind., 1521 (1965).

45. Sr. M.D. Glonek, C. Curran and J.V. Quagliano, J. Am. Chem. Soc., 84, 2014 (1962).

46. A.B.P. Lever, J. Lewis and R.S. Nyholm, J. Chem. Soc., 1235 (1962).

47. J.R. Allan, D.H. Brown, R.M. Nuttall and D.W.A. Sharp, J. Inorg. Nucl. Chem., 27, 1865 (1965).

48. L.R. Ocone, J.R. Soulen and B.P. Block, J. Inorg. Nucl. Chem., 15, 76 (1960).

49. J.R. Allan, D.H. Brown, R.M. Nuttall and D.W.A. Sharp, J. Inorg. Nucl. Chem., 26, 1895 (1964).

50. Gmelins Handbuch der Anorganischen Chemie, Cobalt, System-Nummer 58, Teil B.

51. J.R. Allan, D.H. Brown, R.H. Nuttall and D.W.A. Sharp, J. Inorg. Bucl. Chem., 27, 1529 (1965).

52. F.T. Welcher "Organic Analytical Reagent", New York, 1947, Vol. III.

53. R. Zanetti and R. Serra, Gazz. Chim. Ital. 90, 328 (1960).

54. R. Ripan, Bull. Soc. Stiinte Cluj. România, 4, 80 (1928).

55. O. Baudisch and W.H. Hartung, Inorg. Syn. 1, 184 (1939).

56. D.M.L. Goodgame, M. Goodgame, M.A. Hitchman and M.J. Weeks, Inorg. Chem., 5, 635 (1966).

57. A.B.P. Lever, J. Lewis and R.S. Nyholm, J. Chem. Soc. 1235 (1962).

58. E. Koros, S.M. Nelson, F. Paulik, L. Erdey and F. Ruff, Proceedings of the Symposium on Coordination Chemistry, Hungary, 1964, p.295-308.

59. A.B.P. Lever, J. Lewis and R.S. Nyholm, J. Chem. Soc. 5042 (1963).

60. I.S. Ahuja, D.H. Brown, R.H. Nuttall and D.W.A. Sharp, J. Inorg. Nucl. Chem., 27, 1105 (1965).

61. G. Booth in "Advances in Inorganic Chemistry and Radiochemistry", Vol. 6, Academic Press, New York, 1966.

62. The details of this method were kindly supplied by Mr. A.W. Cooper of The North Staffordshire College of Technology, Stoke-on-Trent.

63. The basis of the method may be found in "Calorimetric Determination of Elements", by G. Charlot, Elsevier Pub. Co., Amsterdam 1964.

64. G. Beech, S.J. Ashcroft and C.T. Mortimer, J. Chem. Soc. (A) 929 (1967).

65. A.F. Bedford, D.M. Heinekey, I.T. Millar and C.T. Mortimer, J. Chem. Soc., 2932 (1962).

66. N.S. Gill, R.S. Nyholm, G.A. Barclay, T.I. Christie and P.J. Pauling, J. Inorg. Nucl. Chem., 18, 88 (1961).

67. J.D. Dunitz, Acta. Cryst., 10, 307 (1957).

68. M.A. Porai-Koshits, L.O. Atovmyan and G.N. Tishchenko, Zhur. Shuht. Khim., 1, 337 (1960).

69. D.G. Holah and J.P. Fackler (Jr.), Inorg. Chem., 4, 112 (1965).

70. M.A. Porai-Koshits, Tr. Inst. Krist. Akad. Nank. S.S.S.R., 10, 117 (1954).

71. A.S. Antsishkina and M.A. Porai-Koshits, Kristallografiya, 3, 676 (1958).

72. M.A. Porai-Koshits and A.S. Antsishkina, Kristallografiya, 3, 386 (1958).

73. M. Delepine, Bull. Soc. Chim. France, 45, 235 (1929).

74. A.B.P. Lever, J. Lewis and R.S. Nyholm, Nature 189, 58 (1961).

75. A.V. Ablov and Ts. B. Konunova, Russ. J. Inorg. Chem. 8, 582 (1963).

76. J.L. Wood and M.M. Jones, Inorg. Chem. 3, 1555 (1964).

77. S.M. Nelson, personal communication.

78. W.W. Wendlandt, Chemist-Analyst, 53, 71 (1964). (Published by J.T. Baker, Chem. Co., New Jersey, U.S.A.).

79. R.J.H. Clark and C.S. Williams, Inorg. Chem., 4, 350 (1965).

80. C.W. Frank and L. B. Rogers, Inorg. Chem. 5, 615 (1966).

81. A.B.P. Lever, S.M. Nelson and T.M. Shepherd, Inorg. Chem. 4, 810 (1965).

82. S.M. Nelson and T.M. Shepherd, J. Chem. Soc., 3284 (1965).

83. H.C.A. King, E. Koros and S.M. Nelson, J. Chem. Soc, 5449 (1963).

84. H.C.A. King, E. Koros and S.M. Nelson, J. Chem. Soc., 4832 (1964).

85. H.C.A. King, E. Koros and S.M. Nelson, Nature, 196, 572 (1966).

86. J. De O. Cabral, H.C.A. King, S.M. Nelson and (in part) E. Koros, J. Chem. Soc., 1348 (1966).

87. W. Libus and I. Uruska, Inorg. Chem., 5, 256 (1966).

88. N.S. Gill and R.S. Nyholm, J. Chem. Soc., 3997 (1959).

89. A.B. Blake and F.A. Cotton, Inorg. Chem., 3, 5 (1964).

90. A.R. Leeds, J. Amer. Chem. Soc., 1, 134 (1879).

91. A.V. Ablov, Ts. B. Konunova-Frid and V.A. Palkin, Russ. J. Inorg. Chem., 5, 747 (1960).

92. A.V. Butcher, D.J. Phillips and J.P. Redfern, J. Inorg. Nucl. Chem., 28, 2765 (1966).

93. R.J.H. Clark and C.S. Williams, Chem. and Ind. 1317 (1964).

94. A.B.P. Lever, J. Lewis and R.S. Nyholm, J. Chem. Soc. 4761 (1964).

95. C. Reimann and G. Gordon, Nature 205, 902 (1965).

96. G.E. Coates, "Organo-Metallic Compounds" 2nd Ed., Methuen and Co. Ltd., London, 1960.

97. Handbook of Chemistry and Physics, 44th Edn., Chemical Rubber Pub. Co., Cleveland, Ohio, 1961.

98. E. Tomus and E. Segal, Anal. Univ. Bucuresti, 41, 103 (1963).

99. W.A. Roth, I. Meyer, M. Zeumer, Z. Anorg. Chem., 214, 309 (1933).

100. O. Kubaschewski and E. LL. Evans, "Metallurgical Thermochemistry", Pergamon Press, London, 1958.

101. W.E. Hatton, D.L. Hildenbrand, G.C. Sinke and D.R. Stull, J. Chem. Eng. Data 7, 229 (1962).

102. G. Nagarajan, J. Sci. Industr. Res., 218, 255 (1962).

103. D.W. Scott et al. J. Phys. Chem., 67, 685 (1963).

104. D.W. Scott et al., J. Phys. Chem., 67, 680 (1963).

105. D.S. Douslin, U.S. Department of the Interior, personal communication.